

EUROPEAN ORGANISATION FOR NUCLEAR RESEARCH (CERN)



Phys. Rev. D 105 (2022) 012006
DOI: [10.1103/PhysRevD.105.012006](https://doi.org/10.1103/PhysRevD.105.012006)



CERN-EP-2021-157
7th February 2022

Search for Higgs boson decays into a pair of pseudoscalar particles in the $bb\mu\mu$ final state with the ATLAS detector in $p p$ collisions at $\sqrt{s} = 13$ TeV

The ATLAS Collaboration

This paper presents a search for decays of the Higgs boson with a mass of 125 GeV into a pair of new pseudoscalar particles, $H \rightarrow aa$, where one a -boson decays into a b -quark pair and the other into a muon pair. The search uses 139 fb^{-1} of proton–proton collision data at a center-of-mass energy of $\sqrt{s} = 13$ TeV recorded between 2015 and 2018 by the ATLAS experiment at the LHC. A narrow dimuon resonance is searched for in the invariant mass spectrum between 16 GeV and 62 GeV. The largest excess of events above the Standard Model backgrounds is observed at a dimuon invariant mass of 52 GeV and corresponds to a local (global) significance of 3.3σ (1.7σ). Upper limits at 95% confidence level are placed on the branching ratio of the Higgs boson to the $bb\mu\mu$ final state, $\mathcal{B}(H \rightarrow aa \rightarrow bb\mu\mu)$, and are in the range $(0.2\text{--}4.0) \times 10^{-4}$, depending on the signal mass hypothesis.

1 Introduction

Light (pseudo) scalars that couple to the 125 GeV Higgs boson [1, 2] appear in many well-motivated extensions of the Standard Model (SM) [3–8]. These include models addressing the baryon asymmetry of the universe [9, 10], offering a solution to the naturalness problem [11, 12], or providing insights into the nature of dark matter [13–19]. Light bosons produced in Higgs boson decays could also be mediators to dark sectors that do not couple to the SM otherwise [20–24]. Furthermore, pseudoscalar mediators appear in models, such as those described in Ref. [25], that were proposed to explain the anomalous muon magnetic moment [26]. A combination of ATLAS measurements of the Higgs boson production cross-sections and branching ratios constrains the branching ratios into invisible and undetected states to be $\mathcal{B}(H \rightarrow \text{inv}) < 30\%$ and $\mathcal{B}(H \rightarrow \text{undetected}) < 21\%$, respectively, whereas the overall branching fraction of the Higgs boson into beyond-the-SM (BSM) states is determined to be less than 47% at 95% confidence level (CL) [27]. Combined measurements of Higgs boson couplings performed by the CMS Collaboration set upper limits of $\mathcal{B}(H \rightarrow \text{inv}) < 22\%$ and $\mathcal{B}(H \rightarrow \text{undetected}) < 38\%$ at 95% CL [28]. This motivates searches for light states in the Higgs boson decays that probe this potentially large $\mathcal{B}(H \rightarrow \text{BSM})$.

This paper presents a search for decays of the 125 GeV Higgs boson into two pseudoscalars, denoted by a , in proton–proton (pp) collisions at the LHC [29]. The search is performed in events where one a -boson decays into two b -quarks and the other into two muons, $H \rightarrow aa \rightarrow b\bar{b}\mu^+\mu^-$.¹ The a -bosons are assumed to have a decay width that is narrow compared to the detector resolution. As pseudoscalar couplings are generally proportional to mass, which is for example the case in two-Higgs-doublet models [20, 30], the $bb\mu\mu$ final state provides a good balance between a high branching ratio from the $a \rightarrow bb$ decay and a clean, high mass-resolution, dimuon resonance signature that is easy to trigger on from the $a \rightarrow \mu\mu$ decay. In scenarios with enhanced lepton couplings, the $a \rightarrow \mu\mu$ branching ratio can also be relatively large, resulting in $\mathcal{B}(H \rightarrow aa \rightarrow bb\mu\mu)/\mathcal{B}(H \rightarrow aa)$ of up to 0.16% [31].

Light resonances in Higgs boson decays have been searched for by ATLAS and CMS in many different channels, i.e. in the final states involving 4μ [32, 33], $2\mu 2\tau$ or 4τ [34–38], $2b2\tau$ [39], $4b$ [40, 41], 4γ [42] and $2\gamma + 2\text{jets}$ [43]. A search for a dimuon resonance produced in association with b -jets has been performed by CMS [44] and a light resonance decaying to two muons has been searched for by LHCb [45]. CMS has performed a search for $H \rightarrow aa \rightarrow bb\mu\mu$ in 35.9 fb^{-1} of pp collision data at a center-of-mass energy of $\sqrt{s} = 13 \text{ TeV}$ that sets upper limits on $\mathcal{B}(H \rightarrow aa \rightarrow bb\mu\mu)$ of $(1\text{--}7) \times 10^{-4}$ for a -boson masses (m_a) in the range $20 \leq m_a \leq 62.5 \text{ GeV}$ [46]. The ATLAS search based on 36 fb^{-1} of Run 2 data [47] sets upper limits on $\mathcal{B}(H \rightarrow aa \rightarrow bb\mu\mu)$ between 1.2×10^{-4} and 8.4×10^{-4} for a -boson masses in the range $20 \leq m_a \leq 60 \text{ GeV}$. In this paper, the full Run 2 dataset corresponding to an integrated luminosity of 139 fb^{-1} is used and the search is extended down to $m_a = 16 \text{ GeV}$ and up to $m_a = 62 \text{ GeV}$. Additionally, boosted decision tree (BDT) techniques are used to improve the separation of the signal from the SM backgrounds, increasing the analysis sensitivity, especially for higher m_a .

¹ Denoted by $H \rightarrow aa \rightarrow bb\mu\mu$ from now on for the rest of the paper.

2 ATLAS detector

The ATLAS experiment [48, 49] is a multipurpose particle detector with a forward–backward symmetric cylindrical geometry and a nearly 4π coverage in solid angle.² It consists of an inner detector (ID) surrounded by a thin superconducting solenoid providing a 2 T axial magnetic field, electromagnetic (EM) and hadron calorimeters, and a muon spectrometer (MS). The inner tracking detector covers the pseudorapidity range $|\eta| < 2.5$. It consists of silicon pixel, silicon microstrip, and transition radiation tracking detectors. Lead/liquid-argon (LAr) sampling calorimeters provide electromagnetic energy measurements with high granularity. A steel/scintillator-tile hadron calorimeter covers the central pseudorapidity range $|\eta| < 1.7$. The endcap and forward regions are instrumented with LAr calorimeters for both the EM and hadronic energy measurements up to $|\eta| = 4.9$. The MS surrounds the calorimeters and is based on three large superconducting air-core toroidal magnets with eight coils each. The field integral of the toroids ranges between 2.0 Tm and 6.0 Tm across most of the detector. The MS includes a system of precision tracking chambers and fast detectors for triggering. A two-level trigger system is used to select events. The first-level trigger is implemented in hardware and uses a subset of the detector information to accept events at a rate below 100 kHz [50]. This is followed by a software-based trigger that reduces the accepted event rate to 1 kHz on average. An extensive software suite [51] is used in the reconstruction and analysis of real and simulated data, in detector operations, and in the trigger and data acquisition systems of the experiment.

3 Dataset and simulated events

The data used in this analysis were collected in Run 2 of the LHC during the 2015–2018 data-taking period with pp collisions at a center-of-mass energy of $\sqrt{s} = 13$ TeV. The dataset corresponds to an integrated luminosity of 139 fb^{-1} . The lowest-threshold unprescaled single-muon and dimuon triggers are used to select the events [52]. Single-muon triggers require the transverse momentum (p_T) of the muon to be above 20 GeV or 26 GeV, depending on the data-taking period, while the dimuon trigger requires both muons to have a p_T above 14 GeV.

Simulated events are used in the estimation of the SM backgrounds. SHERPA 2.2.1 [53, 54] was used as the baseline generator for the Drell–Yan (DY) + jets, $W(\rightarrow \ell\nu)$ +jets, diboson and triboson backgrounds. It is a multiparton matrix element and parton shower (PS) generator including hadronization [55–59], with the NNPDF3.0 parton distribution function (PDF) set at next-to-next-to-leading-order (NNLO) accuracy [60]. The DY+jets and multiboson samples were generated with a minimum dilepton mass of 10 GeV and 4 GeV, respectively. The $t\bar{t}$ and single-top-quark samples were generated with PowHEG-Box v2 [61–65] using the NNPDF3.0NLO PDF in matrix element interfaced to PYTHIA 8.230 [66] for the PS. For the underlying-event description a set of tuned parameters called the A14 tune [67] was used, along with the NNPDF2.3LO PDF [68]. The $t\bar{t}$ + vector-boson processes ($t\bar{t}+V$) were generated with MADGRAPH5_aMC@NLO 2.3.3 [69] interfaced to PYTHIA 8.210 for the PS. The underlying-event tune was the same as for the $t\bar{t}$ sample. EvtGen [70] was used for the properties of the bottom and charm hadron decays in all simulated samples, except those simulated with SHERPA.

² ATLAS uses a right-handed coordinate system with its origin at the nominal interaction point (IP) in the center of the detector and the z -axis along the beam pipe. The x -axis points from the IP to the center of the LHC ring, and the y -axis points upwards. Cylindrical coordinates (r, ϕ) are used in the transverse plane, ϕ being the azimuthal angle around the z -axis. The pseudorapidity is defined in terms of the polar angle θ as $\eta = -\ln \tan(\theta/2)$. Angular distance is measured in units of $\Delta R \equiv \sqrt{(\Delta\eta)^2 + (\Delta\phi)^2}$.

Higgs boson production through gluon–gluon fusion (ggF) was generated using the NNLOPS program [71, 72] with PowHEG-Box v2 [61, 63, 73, 74]. The vector-boson fusion (VBF) processes were generated with PowHEG-Box v2 at NLO accuracy [75]. The Higgs boson mass was set to 125 GeV. For both the ggF and VBF production processes, PowHEG-Box was interfaced with PYTHIA 8.212 using the AZNLO tune [76] for the simulation of the $H \rightarrow aa \rightarrow bb\mu\mu$ decays, where the a -boson is a pseudoscalar, as well as for parton showering, hadronization and the underlying event. The ggF Higgs boson production rate is normalized to the total cross-section predicted at next-to-next-to-next-to-leading-order accuracy in QCD with NLO electroweak corrections applied [77–81] and amounts to 48.58 pb. The VBF production rate is normalized to an approximate NNLO cross-section with the NLO electroweak corrections applied [82–85], which amounts to 3.8 pb. The contribution from the associated production of a Higgs boson and a vector boson (VH) is calculated to be 3.5% of the total ggF+VBF cross-section and is accounted for by scaling the simulated ggF and VBF samples. The contribution from Higgs boson production in association with a pair of top quarks is found to be negligible (below the percent level) and is neglected in the analysis. Thirteen mass points were simulated for the ggF and VBF production modes, with the a -boson mass in the range $m_a = 16\text{--}62\text{ GeV}$.³ Below $m_a = 16\text{ GeV}$ the b -quarks coming from the decays of the a -boson tend to be so collimated due to its boost that they cannot be reconstructed as two separate b -jets (with a radius parameter of $R = 0.4$). Another effect is that in the highly asymmetric decays of low-mass a -bosons, the subleading b -jet falls below the jet reconstruction threshold of 20 GeV [86]. As a result, the signal acceptance falls below 0.2% and the analysis loses sensitivity.

The effects of additional interactions in the same and neighboring beam-bunch crossings (pileup) were modeled for all simulated events by overlaying additional pp collisions generated with PYTHIA 8.186 using the NNPDF2.3LO PDF set and the A3 tune [87]. Simulated event samples are weighted to reproduce the distribution of the number of pileup interactions observed in the data. All the generated background and signal samples are processed through the ATLAS detector simulation [88] based on GEANT4 [89] and reconstructed using the same software as for the data.

4 Event reconstruction and selection

Muons are reconstructed by combining track information from the MS with tracks found in the ID [90]. They also have to satisfy $p_T > 5\text{ GeV}$ and $|\eta| < 2.7$ (for $|\eta| > 2.5$, only tracking information from the MS is used), and pass the *LowPt* working point identification requirement defined in Ref. [90]. Muon tracks must have a longitudinal impact parameter z_0 satisfying $|z_0 \sin \theta| < 0.5\text{ mm}$ and a transverse impact parameter significance $|d_0|/\sigma_{d_0} < 3$ relative to the primary interaction vertex, chosen as the reconstructed vertex with the highest sum of the p_T^2 of its associated tracks. Furthermore, muons are required to be isolated from the surrounding detector activity by requiring that the scalar sum of the p_T of additional inner detector tracks and the sum of the transverse momentum E_T of calorimeter energy deposits within a cone of size $\Delta R = 0.2$ around a muon be less than 15% and 30% of the muon p_T , respectively.

Jets are reconstructed using the anti- k_t algorithm [91] implemented in the FASTJET package [92] with a radius parameter of $R = 0.4$. The inputs to the jet clustering are built by combining the information from both the calorimeters and the ID using a particle-flow algorithm [86, 93]. Jets with $p_T < 60\text{ GeV}$ originating from pileup are suppressed with the jet-vertex-tagger (JVT) [94], a multivariate algorithm combining track-based variables. Selected jets are required to have $p_T > 20\text{ GeV}$ and $|\eta| < 2.5$. An algorithm (MV2c10) relying on multivariate techniques, taking as input the properties of displaced tracks

³ More specifically, the simulated mass points are at $m_a = 16, 18, 20, 25, 30, 35, 40, 45, 50, 52, 55, 60$ and 62 GeV .

and vertices reconstructed within a jet, is employed to identify (tag) jets containing b -hadrons [95]. The MV2c10 tagger is used at 77% b -jet identification efficiency, with an approximate misidentification probability of 25% for jets arising from charm quarks, 6.3% for hadronically decaying τ -leptons, and 0.8% for light-flavor jets as measured in simulated $t\bar{t}$ events.

The missing transverse momentum (E_T^{miss}) is calculated as the magnitude of the negative vector sum of the transverse momenta of all the reconstructed and calibrated objects in the event, including a soft term that accounts for charged particles that are associated with the primary vertex, but not with any reconstructed object [96, 97].

The events selected for the analysis are required to have two muons of opposite charge, either with the leading and subleading muons satisfying $p_T^{\text{leading}} > 27 \text{ GeV}$ and $p_T^{\text{subleading}} > 5 \text{ GeV}$, and the event being triggered by a single-muon trigger, or with both muons having $p_T > 15 \text{ GeV}$, and the event being triggered by a dimuon trigger. The dimuon invariant mass, $m_{\mu\mu}$, is required to be between 15 GeV and 65 GeV. Furthermore, the events must contain exactly two b -tagged jets with p_T above 20 GeV.

A kinematic likelihood (KL) [98] fit exploiting the equal invariant masses of the bb and $\mu\mu$ systems in $H \rightarrow aa$ decays is performed to improve the four-body invariant mass ($m_{bb\mu\mu}$) resolution and reduce the SM backgrounds. The same fit approach as considered in the previous ATLAS publication [47] is used. The dimuon invariant mass, $m_{\mu\mu}$, is used to constrain the di- b -jet mass, as the former has a resolution approximately ten times better than the latter. The $m_{\mu\mu}$ resolution ranges between 0.4 GeV at $m_a = 16 \text{ GeV}$ and 1.3 GeV at $m_a = 62 \text{ GeV}$. The fit maximizes the likelihood by shifting the b -jet energies within the resolution in order to satisfy the constraint $m_{\mu\mu} \simeq m_{bb}$. The output of the fit is the logarithm of the maximum likelihood value, $\ln(L^{\text{max}})$, which quantifies how well the event matches the $m_{\mu\mu} = m_{bb}$ hypothesis, characteristic of signal events. The four-body invariant mass, recomputed after the KL fit, is denoted by $m_{bb\mu\mu}^{\text{KL}}$ and is used for further event categorization.

Signal-like events are chosen by requiring that $110 < m_{bb\mu\mu}^{\text{KL}} < 140 \text{ GeV}$, and that $\ln(L^{\text{max}}) > -8$, which ensures that m_{bb} is compatible with $m_{\mu\mu}$. Finally, E_T^{miss} is required to be less than 60 GeV to reduce the background from $t\bar{t}$ events, which is one of the two major backgrounds and can contain large E_T^{miss} from neutrinos in top-quark decays. This selection defines the “inclusive” signal region (SRincl) and is summarized in Table 1, along with the selection requirements for other analysis regions described later in the text.

A boosted decision tree (BDT) classifier implemented using the TMVA framework [99] is employed to further reduce the SM backgrounds. Its training is done in partially overlapping 8-GeV-wide $m_{\mu\mu}$ windows centered at the m_a values of each of the 12 generated signals,⁴ in order to fully exploit their kinematic differences. The background sample consists of $t\bar{t}$ and DY+jets events, the two dominant backgrounds, combined in the proportions extracted from the background validation fit described in Section 7. The signal samples used for the training include ggF and VBF Higgs boson production samples combined according to their cross-sections. The seven kinematic variables included in the training are:

- m_{bb} ,
- $\ln(L^{\text{max}})$,
- $\Delta R_{b_1 b_2}$ (the angular distance between the two b -jets),

⁴ One BDT was trained for each generated signal MC sample, except for $m_a = 52 \text{ GeV}$, as this sample was produced only at a later analysis stage.

- $\text{diff}\Delta R_b R_\mu = \Delta R_{b_1 b_2} - \Delta R_{\mu_1 \mu_2}$ (the difference between the angular separations between the two b -jets and the two muons),
- $\Delta R_{bb\mu\mu}$ (the angular distance between the bb and $\mu\mu$ systems),
- $\overline{\Delta R_{b,\mu}} = [\Delta R_{b_1 \mu_1} + \Delta R_{b_1 \mu_2} + \Delta R_{b_2 \mu_1} + \Delta R_{b_2 \mu_2}] / 4$ (the average angular distance of all four combinations of a b -jet and a muon),
- $\overline{m_{b\mu}} = [m_{b_1 \mu_1} + m_{b_1 \mu_2} + m_{b_2 \mu_1} + m_{b_2 \mu_2}] / 4$ (the average mass of all four combinations of a b -jet and a muon).

The distributions of these variables for the background and three representative signal masses are shown in Figure 1.

The m_{bb} variable helps separate the low-mass signal from the backgrounds, as m_{bb} peaks around 60 GeV for the $t\bar{t}$ and DY processes. The $\ln(L^{\max})$ peaks at higher values as the signal mass becomes smaller.

Due to a higher boost of a lighter a -boson, its decay products are collimated, resulting in $\Delta R_{b_1 b_2}$ and $\Delta R_{\mu_1 \mu_2}$ being much smaller than for a signal from a heavier a -boson or for background processes. As a consequence, $\text{diff}\Delta R_b R_\mu$ shows a narrow distribution centered around zero, while the background and a higher-mass signal exhibit a much broader $\text{diff}\Delta R_b R_\mu$ distribution.

The $\Delta R_{bb\mu\mu}$ variable helps enhance the sensitivity to higher signal masses. Heavier a -bosons are produced approximately at rest, resulting in the $\Delta R_{bb\mu\mu}$ distribution being relatively flat with a small peak at low values. As the signal mass decreases, the $\Delta R_{bb\mu\mu}$ distribution transitions into a “back-to-back” topology, characteristic of both a low-mass signal and the background events.

Finally, the $\overline{\Delta R_{b,\mu}}$ and $\overline{m_{b,\mu}}$ variables provide another measure of how close the two a -bosons are in ΔR . In the “back-to-back” topology for lower signal masses, the muons are, on average, further away from the b -jets, while for heavier a -bosons produced approximately at rest, the average distance between the muons and the b -jets is smaller. Consequently, $\overline{\Delta R_{b,\mu}}$ and $\overline{m_{b,\mu}}$ peak at high (low) values for low (high) signal masses, while the backgrounds peak somewhere between the two extreme signal topologies.

The output score of the BDT trained for a signal with mass m_a is denoted by $\text{BDT}m_a$. The $\text{BDT}m_a$ distributions for $m_a = 20$ GeV, 40 GeV and 60 GeV are shown in Figure 2.

The final signal region (SR) bin for each signal mass is defined by imposing two requirements in addition to the SRincl selection: $m_a - X < m_{\mu\mu} < m_a + X$ and $\text{BDT}m_a > 0.2$, where $X = 1$ GeV ($X = 1.5$ GeV) for $m_a \leq 45$ GeV ($m_a > 45$ GeV). The widths of the SR bins and the $\text{BDT}m_a$ cut value are optimized to maximize the significance of signal over background events. For masses at which no signal sample was generated, and, consequently, no BDT was trained, the BDT trained for the m_a closest to the one being tested is used. For example, when testing the $m_a = 32$ GeV hypothesis, the requirement $\text{BDT}30 > 0.2$ is applied to select the events for the SR bin. Signal yields for mass points where no signal sample was generated ($m_a = 32$ GeV in this example) are obtained by selecting events with BDT scores above 0.2 for the same $\text{BDT}m_a$ (BDT30 in this case) in all simulated mass points and interpolating using third-order splines. To assess the uncertainty, the yields of the neighboring simulated mass points ($m_a = 30$ GeV and $m_a = 35$ GeV in this case) are interpolated using a linear function. The difference between the yields obtained using the splines and a linear function for the interpolation is assigned as a systematic uncertainty on the interpolated signal yield. Using a BDT at a mass for which the training was not performed results in a negligible loss of significance relative to a BDT that was optimized for that mass point.

Table 1: Summary of the selection requirements for the control (TCR and DYCR), validation (VR1 and VR2) and inclusive signal (SRincl) regions in the analysis, as well as the final SR bins. The control and validation regions are defined in Section 5.

	TCR	DYCR	SRincl	VR1	VR2	
$m_{\mu\mu}$ [GeV]			[15, 65]			
$m_{bb\mu\mu}^{\text{KL}}$ [GeV]	[110, 140]	[80, 110] or [140, 170]	[110, 140]	[170, 300]	[110, 140]	
E_T^{miss} [GeV]	> 60		< 60			
$\ln(L^{\max})$			> -8		[-11, -8]	
SR bins	SRincl & $\text{BDT}m_a > 0.2$ 2-GeV-wide (3-GeV-wide) $m_{\mu\mu}$ bins for $m_a \leq 45$ GeV ($m_a > 45$ GeV)					

The signal acceptance \times efficiency varies between 0.3% and 2.5% for ggF Higgs boson production and between 0.2% and 3.0% for VBF production, where the lowest acceptance \times efficiency is obtained for the lowest m_a , and grows as m_a increases. The largest loss of acceptance occurs when requiring that there are two b -jets in the event, as one of the signal jets tends to fall below the reconstruction threshold of 20 GeV. The fraction of signal events passing the two- b -jet requirement is less than 20% for all mass points.

5 Background estimation

The dominant backgrounds in the analysis arise from the DY dimuon process in association with b -quarks and pair production of top quarks ($t\bar{t}$) where each W boson decays into a muon and a neutrino. These two backgrounds account for more than 96% of background events in all analysis regions.

Two control regions are designed to constrain the $t\bar{t}$ and DY backgrounds. They are chosen so that they have negligible signal contamination, are kinematically as close as possible to SRincl, and maximize the contribution of one of the respective background processes. A top-quark control region (TCR) is defined by inverting the E_T^{miss} selection criterion in SRincl to $E_T^{\text{miss}} > 60$ GeV. This results in an event sample approximately 93% pure in $t\bar{t}$ events. The DY control region (DYCR) is defined in the 30 GeV-wide $m_{bb\mu\mu}^{\text{KL}}$ sidebands of SRincl, i.e. by requiring $80 < m_{bb\mu\mu}^{\text{KL}} < 110$ GeV or $140 < m_{bb\mu\mu}^{\text{KL}} < 170$ GeV. Approximately 50% of the events in DYCR originate from the DY process, whereas the rest mostly come from $t\bar{t}$ production. Two validation regions (VR1 and VR2) are used to validate the normalizations of the backgrounds. VR1 is defined in the $170 < m_{bb\mu\mu}^{\text{KL}} < 300$ GeV range, while VR2 is obtained by inverting the $\ln(L^{\max})$ selection criterion of SRincl to $-11 < \ln(L^{\max}) < -8$. All the analysis regions are summarized in Table 1 and illustrated in Figure 3.

The shapes of the $t\bar{t}$ kinematic variable distributions are obtained from simulation, while the overall normalization is extracted from the fits described in Section 7. The distributions for the DY background are taken from data templates because the limited sizes of the simulated event samples do not allow a reliable estimate. The template regions are defined in the same way as the analysis regions in Table 1, except that the two- b -tag requirement is replaced by a zero- b -tag requirement. The template regions are >95% pure in

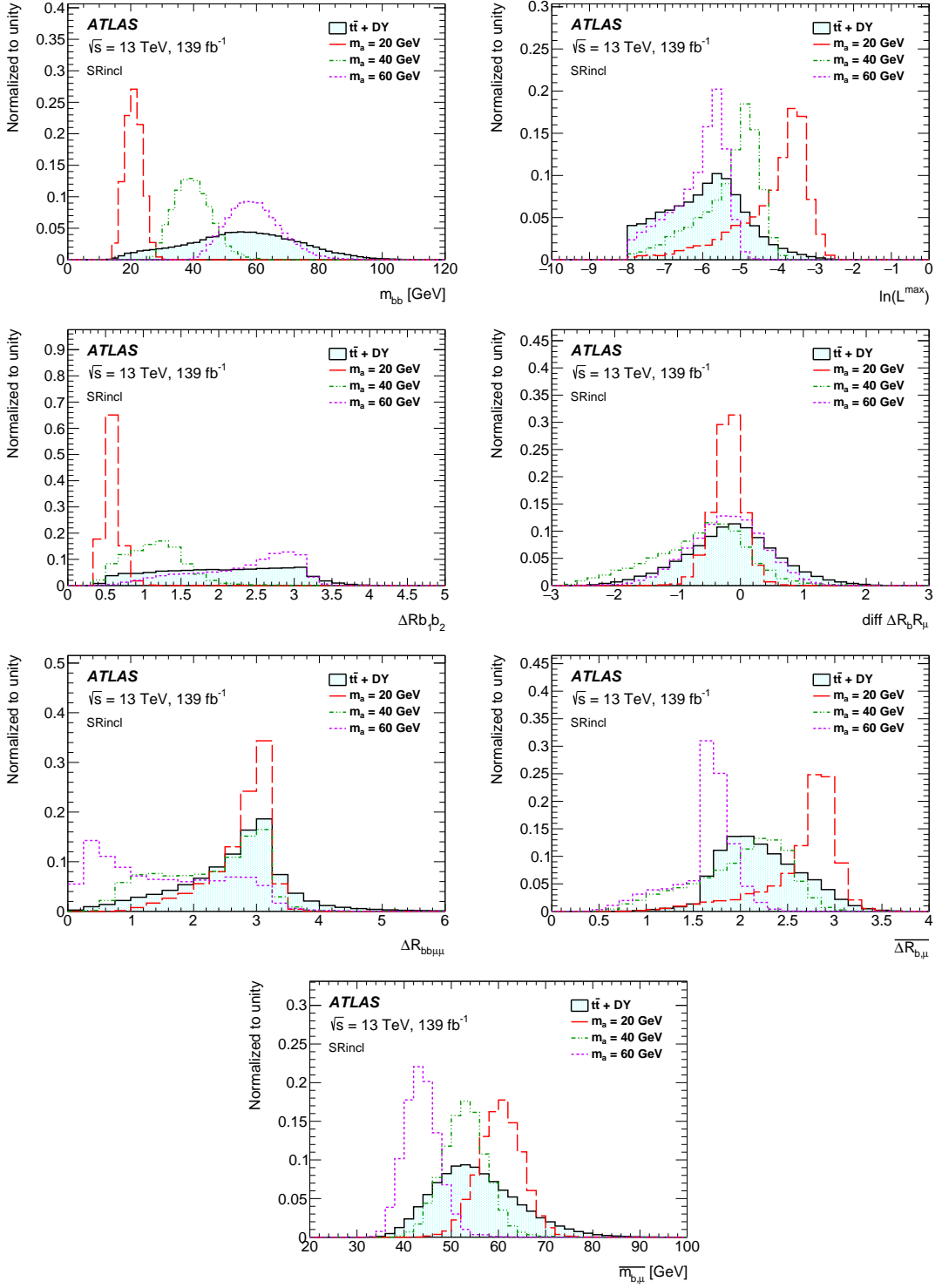


Figure 1: Kinematic variables used as inputs to the BDT training. From top left to bottom right: m_{bb} , $\ln(L^{\max})$, $\Delta R_{b_1 b_2}$, $\text{diff } \Delta R_{b R_\mu}$, $\Delta R_{bb\mu\mu}$, $\overline{\Delta R}_{b,\mu}$. The variables are plotted in SRincl. All the distributions are normalized to unit area. The background histogram is the sum of the $t\bar{t}$ and DY event templates, combined in the proportions extracted from the background validation fit described in Section 7.

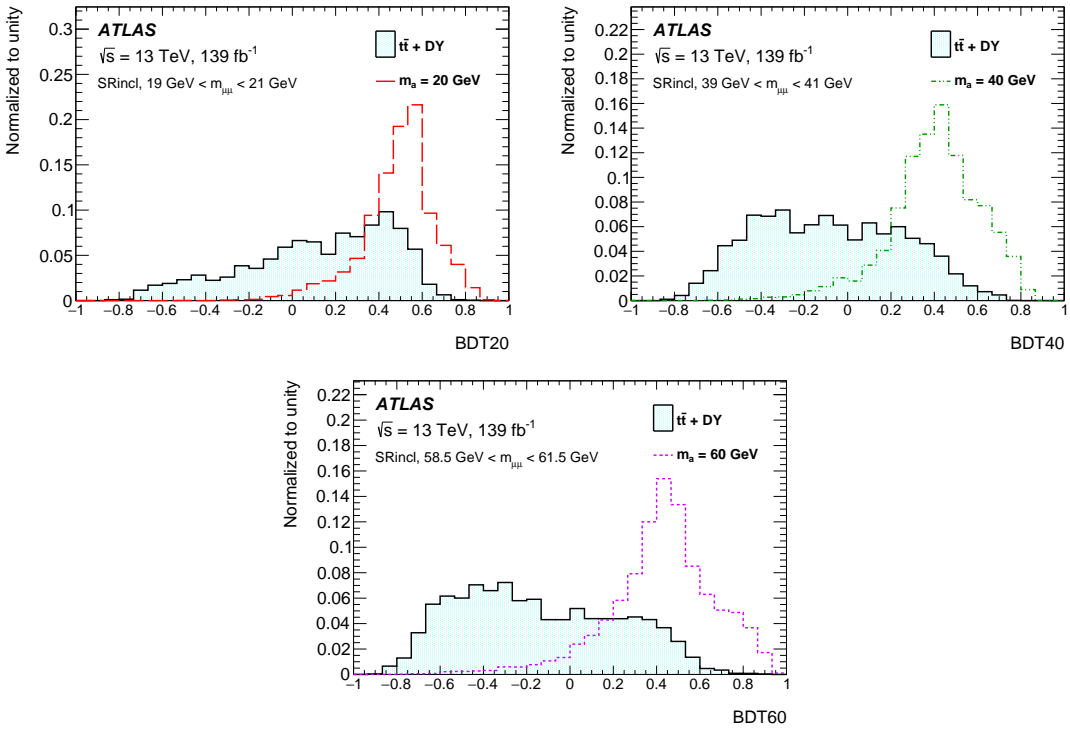


Figure 2: Three BDT m_a distributions, BDT20, BDT40, and BDT60, plotted in the $m_{\mu\mu}$ windows of SRincl, as indicated in the figures. The distributions are normalized to unit area. The background histogram is the sum of the $t\bar{t}$ and DY event templates, combined in the proportions extracted from the background validation fit described in Section 7.

DY events. Contributions from other processes, namely $t\bar{t}$, W +jets, diboson and single-top, are subtracted using simulation. Following the subtraction, the DY templates are corrected to account for kinematic differences between event samples dominated by jets originating from light quarks or gluons (template regions) and event samples dominated by b -jets (analysis regions). The correction is applied as a per-event weight, where the reweighting is derived from a comparison between two- b -tag and zero- b -tag kinematic distributions in simulated DY events. Two sets of event weights are derived and applied sequentially. First, the jet multiplicity of the zero- b -tag MC sample is reweighted to the one in the two- b -tag sample. It is the distribution with the largest difference between the zero- and two- b -tag samples and was hence corrected first. Secondly, a BDT-based reweighting is employed to further correct the zero- b -tag template kinematics. A BDT is trained on the zero- b -tag versus the two- b -tag simulated DY samples. The BDT input consists of kinematic properties and angular distributions of the b -jets, muons and the two corresponding a -boson candidates, as well as E_T^{miss} and $m_{bb\mu\mu}^{\text{KL}}$. The ratio of the BDT score distributions obtained for the two- b -tag and zero- b -tag simulated events is then applied as a weight to every event from the zero- b -tag DY template, as a function of its BDT score. Following the BDT-based reweighting, the $m_{bb\mu\mu}^{\text{KL}}$ and E_T^{miss} distributions are corrected by up to 20%. The DY templates are normalized to data in the fits described in Section 7.

Minor backgrounds include diboson and single-top-quark production, production of a $t\bar{t}$ pair in association with a vector boson, and W boson production in association with b -jets. The estimation of these minor backgrounds relies purely on simulation normalized to the best available theoretical prediction. The events where a jet is misidentified as a muon are taken into account as follows: non-prompt/misidentified muons in W +jets and $t\bar{t}$ events are included in the analysis on the basis of simulation, any contribution of

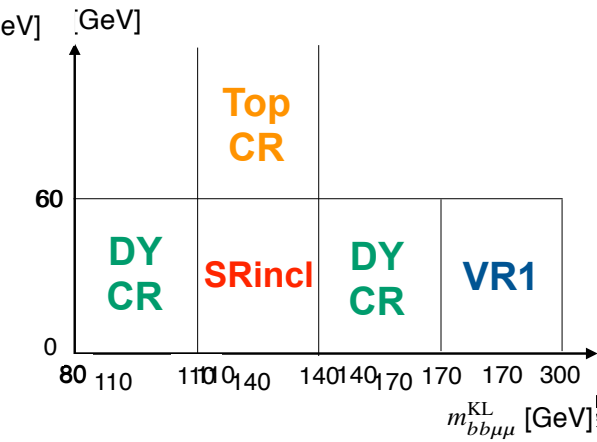


Figure 3: Illustration of the signal, control, and validation regions used in the analysis. VR2 (not shown) is defined by the same selection as SRincl, except that the requirement on $\ln(L^{\max})$ is inverted to $-11 < \ln(L^{\max}) < -8$.

non-prompt/misidentified muons in the DY+jets component is accounted for by the data template, and the potential contribution from multijet events is found to be negligible.

6 Systematic uncertainties

Systematic uncertainties in the analysis are divided into three categories: experimental uncertainties affecting the simulated background and signal processes, uncertainties in the modeling of the DY template, and theoretical uncertainties of the simulated background and signal samples. Table 2 shows a summary of the dominant systematic uncertainties in the total background and signal yields in the signal region bins, as resulting from the fits described in Section 7 and hereafter denoted by "post-fit".

Among the experimental uncertainties, the leading effects come from those associated with the calibration and resolution of jet energies [100], and with the measurement of the b -tagging efficiency [95]. The impact of these uncertainties on the total background (signal) yields in the SR bins is as large as 3% (10%). The uncertainty in the combined 2015–2018 integrated luminosity is 1.7% [101], obtained using the LUCID-2 detector [102] for the primary luminosity measurement. Other uncertainties, such as those arising from the muon identification efficiency, momentum scale and resolution [90, 103], and pileup are found to have a negligible impact on the final yields.

The uncertainty arising from limited MC sample sizes ranges from 8% to as large as 40% in the low m_a mass bins due to there being few $t\bar{t}$ events in this region.

Five sources of uncertainty in the data-driven DY template are considered. The uncertainty in subtracting non-DY events from the non-reweighted template in the analysis regions is assessed by comparing the nominal template, for which the simulated non-DY backgrounds had been subtracted before reweighting, with an alternative template for which no subtraction had been performed. The uncertainties in the template kinematics modeling are derived by comparing the DY template with simulation in two key variables: E_T^{miss} and $m_{bb\mu\mu}^{\text{KL}}$. The ratios of the template to the simulated DY events are fit with linear functions and used in assigning uncertainties to the shapes of the E_T^{miss} and $m_{bb\mu\mu}^{\text{KL}}$ distributions. Similarly, the uncertainty in the $m_{\mu\mu}$ template shape is assessed by comparing the template with the smoothed simulated sample and

Table 2: Summary of the dominant post-fit systematic uncertainties in the background and signal yields. The uncertainties are expressed as a percentage of the total background and signal yields per $m_{\mu\mu}$ bin of the signal region. Only uncertainties exceeding 2% in at least one SR bin are shown.

Category	Source	Total background [%]	Signal [%]
DY	BDT m_a selection	7–14	–
	normalization	5–10	–
	$m_{\mu\mu}$ shape	1–8	–
	kinematics	0.3–6	–
	background subtraction	0.6–3	–
$t\bar{t}$	hadronization/PS	0.3–4	–
	hard-scatter generation	0.2–3	–
	normalization	0.2–3	–
Overall MC	Sample statistics	8–40	1–2
Jets	b -tagging	0.03–0.7	9–10
	Jet-energy resolution	1–3	6–7
	Jet-energy scale	1–3	4–5
Signal	FSR	–	5
	PS	–	4
	VH contribution	–	3.5
	MPI	–	3
	QCD scale	–	3
	ISR	–	3
	ggF cross-section	–	5
	- missing higher-order QCD	–	5
	- PDF & α_S	–	3

applying the observed difference as a systematic uncertainty. The uncertainty in the normalization of the DY template is obtained from the fits to data. Finally, the uncertainty in the efficiency of the BDT m_a selection criteria is evaluated by taking the difference in the BDT m_a cut efficiency, $N_{\text{DY events SR}}^{\text{BDT}m_a>0.2} / N_{\text{DY events SR}}^{\text{no BDT}m_a \text{ cut}}$, between the template and the simulation. All one-sided DY template uncertainties are symmetrized around the nominal value.

To assess the uncertainties in the generation of the hard-scatter $t\bar{t}$ process, the PowHEG sample is compared with a sample generated using `MADGRAPH5_aMC@NLO` 2.3.3. The hadronization and fragmentation uncertainties in the PS are evaluated by comparing the nominal sample showered by `Pythia` 8.230 with an alternative sample generated by PowHEG using the same PDF in matrix element as for the nominal sample, but showered with `HERWIG` 7.0.4 [104, 105]. The initial- and final-state radiation (ISR and FSR) uncertainties of the $t\bar{t}$ sample are assessed by varying the internal `Pythia` 8.230 showering parameters. Finally, the uncertainties due to the PDF choice are evaluated using the internal variations of the nominal `PDF4LHC15_NLO_30` set [106].

Uncertainties in the calculation of the ggF and VBF Higgs boson production cross-sections are assessed by

following the recommendations of the LHC Higgs Working Group given in Refs. [77, 82]. As no VH signal sample was generated, a conservative 100% uncertainty is assigned to the estimated VH yield. To evaluate the uncertainties due to the PDF choice, the yields obtained with the baseline NNPDF30_NLO_AS_0118 set are compared with the yields obtained using the internal variations of NNPDF30_NLO_AS_0118 and with the yields obtained with the nominal MMHT2014NLO68CLAS118 [107] and CT14NLO [108] sets. The largest difference is taken as the overall PDF uncertainty for all signal mass points. Furthermore, the effects of uncertainties in the ISR, FSR, multiparton interactions (MPI) in PYTHIA, parton showering, and renormalization and factorization scales are also assessed. Uncertainties from these sources have an impact of 1–6% on the signal yields, with the largest contributions arising from the ggF production cross-section and FSR uncertainties.

7 Analysis and results

The final background and signal estimates are obtained in a set of binned likelihood fits [109] using the HistFitter [110] package. The likelihood is a product of Poisson probability functions, describing the observed and predicted numbers of events in each region, and Gaussian distributions that constrain the nuisance parameters associated with the systematic uncertainties. In the background validation fit, the data in TCR and DYCR are used to extract the normalization of the $t\bar{t}$ and DY backgrounds, respectively. As the $t\bar{t}$ sample in TCR is modeled very well, it is implemented as only one bin in the fit, whereas DYCR is divided into five equal-width bins in $m_{\mu\mu}$ to provide greater sensitivity to the DY template shape. The purpose of this fit is to validate the modeling of the background in the control and validation regions and in SRincl. The fitted $t\bar{t}$ normalization factor is $\mu_{t\bar{t}} = 1.07^{+0.06}_{-0.07}$, while the value of μ_{DY} has no physical meaning because it is scaled from a template region and is thus not quoted. Figures 4 and 5 show post-fit distributions of $m_{bb\mu\mu}^{\text{KL}}$, E_T^{miss} , $\ln(L^{\text{max}})$, and $m_{\mu\mu}$ spanning various analysis regions, while Figure 6 shows BDT20 and BDT50 in SRincl. Good agreement between the estimated backgrounds and the data is observed in the kinematic distributions. In SRincl, 1185 events are observed, which is compatible with the total estimated background of 1155.3 ± 13.6 . The yields in several representative SR bins, i.e. $m_{\mu\mu}$ windows after applying the BDT selection, as obtained from the background validation fit above, are shown in Table 3. When comparing the systematic uncertainty with the statistical uncertainty, it can be seen that the analysis is clearly statistically limited. Figure 7 shows the data and the estimated backgrounds in all final SR bins. Due to the limited statistics of the background samples, the estimates are not perfectly smooth; however, the bin-to-bin fluctuations are much smaller than the statistical uncertainty of the data. Larger jumps, which occur at $m_a = 23, 28, 33, 38$ GeV etc., appear when the BDT discriminant used for the selection changes from the one trained in the lower mass range to the one trained in the higher mass range.

To test for the presence of new phenomena, fits are performed for each of the 47 hypothesized signal masses in the range $16 \leq m_{\mu\mu} \leq 62$ GeV in 1 GeV steps. It was verified that the analysis is also sufficiently sensitive to a signal with $m_{\mu\mu}$ centered in between these 1 GeV steps. TCR, DYCR, and the respective SR bin are included in each fit in order to constrain the backgrounds and the signal to the data.

A model-independent fit, i.e. not including any signal sample, is performed to test whether the data are compatible with the background-only hypothesis. The result is a scan of p_0 -values as shown in Figure 8. The largest discrepancy is found at $m_{\mu\mu} = 52$ GeV, corresponding to a local (global) p_0 -value of 0.00054 (0.048) and a local (global) significance of 3.3σ (1.7σ). The global significance was calculated from the asymptotic formulae in Refs. [109, 111].

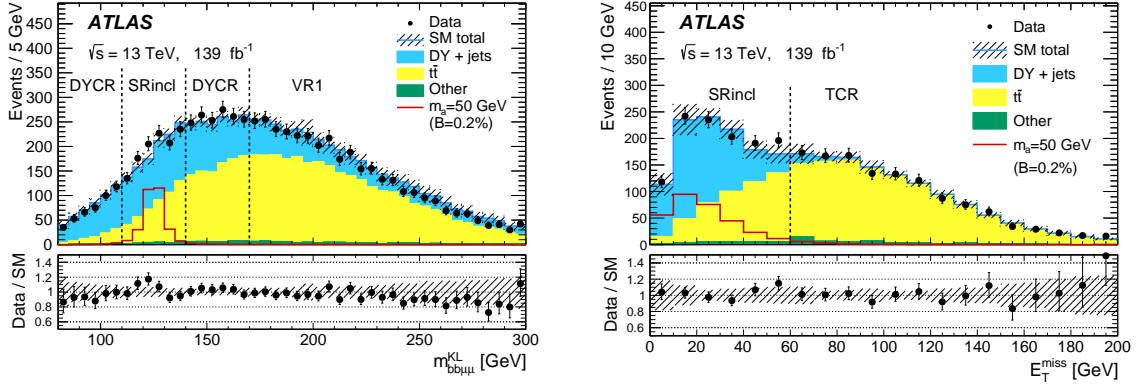


Figure 4: Post-fit $m_{bb\mu\mu}^{KL}$ in DYCR, SRincl and VR1 (left); E_T^{miss} in SRincl and TCR (right). No selection based on the BDT discriminants is applied in the analysis regions shown in the figures. The signal distributions are normalized to the SM Higgs boson cross-section (including ggF, VBF, and VH production) and assume $\mathcal{B}(H \rightarrow aa \rightarrow bb\mu\mu)$ as indicated in the legends of the figures (chosen to ensure good visibility in the plot). The hatched bands show the total post-fit statistical and systematic uncertainties of the backgrounds. The histogram labeled as “Other” in the legend includes the contributions from the diboson, single-top-quark, $t\bar{t}+V$ and $W+jets$ backgrounds.

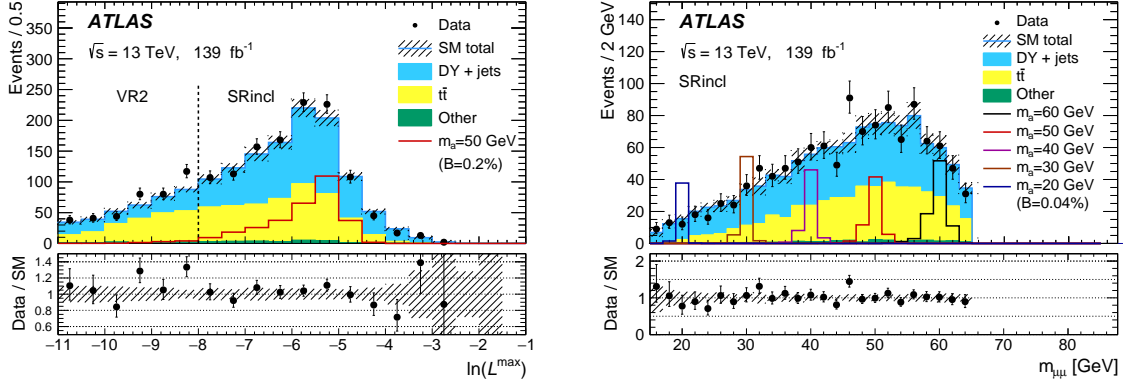


Figure 5: Post-fit $\ln(L^{\text{max}})$ in VR2 and SRincl (left); $m_{\mu\mu}$ in SRincl (right). No selection based on the BDT discriminants is applied in the analysis regions shown in the figures. The signal distributions are normalized to the SM Higgs boson cross-section (including ggF, VBF, and VH production) and assume $\mathcal{B}(H \rightarrow aa \rightarrow bb\mu\mu)$ as indicated in the legends of the figures (chosen to ensure good visibility in the plot). The hatched bands show the total post-fit statistical and systematic uncertainties of the backgrounds. The histogram labeled as “Other” in the legend includes the contributions from the diboson, single-top-quark, $t\bar{t}+V$ and $W+jets$ backgrounds.

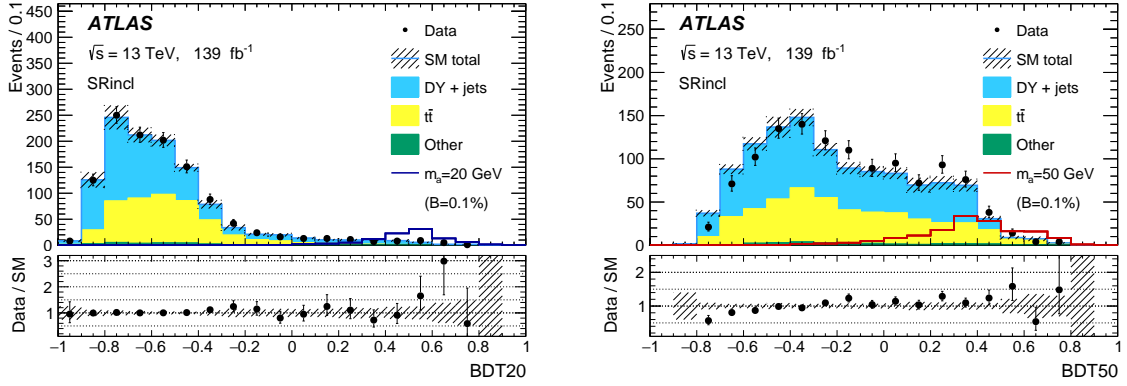


Figure 6: Post-fit BDT20 (left) and BDT50 (right) distributions in SRincl. The signal distributions are normalized to the SM Higgs boson cross-section (including ggF, VBF, and VH production) and assume $\mathcal{B}(H \rightarrow aa \rightarrow bb\mu\mu)$ as indicated in the legends of the figures (chosen to ensure good visibility in the plot). The hatched bands show the total post-fit statistical and systematic uncertainties of the backgrounds. The histogram labeled as “Other” in the legend includes the contributions from the diboson, single-top-quark, $t\bar{t}+V$ and $W+jets$ backgrounds.

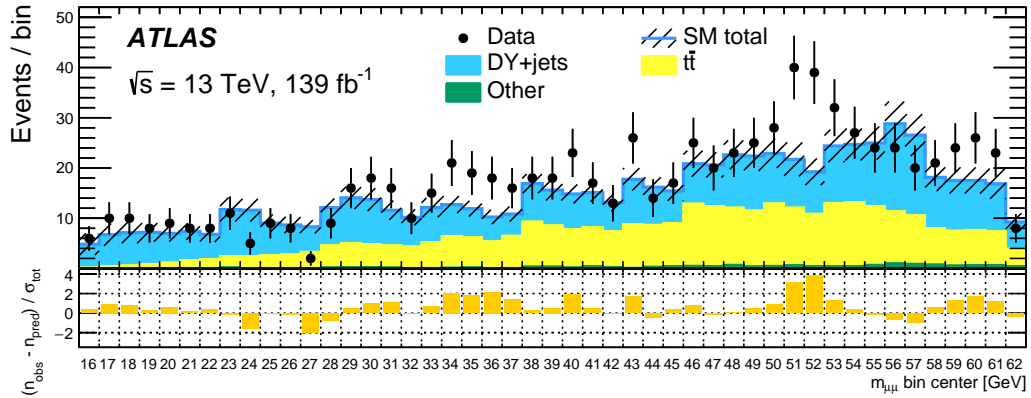


Figure 7: Post-background-validation-fit number of events in all SR bins (after applying the BDT selection) that are tested for the presence of signal. The bin widths are 2 GeV (3 GeV) in $m_{\mu\mu}$ for $m_a \leq 45$ GeV ($m_a > 45$ GeV). Neighboring bins partially overlap, hence they are not statistically independent. The bottom panel shows the pull in each bin, defined as $(n_{\text{obs}} - n_{\text{pred}})/\sigma_{\text{tot}}$, where n_{obs} is the number of events in the data, n_{pred} is the number of fitted background events and σ_{tot} is the total (systematic and statistical, added in quadrature) uncertainty in the fitted background yield. Discontinuities in the background predictions appear when the BDT discriminant used for the selection changes from the one trained in the lower mass range to the one trained in the higher mass range. The histogram labeled as “Other” in the legend includes the contributions from the diboson, single-top-quark, $t\bar{t}+V$ and $W+jets$ backgrounds.

Table 3: Total and individual background yields in six representative $m_{\mu\mu}$ bins of the signal region after the BDT selection is applied. The yields are the post-fit values as determined by the background validation fit. The uncertainties shown include all systematic and statistical uncertainties. As the diboson, single top quark, $t\bar{t}V$, and $W+jets$ contributions are very small, they are summed in the table under "Other".

$m_{\mu\mu}$ bin [GeV]	[15–17]	[24–26]	[34–36]	[44–46]	[50.5–53.5]	[60.5–63.5]
Observed events	6	9	19	17	39	8
Total background	4.8 ± 2.2	9.0 ± 1.8	11.9 ± 1.6	15.5 ± 2.0	19.3 ± 2.7	9.3 ± 1.7
DY	4.6 ± 2.1	6.4 ± 1.5	5.7 ± 1.1	6.4 ± 1.5	8.3 ± 2.1	5.3 ± 1.4
$t\bar{t}$	0.2 ± 0.1	2.6 ± 0.8	6.0 ± 1.1	8.5 ± 1.4	10.4 ± 2.4	3.5 ± 0.9
Other	0.03 ± 0.01	0.03 ± 0.00	0.24 ± 0.12	0.50 ± 0.40	0.50 ± 0.12	0.45 ± 0.19

Upper limits, derived using the CL_s technique [112, 113], are set on $\mathcal{B}(H \rightarrow aa \rightarrow bb\mu\mu)$ in a series of conditional fits, this time also including the signal samples. The limits as a function of m_a are shown in Figure 9. Uniform sensitivity is achieved for all masses above 18 GeV, while for lower signal masses, $m_a \leq 18$ GeV, the sensitivity of the analysis decreases due to b -jets falling below the reconstruction threshold or merging into one reconstructed jet. Figure 10 shows $m_{\mu\mu}$ and $BDTm_a$ distributions after the signal+background fit for two SR bins, $m_a = 35$ GeV and $m_a = 52$ GeV, where the two largest deviations from the background-only hypothesis are observed. The signal in the plots is scaled to the best-fit value, corresponding to $\mathcal{B}(H \rightarrow aa \rightarrow bb\mu\mu) = 6.4 \times 10^{-5}$ (1.9×10^{-4}) for $m_a = 35$ GeV ($m_a = 52$ GeV).

The upper limits at 95% CL on $\mathcal{B}(H \rightarrow aa \rightarrow bb\mu\mu)$ range between 0.2×10^{-4} and 4.0×10^{-4} , depending on m_a . These limits improve upon the previous ATLAS result based on 36 fb^{-1} of data [47] by a factor of 2–5 over the full $m_{\mu\mu}$ range. A factor of ~ 2 improvement in sensitivity comes from the larger dataset, and a further factor of ~ 2 is achieved thanks to the use of multivariate techniques to discriminate between the signal and the SM backgrounds. Due to small number of background events at lower signal masses m_a , the BDT training is less efficient in this region, and the gain from applying the $BDTm_a$ selection criteria is higher at higher m_a . Taking as an example the favorable scenario with $\mathcal{B}(H \rightarrow aa \rightarrow bb\mu\mu)/\mathcal{B}(H \rightarrow aa) = 0.16\%$, the analysis probes the Higgs boson branching fraction into pseudoscalars down to $\mathcal{B}(H \rightarrow aa) = 1.3\%$, much lower than the limits derived from combinations of the Higgs boson measurements.

So as not to restrict the analysis sensitivity solely to models where the a -particle is a pseudoscalar, upper limits obtained without employing the BDT discriminants are also derived as shown in Figure 11. In addition to being less sensitive to the particle's CP properties, the limits in SRincl without the BDT selection also facilitate reinterpretations of the analysis. These limits are derived in the same way as described above, i.e. by scanning the $m_{\mu\mu}$ windows of SRincl, but omitting the final selection on the BDT discriminants. The expected limits obtained when employing the baseline analysis strategy are also shown in Figure 11 for comparison, illustrating the significant improvement in sensitivity to pseudoscalars when using the BDTs. The excess observed at $m_{\mu\mu} = 52$ GeV in the BDT analysis is not supported by the limits derived without the BDTs. Figure 12 shows the data and the estimated backgrounds in all final SR bins, without applying the BDT selection.

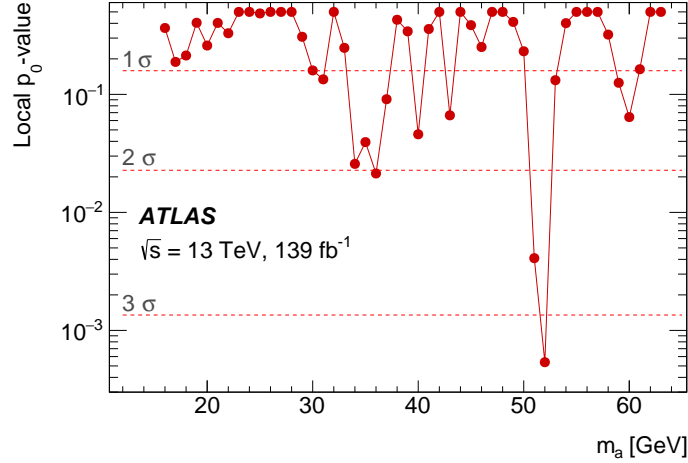


Figure 8: The local p_0 -values are quantified in standard deviations σ and plotted as a function of the signal mass hypothesis. Between the points, the p_0 -values are interpolated and may not be fully representative of the actual sensitivity.

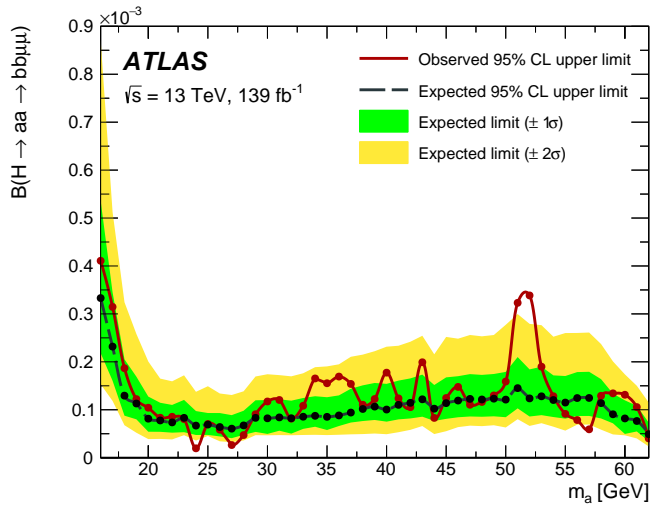


Figure 9: Upper limits on $\mathcal{B}(H \rightarrow aa \rightarrow bb\mu\mu)$ at 95% CL, including the BDT selection, as a function of the signal mass hypothesis. Black and red dots show masses for which the hypothesis testing was done. Between these points, the limits are interpolated and may not be fully representative of the actual sensitivity.

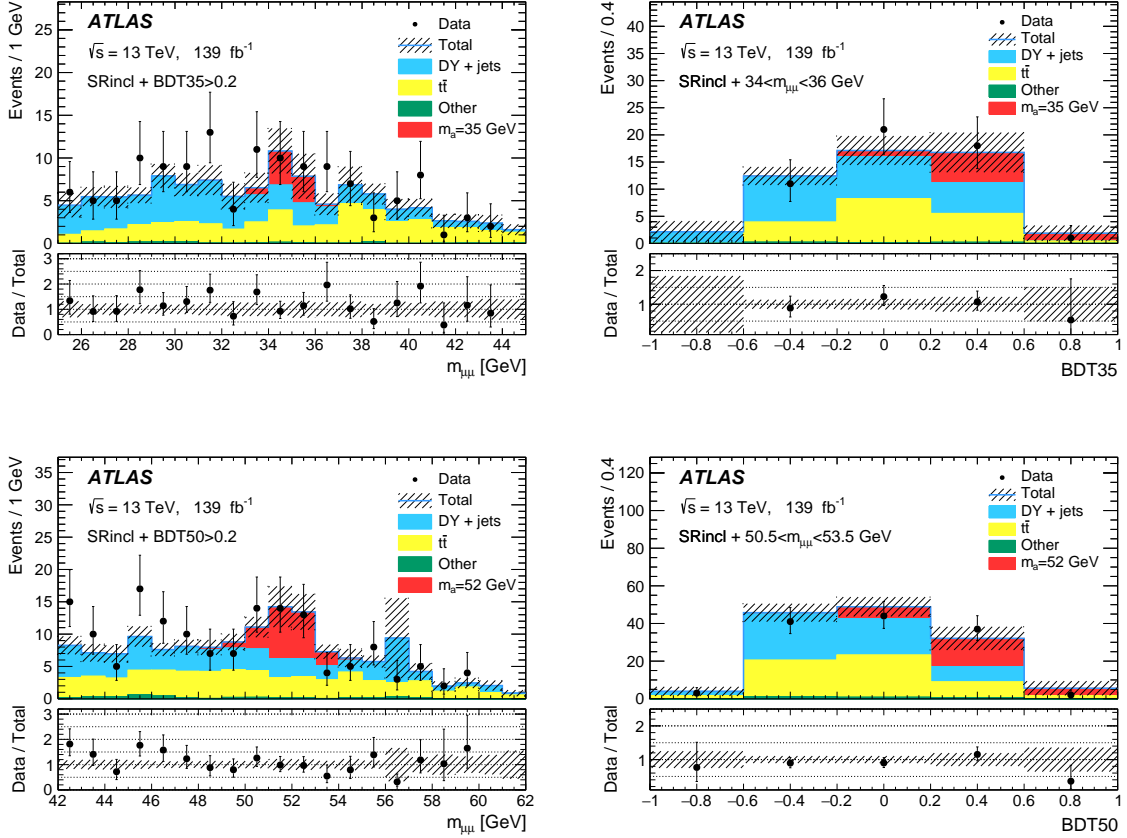


Figure 10: $m_{\mu\mu}$ distributions in the SRincl after the $\text{BDT35} > 0.2$ selection (top left) and $\text{BDT50} > 0.2$ selection (bottom left), and BDT35 (top right) and BDT50 (bottom right) distributions in the SRincl in the $m_{\mu\mu}$ window 34 – 36 GeV and 50.5 – 53.5 GeV, respectively. The signal is scaled to the best-fit value, $\mathcal{B}(H \rightarrow aa \rightarrow bb\mu\mu) = 6.4 \times 10^{-5}$ for the top plots, and 1.9×10^{-4} for the bottom plots, assuming the SM Higgs boson cross-section (including ggF, VBF, and VH production). The hatched bands show the total post-fit statistical and systematic uncertainties of the backgrounds and the signal. The histogram labeled as “Other” in the legend includes the contributions from the diboson, single-top-quark, $t\bar{t}+V$ and $W+V$ backgrounds.

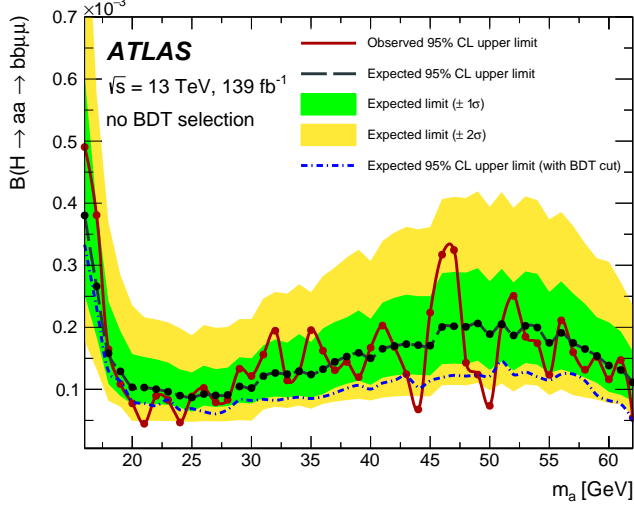


Figure 11: Upper limits on $\mathcal{B}(H \rightarrow aa \rightarrow bb\mu\mu)$ at 95% CL, with no BDT selection applied, as a function of the signal mass hypothesis. The dash-dotted blue line indicates the expected limit set in the analysis with the BDT selection. Black and red dots show masses for which the hypothesis testing was done. Between these points, the limits are interpolated and may not be fully representative of the actual sensitivity.

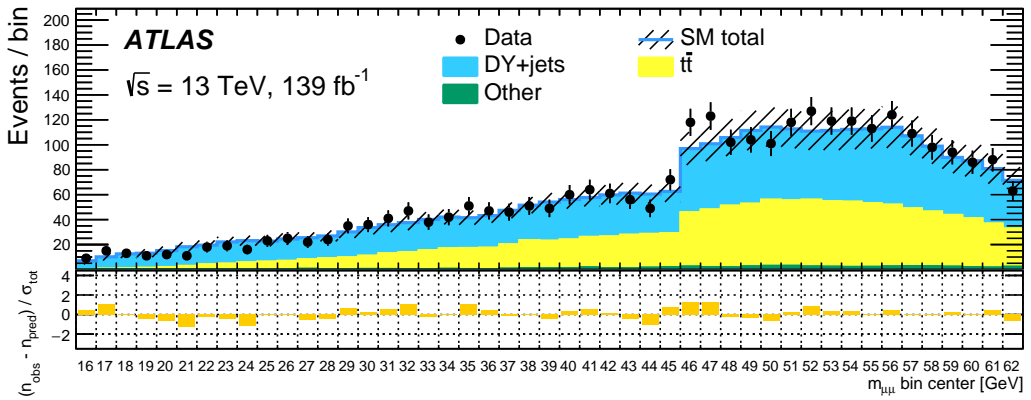


Figure 12: Post-background-validation-fit number of events in all SR bins (without applying the BDT selection) that are tested for the presence of signal. The bin widths are 2 GeV (3 GeV) in $m_{\mu\mu}$ for $m_a \leq 45$ GeV ($m_a > 45$ GeV). Neighboring bins partially overlap, hence they are not statistically independent. The bottom panel shows the pull in each bin, defined as $(n_{\text{obs}} - n_{\text{pred}})/\sigma_{\text{tot}}$, where n_{obs} is the number of events in the data, n_{pred} is the number of fitted background events and σ_{tot} is the total (systematic and statistical, added in quadrature) uncertainty in the fitted background yield. The discontinuity at $m_a = 45$ GeV appears where the $m_{\mu\mu}$ window size is changed. The histogram labeled as ‘‘Other’’ in the legend includes the contributions from the diboson, single-top-quark, $t\bar{t}+V$ and $W+jets$ backgrounds.

8 Conclusion

A search for light pseudoscalar particles (denoted by a) in the decays of the 125 GeV Higgs boson in the final state with two muons and two b -tagged jets, $H \rightarrow aa \rightarrow bb\mu\mu$, is presented. The analysis is performed using 139 fb^{-1} of $\sqrt{s} = 13$ TeV pp collision data recorded by the ATLAS detector at the LHC between 2015 and 2018. A narrow resonance is searched for in the dimuon invariant mass spectrum in the range $16 \leq m_{\mu\mu} \leq 62$ GeV. BDT classifiers are trained to distinguish the $H \rightarrow aa$ signal, where a is a pseudoscalar, from the SM backgrounds. Additionally, the result without selection on the BDT discriminants is also provided to ensure sensitivity to models where the a -particle is not necessarily a pseudoscalar, as well as to facilitate reinterpretations of the analysis. No significant excess of the data above the SM backgrounds is observed. In the BDT analysis, the lowest local p_0 -value of 0.00054 is observed at $m_{\mu\mu} = 52$ GeV and corresponds to a local significance of 3.3σ . The global significance of that excess is determined to be 1.7σ . Upper limits at 95% CL including (excluding) the BDT selection criteria are set on $\mathcal{B}(H \rightarrow aa \rightarrow bb\mu\mu)$ and range between 0.2×10^{-4} and 4.0×10^{-4} (0.5×10^{-4} and 5.0×10^{-4}), depending on m_a . The result including the BDT selection criteria improves upon previous ATLAS and CMS limits by about a factor of 2–5 for $m_a > 20$ GeV, while both results (with and without the BDT) extend the search down to m_a values of 16 GeV.

Acknowledgments

We thank CERN for the very successful operation of the LHC, as well as the support staff from our institutions without whom ATLAS could not be operated efficiently.

We acknowledge the support of ANPCyT, Argentina; YerPhI, Armenia; ARC, Australia; BMWFW and FWF, Austria; ANAS, Azerbaijan; SSTC, Belarus; CNPq and FAPESP, Brazil; NSERC, NRC and CFI, Canada; CERN; ANID, Chile; CAS, MOST and NSFC, China; Minciencias, Colombia; MSMT CR, MPO CR and VSC CR, Czech Republic; DNRF and DNSRC, Denmark; IN2P3-CNRS and CEA-DRF/IRFU, France; SRNSFG, Georgia; BMBF, HGF and MPG, Germany; GSRI, Greece; RGC and Hong Kong SAR, China; ISF and Benoziyo Center, Israel; INFN, Italy; MEXT and JSPS, Japan; CNRST, Morocco; NWO, Netherlands; RCN, Norway; MEiN, Poland; FCT, Portugal; MNE/IFA, Romania; JINR; MES of Russia and NRC KI, Russian Federation; MESTD, Serbia; MSSR, Slovakia; ARRS and MIZŠ, Slovenia; DS/ NRF, South Africa; MICINN, Spain; SRC and Wallenberg Foundation, Sweden; SERI, SNSF and Cantons of Bern and Geneva, Switzerland; MOST, Taiwan; TAEK, Turkey; STFC, United Kingdom; DOE and NSF, United States of America. In addition, individual groups and members have received support from BCKDF, CANARIE, Compute Canada and CRC, Canada; COST, ERC, ERDF, Horizon 2020 and Marie Skłodowska-Curie Actions, European Union; Investissements d’Avenir Labex, Investissements d’Avenir Idex and ANR, France; DFG and AvH Foundation, Germany; Herakleitos, Thales and Aristeia programmes co-financed by EU-ESF and the Greek NSRF, Greece; BSF-NSF and GIF, Israel; Norwegian Financial Mechanism 2014-2021, Norway; NCN and NAWA, Poland; La Caixa Banking Foundation, CERCA Programme Generalitat de Catalunya and PROMETEO and GenT Programmes Generalitat Valenciana, Spain; Göran Gustafssons Stiftelse, Sweden; The Royal Society and Leverhulme Trust, United Kingdom.

The crucial computing support from all WLCG partners is acknowledged gratefully, in particular from CERN, the ATLAS Tier-1 facilities at TRIUMF (Canada), NDGF (Denmark, Norway, Sweden), CC-IN2P3 (France), KIT/GridKA (Germany), INFN-CNAF (Italy), NL-T1 (Netherlands), PIC (Spain), ASGC

(Taiwan), RAL (UK) and BNL (USA), the Tier-2 facilities worldwide and large non-WLCG resource providers. Major contributors of computing resources are listed in Ref. [114].

References

- [1] ATLAS Collaboration, *Observation of a new particle in the search for the Standard Model Higgs boson with the ATLAS detector at the LHC*, *Phys. Lett. B* **716** (2012) 1, arXiv: [1207.7214 \[hep-ex\]](#).
- [2] CMS Collaboration, *Observation of a new boson at a mass of 125 GeV with the CMS experiment at the LHC*, *Phys. Lett. B* **716** (2012) 30, arXiv: [1207.7235 \[hep-ex\]](#).
- [3] B. A. Dobrescu and K. T. Matchev, *Light axion within the next-to-minimal supersymmetric standard model*, *JHEP* **09** (2000) 031, arXiv: [hep-ph/0008192 \[hep-ph\]](#).
- [4] U. Ellwanger, J. F. Gunion, C. Hugonie and S. Moretti, *Towards a No-Lose Theorem for NMSSM Higgs Discovery at the LHC*, (2003), arXiv: [hep-ph/0305109](#).
- [5] R. Dermisek and J. F. Gunion, *Escaping the Large Fine Tuning and Little Hierarchy Problems in the Next to Minimal Supersymmetric Model and $h \rightarrow aa$ decays*, *Phys. Rev. Lett.* **95** (2005) 041801, arXiv: [hep-ph/0502105](#).
- [6] S. Chang, R. Dermisek, J. F. Gunion and N. Weiner, *Nonstandard Higgs Boson Decays*, *Ann. Rev. Nucl. Part. Sci.* **58** (2008) 75, arXiv: [0801.4554 \[hep-ph\]](#).
- [7] D. E. Morrissey and A. Pierce, *Modified Higgs boson phenomenology from gauge or gaugino mediation in the next-to-minimal supersymmetric standard model*, *Phys. Rev. D* **78** (2008) 075029, arXiv: [0807.2259 \[hep-ph\]](#).
- [8] G. Belanger, B. Dumont, U. Ellwanger, J. F. Gunion and S. Kraml, *Status of invisible Higgs decays*, *Phys. Lett. B* **723** (2013) 340, arXiv: [1302.5694 \[hep-ph\]](#).
- [9] S. Profumo, M. J. Ramsey-Musolf and G. Shaughnessy, *Singlet Higgs phenomenology and the electroweak phase transition*, *JHEP* **08** (2007) 010, arXiv: [0705.2425 \[hep-ph\]](#).
- [10] N. Blinov, J. Kozaczuk, D. E. Morrissey and C. Tamarit, *Electroweak Baryogenesis from Exotic Electroweak Symmetry Breaking*, *Phys. Rev. D* **92** (2015) 035012, arXiv: [1504.05195 \[hep-ph\]](#).
- [11] N. Craig, A. Katz, M. Strassler and R. Sundrum, *Naturalness in the Dark at the LHC*, *JHEP* **07** (2015) 105, arXiv: [1501.05310 \[hep-ph\]](#).
- [12] D. Curtin and C. B. Verhaaren, *Discovering Uncolored Naturalness in Exotic Higgs Decays*, *JHEP* **12** (2015) 072, arXiv: [1506.06141 \[hep-ph\]](#).
- [13] V. Silveira and A. Zee, *Scalar Phantoms*, *Phys. Lett. B* **161** (1985) 136.
- [14] M. Pospelov, A. Ritz and M. B. Voloshin, *Secluded WIMP Dark Matter*, *Phys. Lett. B* **662** (2008) 53, arXiv: [0711.4866 \[hep-ph\]](#).
- [15] P. Draper, T. Liu, C. E. M. Wagner, L.-T. Wang and H. Zhang, *Dark Light-Higgs Bosons*, *Phys. Rev. Lett.* **106** (2011) 121805, arXiv: [1009.3963 \[hep-ph\]](#).
- [16] S. Ipek, D. McKeen and A. E. Nelson, *Renormalizable model for the Galactic Center gamma-ray excess from dark matter annihilation*, *Phys. Rev. D* **90** (2014) 055021, arXiv: [1404.3716 \[hep-ph\]](#).
- [17] A. Martin, J. Shelton and J. Unwin, *Fitting the Galactic Center Gamma-Ray Excess with Cascade Annihilations*, *Phys. Rev. D* **90** (2014) 103513, arXiv: [1405.0272 \[hep-ph\]](#).
- [18] C. Boehm, M. J. Dolan, C. McCabe, M. Spannowsky and C. J. Wallace, *Extended gamma-ray emission from Coy Dark Matter*, *JCAP* **1405** (2014) 009, arXiv: [1401.6458 \[hep-ph\]](#).

- [19] K. C. Yang, *Hidden Higgs portal vector dark matter for the Galactic center gamma-ray excess from the two-step cascade annihilation, and muon g – 2*, JHEP **08** (2018) 99, arXiv: [1806.05663 \[hep-ph\]](#).
- [20] D. Curtin et al., *Exotic decays of the 125 GeV Higgs boson*, Phys. Rev. D **90** (2014) 075004, arXiv: [1312.4992 \[hep-ph\]](#).
- [21] T. Robens and T. Stefaniak, *Status of the Higgs singlet extension of the standard model after LHC run 1*, Eur. Phys. J. C **75** (2015) 104, arXiv: [1501.02234 \[hep-ph\]](#).
- [22] T. Robens and T. Stefaniak, *LHC benchmark scenarios for the real Higgs singlet extension of the standard model*, Eur. Phys. J. C **76** (2016) 268, arXiv: [1601.07880 \[hep-ph\]](#).
- [23] T. S. Robens and J. T. Wittbrodt, *Two-real-scalar-singlet extension of the SM: LHC phenomenology and benchmark scenarios*, Eur. Phys. J. C **80** (2020) 151, arXiv: [1908.08554 \[hep-ph\]](#).
- [24] M. Bauer, M. Neubert, and A. Thamm, *Collider Probes of Axion-Like Particles*, JHEP **12** (2017) 044, arXiv: [1708.00443 \[hep-ph\]](#).
- [25] J. Liu, C. E. M. Wagner and X.-P. Wang, *A light complex scalar for the electron and muon anomalous magnetic moments*, Journal of High Energy Physics **2019** (2019), ISSN: 1029-8479, URL: [http://dx.doi.org/10.1007/JHEP03\(2019\)008](http://dx.doi.org/10.1007/JHEP03(2019)008).
- [26] B. Abi et al. [Muon g-2], *Measurement of the Positive Muon Anomalous Magnetic Moment to 0.46 ppm*, Phys. Rev. Lett. **126** (2021) 141801, arXiv: [2104.03281 \[hep-ex\]](#).
- [27] ATLAS Collaboration, *Combined measurements of Higgs boson production and decay using up to 80 fb^{-1} of proton–proton collision data at $\sqrt{s} = 13\text{ TeV}$ collected with the ATLAS experiment*, Phys. Rev. D **101** (2020) 012002, arXiv: [1909.02845 \[hep-ex\]](#).
- [28] CMS Collaboration, *Combined measurements of Higgs boson couplings in proton–proton collisions at $\sqrt{s} = 13\text{ TeV}$* , Eur. Phys. J. C **79** (2019) 421, arXiv: [1809.10733 \[hep-ex\]](#).
- [29] L. Evans and P. Bryant, *LHC Machine*, JINST **3** (2008) S08001.
- [30] G. Branco et al., *Theory and phenomenology of two-Higgs-doublet models*, Phys. Rept. **516** (2012) 1, arXiv: [1106.0034 \[hep-ph\]](#).
- [31] D. Curtin, R. Essig and Y. M. Zhong, *Uncovering light scalars with exotic Higgs decays to $b\bar{b}\mu^+\mu^-$* , JHEP **06** (2015) 025, arXiv: [1412.4779 \[hep-ph\]](#).
- [32] CMS Collaboration, *A search for pair production of new light bosons decaying into muons in proton–proton collisions at 13 TeV*, Phys. Lett. B **796** (2019) 131, arXiv: [1812.00380 \[hep-ex\]](#).
- [33] ATLAS Collaboration, *Search for Higgs boson decays to beyond-the-Standard-Model light bosons in four-lepton events with the ATLAS detector at $\sqrt{s} = 13\text{ TeV}$* , JHEP **06** (2018) 166, arXiv: [1802.03388 \[hep-ex\]](#).
- [34] CMS Collaboration, *Search for a light pseudoscalar Higgs boson in the boosted $\mu\mu\tau\tau$ final state in proton–proton collisions at $\sqrt{s} = 13\text{ TeV}$* , JHEP **08** (2020) 139, arXiv: [2005.08694 \[hep-ex\]](#).
- [35] CMS Collaboration, *Search for light pseudoscalar boson pairs produced from decays of the 125 GeV Higgs boson in final states with two muons and two nearby tracks in pp collisions at $\sqrt{s} = 13\text{ TeV}$* , Phys. Lett. B **800** (2020) 135087, arXiv: [1907.07235 \[hep-ex\]](#).
- [36] CMS Collaboration, *Search for an exotic decay of the Higgs boson to a pair of light pseudoscalars in the final state of two muons and two τ leptons in proton–proton collisions at $\sqrt{s} = 13\text{ TeV}$* , JHEP **11** (2018) 018, arXiv: [1805.04865 \[hep-ex\]](#).

- [37] CMS Collaboration, *Search for light bosons in decays of the 125 GeV Higgs boson in proton–proton collisions at $\sqrt{s} = 8$ TeV*, *JHEP* **10** (2017) 076, arXiv: [1701.02032 \[hep-ex\]](#).
- [38] ATLAS Collaboration, *Search for Higgs bosons decaying to aa in the $\mu\mu\tau\tau$ final state in pp collisions at $\sqrt{s} = 8$ TeV with the ATLAS experiment*, *Phys. Rev. D* **92** (2015) 052002, arXiv: [1505.01609 \[hep-ex\]](#).
- [39] CMS Collaboration, *Search for an exotic decay of the Higgs boson to a pair of light pseudoscalars in the final state with two b quarks and two τ leptons in proton–proton collisions at $\sqrt{s} = 13$ TeV*, *Phys. Lett. B* **785** (2018) 462, arXiv: [1805.10191 \[hep-ex\]](#).
- [40] ATLAS Collaboration, *Search for the Higgs boson produced in association with a vector boson and decaying into two spin-zero particles in the $H \rightarrow aa \rightarrow 4b$ channel in pp collisions at $\sqrt{s} = 13$ TeV with the ATLAS detector*, *JHEP* **10** (2018) 031, arXiv: [1806.07355 \[hep-ex\]](#).
- [41] ATLAS Collaboration, *Search for Higgs boson decays into two new low-mass spin-0 particles in the $4b$ channel with the ATLAS detector using pp collisions at $\sqrt{s} = 13$ TeV*, *Phys. Rev. D* **102** (2020) 112006, arXiv: [2005.12236 \[hep-ex\]](#).
- [42] ATLAS Collaboration, *Search for new phenomena in events with at least three photons collected in pp collisions at $\sqrt{s} = 8$ TeV with the ATLAS detector*, *Eur. Phys. J. C* **76** (2016) 210, arXiv: [1509.05051 \[hep-ex\]](#).
- [43] ATLAS Collaboration, *Search for Higgs boson decays into pairs of light (pseudo)scalar particles in the $\gamma\gamma jj$ final state in pp collisions at $\sqrt{s} = 13$ TeV with the ATLAS detector*, *Phys. Lett. B* **782** (2018) 750, arXiv: [1803.11145 \[hep-ex\]](#).
- [44] A. M. Sirunyan et al., *Search for resonances in the mass spectrum of muon pairs produced in association with b quark jets in proton-proton collisions at $\sqrt{s} = 8$ and 13 TeV*, *JHEP* **11** (2018) 161, arXiv: [1808.01890 \[hep-ex\]](#).
- [45] R. Aaij et al., *Searches for low-mass dimuon resonances*, *JHEP* **10** (2020) 156, arXiv: [2007.03923 \[hep-ex\]](#).
- [46] CMS Collaboration, *Search for an exotic decay of the Higgs boson to a pair of light pseudoscalars in the final state with two muons and two b quarks in pp collisions at 13 TeV*, *Phys. Lett. B* **795** (2019) 398, arXiv: [1812.06359 \[hep-ex\]](#).
- [47] ATLAS Collaboration, *Search for Higgs boson decays into a pair of light bosons in the $bb\mu\mu$ final state in pp collision at $\sqrt{s} = 13$ TeV with the ATLAS detector*, *Phys. Lett. B* **790** (2019) 1.
- [48] ATLAS Collaboration, *The ATLAS Experiment at the CERN Large Hadron Collider*, *JINST* **3** (2008) S08003.
- [49] B. Abbott et al., *Production and integration of the ATLAS Insertable B-Layer*, *JINST* **13** (2018) T05008, arXiv: [1803.00844 \[physics.ins-det\]](#).
- [50] ATLAS Collaboration, *Performance of the ATLAS trigger system in 2015*, *Eur. Phys. J. C* **77** (2017) 317, arXiv: [1611.09661 \[hep-ex\]](#).
- [51] ATLAS Collaboration, *ATLAS Computing Acknowledgements*, ATL-SOFT-PUB-2020-001, URL: <https://cds.cern.ch/record/2717821>.
- [52] ATLAS Collaboration, *Performance of the ATLAS muon triggers in Run 2*, *JINST* **15** (2020) P09015, arXiv: [2004.13447 \[hep-ex\]](#).
- [53] T. Gleisberg et al., *Event generation with SHERPA 1.1*, *JHEP* **02** (2009) 007, arXiv: [0811.4622 \[hep-ph\]](#).

- [54] E. Bothmann et al., *Event generation with Sherpa 2.2*, *SciPost Phys.* **7** (2019) 034, arXiv: [1905.09127 \[hep-ph\]](#).
- [55] S. Schumann and F. Krauss, *A parton shower algorithm based on Catani–Seymour dipole factorisation*, *JHEP* **03** (2008) 038, arXiv: [0709.1027 \[hep-ph\]](#).
- [56] S. Höche, F. Krauss, M. Schönher and F. Siegert, *A critical appraisal of NLO+PS matching methods*, *JHEP* **09** (2012) 049, arXiv: [1111.1220 \[hep-ph\]](#).
- [57] S. Höche, F. Krauss, M. Schönher and F. Siegert, *QCD matrix elements + parton showers. The NLO case*, *JHEP* **04** (2013) 027, arXiv: [1207.5030 \[hep-ph\]](#).
- [58] S. Catani, F. Krauss, R. Kuhn and B. R. Webber, *QCD Matrix Elements + Parton Showers*, *JHEP* **11** (2001) 063, arXiv: [hep-ph/0109231](#).
- [59] S. Höche, F. Krauss, S. Schumann and F. Siegert, *QCD matrix elements and truncated showers*, *JHEP* **05** (2009) 053, arXiv: [0903.1219 \[hep-ph\]](#).
- [60] R. D. Ball et al., *Parton distributions for the LHC run II*, *JHEP* **04** (2015) 040, arXiv: [1410.8849 \[hep-ph\]](#).
- [61] S. Frixione, P. Nason and C. Oleari, *Matching NLO QCD computations with parton shower simulations: the POWHEG method*, *JHEP* **11** (2007) 070, arXiv: [0709.2092 \[hep-ph\]](#).
- [62] P. Nason, *A new method for combining NLO QCD with shower Monte Carlo algorithms*, *JHEP* **11** (2004) 040, arXiv: [hep-ph/0409146](#).
- [63] S. Alioli, P. Nason, C. Oleari and E. Re, *A general framework for implementing NLO calculations in shower Monte Carlo programs: the POWHEG BOX*, *JHEP* **06** (2010) 043, arXiv: [1002.2581 \[hep-ph\]](#).
- [64] S. Frixione, P. Nason and G. Ridolfi, *A positive-weight next-to-leading-order Monte Carlo for heavy flavour hadroproduction*, *JHEP* **09** (2007) 126, arXiv: [0707.3088 \[hep-ph\]](#).
- [65] E. Re, *Single-top Wt-channel production matched with parton showers using the POWHEG method*, *Eur. Phys. J. C* **71** (2011) 1547, arXiv: [1009.2450 \[hep-ph\]](#).
- [66] T. Sjöstrand et al., *An introduction to PYTHIA 8.2*, *Comput. Phys. Commun.* **191** (2015) 159, arXiv: [1410.3012 \[hep-ph\]](#).
- [67] ATLAS Collaboration, *ATLAS Pythia8 tunes to 7 TeV data*, ATL-PHYS-PUB-2014-021, 2014, URL: <https://cds.cern.ch/record/1966419/>.
- [68] R. D. Ball et al., *Parton distributions with LHC data*, *Nucl. Phys. B* **867** (2013) 244, arXiv: [1207.1303 \[hep-ph\]](#).
- [69] J. Alwall et al., *The automated computation of tree-level and next-to-leading order differential cross sections, and their matching to parton shower simulations*, *JHEP* **07** (2014) 079, arXiv: [1405.0301 \[hep-ph\]](#).
- [70] D. J. Lange, *The EvtGen particle decay simulation package*, *Nucl. Instrum. Meth. A* **462** (2001) 152.
- [71] K. Hamilton, P. Nason and G. Zanderighi, *MINLO: Multi-Scale Improved NLO*, *JHEP* **10** (2012) 155, arXiv: [1206.3572 \[hep-ph\]](#).
- [72] K. Hamilton, P. Nason and G. Zanderighi, *Finite quark-mass effects in the NNLOPS POWHEG+MiNLO Higgs generator*, *JHEP* **05** (2015) 140, arXiv: [1501.04637 \[hep-ph\]](#).
- [73] J. M. Campbell et al., *NLO Higgs Boson Production Plus One and Two Jets Using the POWHEG BOX, MadGraph4 and MCFM*, *JHEP* **07** (2012) 092, arXiv: [1202.5475 \[hep-ph\]](#).

- [74] K. Hamilton, P. Nason, C. Oleari and G. Zanderighi, *Merging H/W/Z + 0 and 1 jet at NLO with no merging scale: a path to parton shower + NNLO matching*, JHEP **05** (2013) 082, arXiv: [1212.4504 \[hep-ph\]](#).
- [75] P. Nason and C. Oleari, *NLO Higgs boson production via vector-boson fusion matched with shower in POWHEG*, JHEP **02** (2010) 037, arXiv: [0911.5299 \[hep-ph\]](#).
- [76] ATLAS Collaboration, *Measurement of the Z/γ^* boson transverse momentum distribution in pp collisions at $\sqrt{s} = 7$ TeV with the ATLAS detector*, JHEP **09** (2014) 145, arXiv: [1406.3660 \[hep-ex\]](#).
- [77] D. de Florian et al., *Handbook of LHC Higgs Cross Sections: 4. Deciphering the Nature of the Higgs Sector*, (2016), arXiv: [1610.07922 \[hep-ph\]](#).
- [78] C. Anastasiou, C. Duhr, F. Dulat, F. Herzog and B. Mistlberger, *Higgs Boson Gluon-Fusion Production in QCD at Three Loops*, Phys. Rev. Lett. **114** (2015) 212001, arXiv: [1503.06056 \[hep-ph\]](#).
- [79] C. Anastasiou et al., *High precision determination of the gluon fusion Higgs boson cross-section at the LHC*, JHEP **05** (2016) 058, arXiv: [1602.00695 \[hep-ph\]](#).
- [80] S. Actis, G. Passarino, C. Sturm and S. Uccirati, *NLO Electroweak Corrections to Higgs Boson Production at Hadron Colliders*, Phys. Lett. B **670** (2008) 12, arXiv: [0809.1301 \[hep-ph\]](#).
- [81] C. Anastasiou, R. Boughezal and F. Petriello, *Mixed QCD-electroweak corrections to Higgs boson production in gluon fusion*, JHEP **04** (2009) 003, arXiv: [0811.3458 \[hep-ph\]](#).
- [82] J. R. Andersen et al., *Handbook of LHC Higgs Cross Sections: 3. Higgs Properties*, (2013), ed. by S. Heinemeyer, C. Mariotti, G. Passarino and R. Tanaka, arXiv: [1307.1347 \[hep-ph\]](#).
- [83] M. Ciccolini, A. Denner, and S. Dittmaier, *Strong and Electroweak Corrections to the Production of a Higgs Boson + 2Jets via Weak Interactions at the Large Hadron Collider*, Phys. Rev. Lett. **99** (2007) 161803, arXiv: [0707.0381 \[hep-ph\]](#).
- [84] M. Ciccolini, A. Denner, and S. Dittmaier, *Electroweak and QCD corrections to Higgs production via vector-boson fusion at the CERN LHC*, Phys. Rev. D **77** (2008) 013002, arXiv: [0710.4749 \[hep-ph\]](#).
- [85] P. Bolzoni, F. Maltoni, S.-O. Moch and M. Zaro, *Higgs Boson Production via Vector-Boson Fusion at Next-to-Next-to-Leading Order in QCD*, Phys. Rev. Lett. **105** (2010) 011801, arXiv: [1003.4451 \[hep-ph\]](#).
- [86] ATLAS Collaboration, *Jet reconstruction and performance using particle flow with the ATLAS Detector*, Eur. Phys. J. C **77** (2017) 466, arXiv: [1703.10485 \[hep-ex\]](#).
- [87] T. Sjöstrand, S. Mrenna and P. Skands, *A brief introduction to PYTHIA 8.1*, Comput. Phys. Commun. **178** (2008) 852, arXiv: [0710.3820 \[hep-ph\]](#).
- [88] ATLAS Collaboration, *The ATLAS Simulation Infrastructure*, Eur. Phys. J. C **70** (2010) 823, arXiv: [1005.4568 \[physics.ins-det\]](#).
- [89] S. Agostinelli et al., *GEANT4 – a simulation toolkit*, Nucl. Instrum. Meth. A **506** (2003) 250.
- [90] ATLAS Collaboration, *Muon reconstruction and identification efficiency in ATLAS using the full Run 2 pp collision data set at $\sqrt{s} = 13$ TeV*, Eur. Phys. J. C**81** (2020) 578, arXiv: [2012.00578 \[hep-ex\]](#).
- [91] M. Cacciari, G. P. Salam and G. Soyez, *The anti- k_t jet clustering algorithm*, JHEP **04** (2008) 063, arXiv: [0802.1189 \[hep-ph\]](#).

- [92] M. Cacciari, G. P. Salam and G. Soyez, *FastJet user manual*, Eur. Phys. J. C **72** (2012) 1896, arXiv: [1111.6097 \[hep-ph\]](#).
- [93] ATLAS Collaboration, *Jet energy scale and resolution measured in proton–proton collisions at $\sqrt{s} = 13\text{ TeV}$ with the ATLAS detector*, Eur. Phys. J. C **81** (2021) 689, arXiv: [2007.02645 \[hep-ex\]](#).
- [94] ATLAS Collaboration, *Tagging and suppression of pileup jets with the ATLAS detector*, tech. rep. ATLAS-CONF-2014-018, CERN, 2014, URL: <https://cds.cern.ch/record/1700870>.
- [95] ATLAS Collaboration, *ATLAS b -jet identification performance and efficiency measurement with $t\bar{t}$ events in pp collisions at $\sqrt{s} = 13\text{ TeV}$* , Eur. Phys. J. C **79** (2019) 970, arXiv: [1907.05120 \[hep-ex\]](#).
- [96] ATLAS Collaboration, *Performance of missing transverse momentum reconstruction with the ATLAS detector using proton–proton collisions at $\sqrt{s} = 13\text{ TeV}$* , Eur. Phys. J. C **78** (2018) 903, arXiv: [1802.08168 \[hep-ex\]](#).
- [97] ATLAS Collaboration, *E_T^{miss} performance in the ATLAS detector using 2015–2016 LHC pp collisions*, ATLAS-CONF-2018-023, 2018, URL: <https://cds.cern.ch/record/2625233>.
- [98] J. Erdmann et al., *A likelihood-based reconstruction algorithm for top-quark pairs and the KLFitter framework*, Nucl. Instrum. Meth. A **748** (2014) 18, arXiv: [1312.5595 \[hep-ex\]](#).
- [99] P. Speckmayer, A. Hocker, J. Stelzer and H. Voss, *The toolkit for multivariate data analysis, TMVA 4*, J. Phys. Conf. Ser. **219** (2010) 032057, ed. by J. Gruntorad and M. Lokajicek.
- [100] ATLAS Collaboration, *Jet energy scale measurements and their systematic uncertainties in proton–proton collisions at $\sqrt{s} = 13\text{ TeV}$ with the ATLAS detector*, Phys. Rev. D **96** (2017) 072002, arXiv: [1703.09665 \[hep-ex\]](#).
- [101] ATLAS Collaboration, *Luminosity determination in pp collisions at $\sqrt{s} = 13\text{ TeV}$ using the ATLAS detector at the LHC*, ATLAS-CONF-2019-021, 2019, URL: <https://cds.cern.ch/record/2677054>.
- [102] G. Avoni et al., *The new LUCID-2 detector for luminosity measurement and monitoring in ATLAS*, JINST **13** (2018) P07017.
- [103] ATLAS Collaboration, *Muon reconstruction performance of the ATLAS detector in proton–proton collision data at $\sqrt{s} = 13\text{ TeV}$* , Eur. Phys. J. C **76** (2016) 292, arXiv: [1603.05598 \[hep-ex\]](#).
- [104] M. Bähr et al., *Herwig++ physics and manual*, Eur. Phys. J. C **58** (2008) 639, arXiv: [0803.0883 \[hep-ph\]](#).
- [105] J. Bellm et al., *Herwig 7.0/Herwig++ 3.0 release note*, Eur. Phys. J. C **76** (2016) 196, arXiv: [1512.01178 \[hep-ph\]](#).
- [106] J. Butterworth et al., *PDF4LHC recommendations for LHC Run II*, J. Phys. G **43** (2016) 023001, arXiv: [1510.03865 \[hep-ph\]](#).
- [107] L. Harland-Lang, A. Martin, P. Motylinski and R. Thorne, *Parton distributions in the LHC era: MMHT 2014 PDFs*, Eur. Phys. J. C **75** (2015) 204, arXiv: [1412.3989 \[hep-ph\]](#).
- [108] S. Dulat et al., *New parton distribution functions from a global analysis of quantum chromodynamics*, Phys. Rev. D **93** (2016) 033006, arXiv: [1506.07443 \[hep-ph\]](#).
- [109] G. Cowan, K. Cranmer, E. Gross and O. Vitells, *Asymptotic formulae for likelihood-based tests of new physics*, Eur. Phys. J. C **71** (2011) 1554, arXiv: [1007.1727 \[physics.data-an\]](#), Erratum: Eur. Phys. J. C **73** (2013) 2501.

- [110] M. Baak et al., *HistFitter software framework for statistical data analysis*, Eur. Phys. J. C **75** (2015) 153, arXiv: [1410.1280 \[hep-ex\]](https://arxiv.org/abs/1410.1280).
- [111] E. Gross and O. Vitells, *Trial factors for the look elsewhere effect in high energy physics*, Eur. Phys. J. C **70** (2010) 525.
- [112] A. L. Read, *Presentation of search results: the CL_S technique*, J. Phys. G **28** (2002) 2693.
- [113] T. Junk, *Confidence level computation for combining searches with small statistics*, Nucl. Instrum. Meth. A **434** (1999) 435, arXiv: [hep-ex/9902006](https://arxiv.org/abs/hep-ex/9902006).
- [114] ATLAS Collaboration, *ATLAS Computing Acknowledgements*, ATL-SOFT-PUB-2021-003, 2021, URL: <https://cds.cern.ch/record/2776662>.

The ATLAS Collaboration

G. Aad⁹⁸, B. Abbott¹²³, D.C. Abbott⁹⁹, A. Abed Abud³⁴, K. Abeling⁵¹, D.K. Abhayasinghe⁹¹, S.H. Abidi²⁷, A. Aboulhorma^{33e}, H. Abramowicz¹⁵⁶, H. Abreu¹⁵⁵, Y. Abulaiti⁵, A.C. Abusleme Hoffman^{141a}, B.S. Acharya^{64a,64b,o}, B. Achkar⁵¹, L. Adam⁹⁶, C. Adam Bourdarios⁴, L. Adamczyk^{81a}, L. Adamek¹⁶¹, S.V. Addepalli²⁴, J. Adelman¹¹⁶, A. Adiguzel^{11c,ac}, S. Adorni⁵², T. Adye¹³⁸, A.A. Affolder¹⁴⁰, Y. Afik³⁴, C. Agapopoulou⁶², M.N. Agaras¹², J. Agarwala^{68a,68b}, A. Aggarwal¹¹⁴, C. Agheorghiesei^{25c}, J.A. Aguilar-Saavedra^{134f,134a,ab}, A. Ahmad³⁴, F. Ahmadov⁷⁷, W.S. Ahmed¹⁰⁰, X. Ai⁴⁴, G. Aielli^{71a,71b}, I. Aizenberg¹⁷⁴, S. Akatsuwa⁸³, M. Akbiyik⁹⁶, T.P.A. Åkesson⁹⁴, A.V. Akimov¹⁰⁷, K. Al Khoury³⁷, G.L. Alberghi^{21b}, J. Albert¹⁷⁰, P. Albicocco⁴⁹, M.J. Alconada Verzini⁸⁶, S. Alderweireldt⁴⁸, M. Aleksa³⁴, I.N. Aleksandrov⁷⁷, C. Alexa^{25b}, T. Alexopoulos⁹, A. Alfonsi¹¹⁵, F. Alfonsi^{21b}, M. Althroob¹²³, B. Ali¹³⁶, S. Ali¹⁵³, M. Aliev¹⁶⁰, G. Alimonti^{66a}, C. Allaire³⁴, B.M.M. Allbrooke¹⁵¹, P.P. Allport¹⁹, A. Aloisio^{67a,67b}, F. Alonso⁸⁶, C. Alpigiani¹⁴³, E. Alunno Camelia^{71a,71b}, M. Alvarez Estevez⁹⁵, M.G. Alvaggi^{67a,67b}, Y. Amaral Coutinho^{78b}, A. Ambler¹⁰⁰, L. Ambroz¹²⁹, C. Amelung³⁴, D. Amidei¹⁰², S.P. Amor Dos Santos^{134a}, S. Amoroso⁴⁴, C.S. Amrouche⁵², V. Ananiev¹²⁸, C. Anastopoulos¹⁴⁴, N. Andari¹³⁹, T. Andeen¹⁰, J.K. Anders¹⁸, S.Y. Andrean^{43a,43b}, A. Andreazza^{66a,66b}, S. Angelidakis⁸, A. Angerami³⁷, A.V. Anisenkov^{117b,117a}, A. Annovi^{69a}, C. Antel⁵², M.T. Anthony¹⁴⁴, E. Antipov¹²⁴, M. Antonelli⁴⁹, D.J.A. Antrim¹⁶, F. Anulli^{70a}, M. Aoki⁷⁹, J.A. Aparisi Pozo¹⁶⁸, M.A. Aparo¹⁵¹, L. Aperio Bella⁴⁴, N. Aranzabal³⁴, V. Araujo Ferraz^{78a}, C. Arcangeletti⁴⁹, A.T.H. Arce⁴⁷, E. Arena⁸⁸, J-F. Arguin¹⁰⁶, S. Argyropoulos⁵⁰, J.-H. Arling⁴⁴, A.J. Armbruster³⁴, A. Armstrong¹⁶⁵, O. Arnaez¹⁶¹, H. Arnold³⁴, Z.P. Arrubarrena Tame¹¹⁰, G. Artoni¹²⁹, H. Asada¹¹², K. Asai¹²¹, S. Asai¹⁵⁸, N.A. Asbah⁵⁷, E.M. Asimakopoulou¹⁶⁶, L. Asquith¹⁵¹, J. Assahsah^{33d}, K. Assamagan²⁷, R. Astalos^{26a}, R.J. Atkin^{31a}, M. Atkinson¹⁶⁷, N.B. Atlay¹⁷, H. Atmani^{58b}, P.A. Atmasiddha¹⁰², K. Augsten¹³⁶, S. Auricchio^{67a,67b}, V.A. Aastrup¹⁷⁶, G. Avner¹⁵⁵, G. Avolio³⁴, M.K. Ayoub^{13c}, G. Azuelos^{106,aj}, D. Babal^{26a}, H. Bachacou¹³⁹, K. Bachas¹⁵⁷, A. Bachiu³², F. Backman^{43a,43b}, A. Badea⁵⁷, P. Bagnaia^{70a,70b}, H. Bahrasemani¹⁴⁷, A.J. Bailey¹⁶⁸, V.R. Bailey¹⁶⁷, J.T. Baines¹³⁸, C. Bakalis⁹, O.K. Baker¹⁷⁷, P.J. Bakker¹¹⁵, E. Bakos¹⁴, D. Bakshi Gupta⁷, S. Balaji¹⁵², R. Balasubramanian¹¹⁵, E.M. Baldin^{117b,117a}, P. Balek¹³⁷, E. Ballabene^{66a,66b}, F. Balli¹³⁹, W.K. Balunas¹²⁹, J. Balz⁹⁶, E. Banas⁸², M. Bandieramonte¹³³, A. Bandyopadhyay¹⁷, S. Bansal²², L. Barak¹⁵⁶, E.L. Barberio¹⁰¹, D. Barberis^{53b,53a}, M. Barbero⁹⁸, G. Barbour⁹², K.N. Barends^{31a}, T. Barillari¹¹¹, M-S. Barisits³⁴, J. Barkeloo¹²⁶, T. Barklow¹⁴⁸, B.M. Barnett¹³⁸, R.M. Barnett¹⁶, A. Baroncelli^{58a}, G. Barone²⁷, A.J. Barr¹²⁹, L. Barranco Navarro^{43a,43b}, F. Barreiro⁹⁵, J. Barreiro Guimarães da Costa^{13a}, U. Barron¹⁵⁶, S. Barsov¹³², F. Bartels^{59a}, R. Bartoldus¹⁴⁸, G. Bartolini⁹⁸, A.E. Barton⁸⁷, P. Bartos^{26a}, A. Basalaev⁴⁴, A. Basan⁹⁶, M. Baselga⁴⁴, I. Bashta^{72a,72b}, A. Bassalat^{62,ag}, M.J. Basso¹⁶¹, C.R. Basson⁹⁷, R.L. Bates⁵⁵, S. Batlamous^{33e}, J.R. Batley³⁰, B. Batool¹⁴⁶, M. Battaglia¹⁴⁰, M. Bauce^{70a,70b}, F. Bauer^{139,*}, P. Bauer²², H.S. Bawa²⁹, A. Bayirli^{11c}, J.B. Beacham⁴⁷, T. Beau¹³⁰, P.H. Beauchemin¹⁶⁴, F. Becherer⁵⁰, P. Bechtle²², H.P. Beck^{18,q}, K. Becker¹⁷², C. Becot⁴⁴, A.J. Beddall^{11a}, V.A. Bednyakov⁷⁷, C.P. Bee¹⁵⁰, T.A. Beermann³⁴, M. Begalli^{78b}, M. Begel²⁷, A. Behera¹⁵⁰, J.K. Behr⁴⁴, C. Beirao Da Cruz E Silva³⁴, J.F. Beirer^{51,34}, F. Beisiegel²², M. Belfkir⁴, G. Bella¹⁵⁶, L. Bellagamba^{21b}, A. Bellerive³², P. Bellos¹⁹, K. Beloborodov^{117b,117a}, K. Belotskiy¹⁰⁸, N.L. Belyaev¹⁰⁸, D. Benchekroun^{33a}, Y. Benhammou¹⁵⁶, D.P. Benjamin²⁷, M. Benoit²⁷, J.R. Bensinger²⁴, S. Bentvelsen¹¹⁵, L. Beresford³⁴, M. Beretta⁴⁹, D. Berge¹⁷, E. Bergeaas Kuutmann¹⁶⁶, N. Berger⁴, B. Bergmann¹³⁶, L.J. Bergsten²⁴, J. Beringer¹⁶, S. Berlendis⁶, G. Bernardi¹³⁰, C. Bernius¹⁴⁸, F.U. Bernlochner²², T. Berry⁹¹, P. Berta¹³⁷, A. Berthold⁴⁶, I.A. Bertram⁸⁷, O. Bessidskaia Bylund¹⁷⁶, S. Bethke¹¹¹, A. Betti⁴⁰, A.J. Bevan⁹⁰, S. Bhattacharyya¹⁷¹, P. Bhattacharai²⁴, V.S. Bhopatkar⁵, R. Bi¹³³, R.M. Bianchi¹³³, O. Biebel¹¹⁰, R. Bielski¹²⁶, N.V. Biesuz^{69a,69b}, M. Biglietti^{72a}, T.R.V. Billoud¹³⁶, M. Bindi⁵¹, A. Bingul^{11d},

C. Bini^{70a,70b}, S. Biondi^{21b,21a}, A. Biondini⁸⁸, C.J. Birch-sykes⁹⁷, G.A. Bird^{19,138}, M. Birman¹⁷⁴, T. Bisanz³⁴, J.P. Biswal², D. Biswas^{175,j}, A. Bitadze⁹⁷, C. Bittrich⁴⁶, K. Bjørke¹²⁸, I. Bloch⁴⁴, C. Blocker²⁴, A. Blue⁵⁵, U. Blumenschein⁹⁰, J. Blumenthal⁹⁶, G.J. Bobbink¹¹⁵, V.S. Bobrovnikov^{117b,117a}, M. Boehler⁵⁰, D. Bogavac¹², A.G. Bogdanchikov^{117b,117a}, C. Bohm^{43a}, V. Boisvert⁹¹, P. Bokan⁴⁴, T. Bold^{81a}, M. Bomben¹³⁰, M. Bona⁹⁰, M. Boonekamp¹³⁹, C.D. Booth⁹¹, A.G. Borbely⁵⁵, H.M. Borecka-Bielska¹⁰⁶, L.S. Borgna⁹², G. Borissov⁸⁷, D. Bortoletto¹²⁹, D. Boscherini^{21b}, M. Bosman¹², J.D. Bossio Sola³⁴, K. Bouaouda^{33a}, J. Boudreau¹³³, E.V. Bouhova-Thacker⁸⁷, D. Boumediene³⁶, R. Bouquet¹³⁰, A. Boveia¹²², J. Boyd³⁴, D. Boye²⁷, I.R. Boyko⁷⁷, A.J. Bozson⁹¹, J. Bracinik¹⁹, N. Brahimi^{58d,58c}, G. Brandt¹⁷⁶, O. Brandt³⁰, F. Braren⁴⁴, B. Brau⁹⁹, J.E. Brau¹²⁶, W.D. Breaden Madden⁵⁵, K. Brendlinger⁴⁴, R. Brener¹⁷⁴, L. Brenner³⁴, R. Brenner¹⁶⁶, S. Bressler¹⁷⁴, B. Brickwedde⁹⁶, D.L. Briglin¹⁹, D. Britton⁵⁵, D. Britzger¹¹¹, I. Brock²², R. Brock¹⁰³, G. Brooijmans³⁷, W.K. Brooks^{141d}, E. Brost²⁷, P.A. Bruckman de Renstrom⁸², B. Brüters⁴⁴, D. Bruncko^{26b}, A. Bruni^{21b}, G. Bruni^{21b}, M. Bruschi^{21b}, N. Bruscino^{70a,70b}, L. Bryngemark¹⁴⁸, T. Buanes¹⁵, Q. Buat¹⁵⁰, P. Buchholz¹⁴⁶, A.G. Buckley⁵⁵, I.A. Budagov⁷⁷, M.K. Bugge¹²⁸, O. Bulekov¹⁰⁸, B.A. Bullard⁵⁷, S. Burdin⁸⁸, C.D. Burgard⁴⁴, A.M. Burger¹²⁴, B. Burghgrave⁷, J.T.P. Burr⁴⁴, C.D. Burton¹⁰, J.C. Burzynski⁹⁹, E.L. Busch³⁷, V. Büscher⁹⁶, P.J. Bussey⁵⁵, J.M. Butler²³, C.M. Buttar⁵⁵, J.M. Butterworth⁹², W. Buttlinger¹³⁸, C.J. Buxo Vazquez¹⁰³, A.R. Buzykaev^{117b,117a}, G. Cabras^{21b}, S. Cabrera Urbán¹⁶⁸, D. Caforio⁵⁴, H. Cai¹³³, V.M.M. Cairo¹⁴⁸, O. Cakir^{3a}, N. Calace³⁴, P. Calafiura¹⁶, G. Calderini¹³⁰, P. Calfayan⁶³, G. Callea⁵⁵, L.P. Caloba^{78b}, S. Calvente Lopez⁹⁵, D. Calvet³⁶, S. Calvet³⁶, T.P. Calvet⁹⁸, M. Calvetti^{69a,69b}, R. Camacho Toro¹³⁰, S. Camarda³⁴, D. Camarero Munoz⁹⁵, P. Camarri^{71a,71b}, M.T. Camerlingo^{72a,72b}, D. Cameron¹²⁸, C. Camincher¹⁷⁰, M. Campanelli⁹², A. Camplani³⁸, V. Canale^{67a,67b}, A. Canesse¹⁰⁰, M. Cano Bret⁷⁵, J. Cantero¹²⁴, Y. Cao¹⁶⁷, F. Capocasa²⁴, M. Capua^{39b,39a}, A. Carbone^{66a,66b}, R. Cardarelli^{71a}, J.C.J. Cardenas⁷, F. Cardillo¹⁶⁸, G. Carducci^{39b,39a}, T. Carli³⁴, G. Carlino^{67a}, B.T. Carlson¹³³, E.M. Carlson^{170,162a}, L. Carminati^{66a,66b}, M. Carnesale^{70a,70b}, R.M.D. Carney¹⁴⁸, S. Caron¹¹⁴, E. Carquin^{141d}, S. Carrá⁴⁴, G. CarratTA^{21b,21a}, J.W.S. Carter¹⁶¹, T.M. Carter⁴⁸, D. Casadei^{31c}, M.P. Casado^{12,g}, A.F. Casha¹⁶¹, E.G. Castiglia¹⁷⁷, F.L. Castillo^{59a}, L. Castillo Garcia¹², V. Castillo Gimenez¹⁶⁸, N.F. Castro^{134a,134e}, A. Catinaccio³⁴, J.R. Catmore¹²⁸, A. Cattai³⁴, V. Cavalieri²⁷, N. Cavalli^{21b,21a}, V. Cavasinni^{69a,69b}, E. Celebi^{11b}, F. Celli¹²⁹, M.S. Centonze^{65a,65b}, K. Cerny¹²⁵, A.S. Cerqueira^{78a}, A. Cerri¹⁵¹, L. Cerrito^{71a,71b}, F. Cerutti¹⁶, A. Cervelli^{21b}, S.A. Cetin^{11b}, Z. Chadi^{33a}, D. Chakraborty¹¹⁶, M. Chala^{134f}, J. Chan¹⁷⁵, W.S. Chan¹¹⁵, W.Y. Chan⁸⁸, J.D. Chapman³⁰, B. Chargeishvili^{154b}, D.G. Charlton¹⁹, T.P. Charman⁹⁰, M. Chatterjee¹⁸, S. Chekanov⁵, S.V. Chekulaev^{162a}, G.A. Chelkov^{77,ae}, A. Chen¹⁰², B. Chen¹⁵⁶, B. Chen¹⁷⁰, C. Chen^{58a}, C.H. Chen⁷⁶, H. Chen^{13c}, H. Chen²⁷, J. Chen^{58c}, J. Chen²⁴, S. Chen¹³¹, S.J. Chen^{13c}, X. Chen^{58c}, X. Chen^{13b}, Y. Chen^{58a}, Y-H. Chen⁴⁴, C.L. Cheng¹⁷⁵, H.C. Cheng^{60a}, A. Cheplakov⁷⁷, E. Cheremushkina⁴⁴, E. Cherepanova⁷⁷, R. Cherkaoui El Moursli^{33e}, E. Cheu⁶, K. Cheung⁶¹, L. Chevalier¹³⁹, V. Chiarella⁴⁹, G. Chiarelli^{69a}, G. Chiodini^{65a}, A.S. Chisholm¹⁹, A. Chitan^{25b}, Y.H. Chiu¹⁷⁰, M.V. Chizhov^{77,s}, K. Choi¹⁰, A.R. Chomont^{70a,70b}, Y. Chou⁹⁹, Y.S. Chow¹¹⁵, T. Chowdhury^{31f}, L.D. Christopher^{31f}, M.C. Chu^{60a}, X. Chu^{13a,13d}, J. Chudoba¹³⁵, J.J. Chwastowski⁸², D. Cieri¹¹¹, K.M. Ciesla⁸², V. Cindro⁸⁹, I.A. Cioara^{25b}, A. Ciocio¹⁶, F. Cirotto^{67a,67b}, Z.H. Citron^{174,k}, M. Citterio^{66a}, D.A. Ciubotaru^{25b}, B.M. Ciungu¹⁶¹, A. Clark⁵², P.J. Clark⁴⁸, J.M. Clavijo Columbie⁴⁴, S.E. Clawson⁹⁷, C. Clement^{43a,43b}, L. Clissa^{21b,21a}, Y. Coadou⁹⁸, M. Cobal^{64a,64c}, A. Coccaro^{53b}, J. Cochran⁷⁶, R.F. Coelho Barrue^{134a}, R. Coelho Lopes De Sa⁹⁹, S. Coelli^{66a}, H. Cohen¹⁵⁶, A.E.C. Coimbra³⁴, B. Cole³⁷, J. Collot⁵⁶, P. Conde Muñoz^{134a,134h}, S.H. Connell^{131c}, I.A. Connolly⁵⁵, E.I. Conroy¹²⁹, F. Conventi^{67a,ak}, H.G. Cooke¹⁹, A.M. Cooper-Sarkar¹²⁹, F. Cormier¹⁶⁹, L.D. Corpe³⁴, M. Corradi^{70a,70b}, E.E. Corrigan⁹⁴, F. Corriveau^{100,y}, M.J. Costa¹⁶⁸, F. Costanza⁴, D. Costanzo¹⁴⁴, B.M. Cote¹²², G. Cowan⁹¹, J.W. Cowley³⁰, K. Cranmer¹²⁰, S. Crépé-Renaudin⁵⁶, F. Crescioli¹³⁰, M. Cristinziani¹⁴⁶, M. Cristoforetti^{73a,73b,b}, V. Croft¹⁶⁴, G. Crosetti^{39b,39a}, A. Cueto³⁴, T. Cuhadar Donszelmann¹⁶⁵, H. Cui^{13a,13d}, A.R. Cukierman¹⁴⁸,

W.R. Cunningham⁵⁵, F. Curcio^{39b,39a}, P. Czodrowski³⁴, M.M. Czurylo^{59b},
 M.J. Da Cunha Sargedas De Sousa^{58a}, J.V. Da Fonseca Pinto^{78b}, C. Da Via⁹⁷, W. Dabrowski^{81a}, T. Dado⁴⁵,
 S. Dahbi^{31f}, T. Dai¹⁰², C. Dallapiccola⁹⁹, M. Dam³⁸, G. D'amen²⁷, V. D'Amico^{72a,72b}, J. Damp⁹⁶,
 J.R. Dandoy¹³¹, M.F. Daneri²⁸, M. Danninger¹⁴⁷, V. Dao³⁴, G. Darbo^{53b}, S. Darmora⁵, A. Dattagupta¹²⁶,
 S. D'Auria^{66a,66b}, C. David^{162b}, T. Davidek¹³⁷, D.R. Davis⁴⁷, B. Davis-Purcell³², I. Dawson⁹⁰, K. De⁷,
 R. De Asmundis^{67a}, M. De Beurs¹¹⁵, S. De Castro^{21b,21a}, N. De Groot¹¹⁴, P. de Jong¹¹⁵, H. De la Torre¹⁰³,
 A. De Maria^{13c}, D. De Pedis^{70a}, A. De Salvo^{70a}, U. De Sanctis^{71a,71b}, M. De Santis^{71a,71b}, A. De Santo¹⁵¹,
 J.B. De Vivie De Regie⁵⁶, D.V. Dedovich⁷⁷, J. Degens¹¹⁵, A.M. Deiana⁴⁰, J. Del Peso⁹⁵, Y. Delabat Diaz⁴⁴,
 F. Deliot¹³⁹, C.M. Delitzsch⁶, M. Della Pietra^{67a,67b}, D. Della Volpe⁵², A. Dell'Acqua³⁴, L. Dell'Asta^{66a,66b},
 M. Delmastro⁴, P.A. Delsart⁵⁶, S. Demers¹⁷⁷, M. Demichev⁷⁷, S.P. Denisov¹¹⁸, L. D'Eramo¹¹⁶,
 D. Derendarz⁸², J.E. Derkaoui^{33d}, F. Derue¹³⁰, P. Dervan⁸⁸, K. Desch²², K. Dette¹⁶¹, C. Deutsch²²,
 P.O. Deviveiros³⁴, F.A. Di Bello^{70a,70b}, A. Di Ciaccio^{71a,71b}, L. Di Ciaccio⁴, A. Di Domenico^{70a,70b},
 C. Di Donato^{67a,67b}, A. Di Girolamo³⁴, G. Di Gregorio^{69a,69b}, A. Di Luca^{73a,73b}, B. Di Micco^{72a,72b},
 R. Di Nardo^{72a,72b}, C. Diaconu⁹⁸, F.A. Dias¹¹⁵, T. Dias Do Vale^{134a}, M.A. Diaz^{141a}, F.G. Diaz Capriles²²,
 J. Dickinson¹⁶, M. Didenko¹⁶⁸, E.B. Diehl¹⁰², J. Dietrich¹⁷, S. Díez Cornell⁴⁴, C. Diez Pardos¹⁴⁶,
 A. Dimitrievska¹⁶, W. Ding^{13b}, J. Dingfelder²², I-M. Dinu^{25b}, S.J. Dittmeier^{59b}, F. Dittus³⁴, F. Djama⁹⁸,
 T. Djobava^{154b}, J.I. Djuvsland¹⁵, M.A.B. Do Vale¹⁴², D. Dodsworth²⁴, C. Doglioni⁹⁴, J. Dolejsi¹³⁷,
 Z. Dolezal¹³⁷, M. Donadelli^{78c}, B. Dong^{58c}, J. Donini³⁶, A. D'onofrio^{13c}, M. D'Onofrio⁸⁸, J. Dopke¹³⁸,
 A. Doria^{67a}, M.T. Dova⁸⁶, A.T. Doyle⁵⁵, E. Drechsler¹⁴⁷, E. Dreyer¹⁴⁷, T. Dreyer⁵¹, A.S. Drobac¹⁶⁴,
 D. Du^{58a}, T.A. du Pree¹¹⁵, F. Dubinin¹⁰⁷, M. Dubovsky^{26a}, A. Dubreuil⁵², E. Duchovni¹⁷⁴, G. Duckeck¹¹⁰,
 O.A. Ducu^{34,25b}, D. Duda¹¹¹, A. Dudarev³⁴, M. D'uffizi⁹⁷, L. Duflot⁶², M. Dührssen³⁴, C. Dülsen¹⁷⁶,
 A.E. Dumitriu^{25b}, M. Dunford^{59a}, S. Dungs⁴⁵, K. Dunne^{43a,43b}, A. Duperrin⁹⁸, H. Duran Yildiz^{3a},
 M. Düren⁵⁴, A. Durglishvili^{154b}, B. Dutta⁴⁴, G.I. Dyckes¹⁶, M. Dyndal^{81a}, S. Dysch⁹⁷, B.S. Dziedzic⁸²,
 B. Eckerova^{26a}, M.G. Eggleston⁴⁷, E. Egidio Purcino De Souza^{78b}, L.F. Ehrke⁵², T. Eifert⁷, G. Eigen¹⁵,
 K. Einsweiler¹⁶, T. Ekelof¹⁶⁶, Y. El Ghazali^{33b}, H. El Jarrari^{33e}, A. El Moussaouy^{33a}, V. Ellajosyula¹⁶⁶,
 M. Ellert¹⁶⁶, F. Ellinghaus¹⁷⁶, A.A. Elliot⁹⁰, N. Ellis³⁴, J. Elmsheuser²⁷, M. Elsing³⁴, D. Emeliyanov¹³⁸,
 A. Emerman³⁷, Y. Enari¹⁵⁸, J. Erdmann⁴⁵, A. Ereditato¹⁸, P.A. Erland⁸², M. Errenst¹⁷⁶, M. Escalier⁶²,
 C. Escobar¹⁶⁸, O. Estrada Pastor¹⁶⁸, E. Etzion¹⁵⁶, G. Evans^{134a}, H. Evans⁶³, M.O. Evans¹⁵¹, A. Ezhilov¹³²,
 F. Fabbri⁵⁵, L. Fabbri^{21b,21a}, G. Facini¹⁷², V. Fadeyev¹⁴⁰, R.M. Fakhrutdinov¹¹⁸, S. Falciano^{70a},
 P.J. Falke²², S. Falke³⁴, J. Faltova¹³⁷, Y. Fan^{13a}, Y. Fang^{13a}, Y. Fang^{13a}, G. Fanourakis⁴², M. Fanti^{66a,66b},
 M. Faraj^{58c}, A. Farbin⁷, A. Farilla^{72a}, E.M. Farina^{68a,68b}, T. Farooque¹⁰³, S.M. Farrington⁴⁸, P. Farthouat³⁴,
 F. Fassi^{33e}, D. Fassouliotis⁸, M. Faucci Giannelli^{71a,71b}, W.J. Fawcett³⁰, L. Fayard⁶², O.L. Fedin^{132,p},
 M. Feickert¹⁶⁷, L. Feligioni⁹⁸, A. Fell¹⁴⁴, C. Feng^{58b}, M. Feng^{13b}, M.J. Fenton¹⁶⁵, A.B. Fenyuk¹¹⁸,
 S.W. Ferguson⁴¹, J. Ferrando⁴⁴, A. Ferrari¹⁶⁶, P. Ferrari¹¹⁵, R. Ferrari^{68a}, D. Ferrere⁵², C. Ferretti¹⁰²,
 F. Fiedler⁹⁶, A. Filipčič⁸⁹, F. Filthaut¹¹⁴, M.C.N. Fiolhais^{134a,134c,a}, L. Fiorini¹⁶⁸, F. Fischer¹⁴⁶,
 W.C. Fisher¹⁰³, T. Fitschen¹⁹, I. Fleck¹⁴⁶, P. Fleischmann¹⁰², T. Flick¹⁷⁶, B.M. Flierl¹¹⁰, L. Flores¹³¹,
 M. Flores^{31f}, L.R. Flores Castillo^{60a}, F.M. Follega^{73a,73b}, N. Fomin¹⁵, J.H. Foo¹⁶¹, B.C. Forland⁶³,
 A. Formica¹³⁹, F.A. Förster¹², A.C. Forti⁹⁷, E. Fortin⁹⁸, M.G. Foti¹²⁹, L. Fountas⁸, D. Fournier⁶²,
 H. Fox⁸⁷, P. Francavilla^{69a,69b}, S. Francescato⁵⁷, M. Franchini^{21b,21a}, S. Franchino^{59a}, D. Francis³⁴,
 L. Franco⁴, L. Franconi¹⁸, M. Franklin⁵⁷, G. Frattari^{70a,70b}, A.C. Freegard⁹⁰, P.M. Freeman¹⁹,
 W.S. Freund^{78b}, E.M. Freundlich⁴⁵, D. Froidevaux³⁴, J.A. Frost¹²⁹, Y. Fu^{58a}, M. Fujimoto¹²¹,
 E. Fullana Torregrosa¹⁶⁸, J. Fuster¹⁶⁸, A. Gabrielli^{21b,21a}, A. Gabrielli³⁴, P. Gadow⁴⁴, G. Gagliardi^{53b,53a},
 L.G. Gagnon¹⁶, G.E. Gallardo¹²⁹, E.J. Gallas¹²⁹, B.J. Gallop¹³⁸, R. Gamboa Goni⁹⁰, K.K. Gan¹²²,
 S. Ganguly¹⁷⁴, J. Gao^{58a}, Y. Gao⁴⁸, Y.S. Gao^{29,m}, F.M. Garay Walls^{141a}, C. García¹⁶⁸,
 J.E. García Navarro¹⁶⁸, J.A. García Pascual^{13a}, M. Garcia-Sciveres¹⁶, R.W. Gardner³⁵, D. Garg⁷⁵,
 R.B. Garg¹⁴⁸, S. Gargiulo⁵⁰, C.A. Garner¹⁶¹, V. Garonne¹²⁸, S.J. Gasiorowski¹⁴³, P. Gaspar^{78b},
 G. Gaudio^{68a}, P. Gauzzi^{70a,70b}, I.L. Gavrilenko¹⁰⁷, A. Gavriluk¹¹⁹, C. Gay¹⁶⁹, G. Gaycken⁴⁴, E.N. Gazis⁹,

A.A. Geanta^{25b}, C.M. Gee¹⁴⁰, C.N.P. Gee¹³⁸, J. Geisen⁹⁴, M. Geisen⁹⁶, C. Gemme^{53b}, M.H. Genest⁵⁶, S. Gentile^{70a,70b}, S. George⁹¹, W.F. George¹⁹, T. Geralis⁴², L.O. Gerlach⁵¹, P. Gessinger-Befurt³⁴, M. Ghasemi Bostanabad¹⁷⁰, M. Ghneimat¹⁴⁶, A. Ghosh¹⁶⁵, A. Ghosh⁷⁵, B. Giacobbe^{21b}, S. Giagu^{70a,70b}, N. Giangiacomi¹⁶¹, P. Giannetti^{69a}, A. Giannini^{67a,67b}, S.M. Gibson⁹¹, M. Gignac¹⁴⁰, D.T. Gil^{81b}, B.J. Gilbert³⁷, D. Gillberg³², G. Gilles¹¹⁵, N.E.K. Gillwald⁴⁴, D.M. Gingrich^{2,aj}, M.P. Giordani^{64a,64c}, P.F. Giraud¹³⁹, G. Giugliarelli^{64a,64c}, D. Giugni^{66a}, F. Giuli^{71a,71b}, I. Gkalias^{8,h}, P. Gkountoumis⁹, L.K. Gladilin¹⁰⁹, C. Glasman⁹⁵, G.R. Gledhill¹²⁶, M. Glisic¹²⁶, I. Gnesi^{39b,d}, M. Goblirsch-Kolb²⁴, D. Godin¹⁰⁶, S. Goldfarb¹⁰¹, T. Golling⁵², D. Golubkov¹¹⁸, J.P. Gombas¹⁰³, A. Gomes^{134a,134b}, R. Goncalves Gama⁵¹, R. Gonçalo^{134a,134c}, G. Gonella¹²⁶, L. Gonella¹⁹, A. Gongadze⁷⁷, F. Gonnella¹⁹, J.L. Gonski³⁷, S. González de la Hoz¹⁶⁸, S. Gonzalez Fernandez¹², R. Gonzalez Lopez⁸⁸, C. Gonzalez Renteria¹⁶, R. Gonzalez Suarez¹⁶⁶, S. Gonzalez-Sevilla⁵², G.R. Gonzalvo Rodriguez¹⁶⁸, R.Y. González Andana^{141a}, L. Goossens³⁴, N.A. Gorasia¹⁹, P.A. Gorbounov¹¹⁹, H.A. Gordon²⁷, B. Gorini³⁴, E. Gorini^{65a,65b}, A. Gorišek⁸⁹, A.T. Goshaw⁴⁷, M.I. Gostkin⁷⁷, C.A. Gottardo¹¹⁴, M. Gouighri^{33b}, V. Goumarre⁴⁴, A.G. Goussiou¹⁴³, N. Govender^{31c}, C. Goy⁴, I. Grabowska-Bold^{81a}, K. Graham³², E. Gramstad¹²⁸, S. Grancagnolo¹⁷, M. Grandi¹⁵¹, V. Gratchev¹³², P.M. Gravila^{25f}, F.G. Gravili^{65a,65b}, H.M. Gray¹⁶, C. Grefe²², I.M. Gregor⁴⁴, P. Grenier¹⁴⁸, K. Grevtsov⁴⁴, C. Grieco¹², N.A. Grieser¹²³, A.A. Grillo¹⁴⁰, K. Grimm^{29,l}, S. Grinstein^{12,v}, J.-F. Grivaz⁶², S. Groh⁹⁶, E. Gross¹⁷⁴, J. Grosse-Knetter⁵¹, C. Grud¹⁰², A. Grummer¹¹³, J.C. Grundy¹²⁹, L. Guan¹⁰², W. Guan¹⁷⁵, C. Gubbels¹⁶⁹, J. Guenther³⁴, J.G.R. Guerrero Rojas¹⁶⁸, F. Guescini¹¹¹, D. Guest¹⁷, R. Gugel⁹⁶, A. Guida⁴⁴, T. Guillemin⁴, S. Guindon³⁴, J. Guo^{58c}, L. Guo⁶², Y. Guo¹⁰², R. Gupta⁴⁴, S. Gurbuz²², G. Gustavino¹²³, M. Guth⁵², P. Gutierrez¹²³, L.F. Gutierrez Zagazeta¹³¹, C. Gutschow⁹², C. Guyot¹³⁹, C. Gwenlan¹²⁹, C.B. Gwilliam⁸⁸, E.S. Haaland¹²⁸, A. Haas¹²⁰, M. Habedank¹⁷, C. Haber¹⁶, H.K. Hadavand⁷, A. Hadef⁹⁶, S. Hadzic¹¹¹, M. Haleem¹⁷¹, J. Haley¹²⁴, J.J. Hall¹⁴⁴, G. Halladjian¹⁰³, G.D. Hallewell⁹⁸, L. Halser¹⁸, K. Hamano¹⁷⁰, H. Hamdaoui^{33e}, M. Hamer²², G.N. Hamity⁴⁸, K. Han^{58a}, L. Han^{13c}, L. Han^{58a}, S. Han¹⁶, Y.F. Han¹⁶¹, K. Hanagaki^{79,t}, M. Hance¹⁴⁰, M.D. Hank³⁵, R. Hankache⁹⁷, E. Hansen⁹⁴, J.B. Hansen³⁸, J.D. Hansen³⁸, M.C. Hansen²², P.H. Hansen³⁸, K. Hara¹⁶³, T. Harenberg¹⁷⁶, S. Harkusha¹⁰⁴, Y.T. Harris¹²⁹, P.F. Harrison¹⁷², N.M. Hartman¹⁴⁸, N.M. Hartmann¹¹⁰, Y. Hasegawa¹⁴⁵, A. Hasib⁴⁸, S. Hassani¹³⁹, S. Haug¹⁸, R. Hauser¹⁰³, M. Havranek¹³⁶, C.M. Hawkes¹⁹, R.J. Hawkings³⁴, S. Hayashida¹¹², D. Hayden¹⁰³, C. Hayes¹⁰², R.L. Hayes¹⁶⁹, C.P. Hays¹²⁹, J.M. Hays⁹⁰, H.S. Hayward⁸⁸, S.J. Haywood¹³⁸, F. He^{58a}, Y. He¹⁵⁹, Y. He¹³⁰, M.P. Heath⁴⁸, V. Hedberg⁹⁴, A.L. Heggelund¹²⁸, N.D. Hehir⁹⁰, C. Heidegger⁵⁰, K.K. Heidegger⁵⁰, W.D. Heidorn⁷⁶, J. Heilman³², S. Heim⁴⁴, T. Heim¹⁶, B. Heinemann^{44,ah}, J.G. Heinlein¹³¹, J.J. Heinrich¹²⁶, L. Heinrich³⁴, J. Hejbal¹³⁵, L. Helary⁴⁴, A. Held¹²⁰, C.M. Helling¹⁴⁰, S. Hellman^{43a,43b}, C. Helsens³⁴, R.C.W. Henderson⁸⁷, L. Henkelmann³⁰, A.M. Henriques Correia³⁴, H. Herde¹⁴⁸, Y. Hernández Jiménez¹⁵⁰, H. Herr⁹⁶, M.G. Herrmann¹¹⁰, T. Herrmann⁴⁶, G. Herten⁵⁰, R. Hertenberger¹¹⁰, L. Hervas³⁴, N.P. Hessey^{162a}, H. Hibi⁸⁰, S. Higashino⁷⁹, E. Higón-Rodríguez¹⁶⁸, K.H. Hiller⁴⁴, S.J. Hillier¹⁹, M. Hils⁴⁶, I. Hinchliffe¹⁶, F. Hinterkeuser²², M. Hirose¹²⁷, S. Hirose¹⁶³, D. Hirschbuehl¹⁷⁶, B. Hiti⁸⁹, O. Hladík¹³⁵, J. Hobbs¹⁵⁰, R. Hobincu^{25e}, N. Hod¹⁷⁴, M.C. Hodgkinson¹⁴⁴, B.H. Hodgkinson³⁰, A. Hoecker³⁴, J. Hofer⁴⁴, D. Hohn⁵⁰, T. Holm²², T.R. Holmes³⁵, M. Holzbock¹¹¹, L.B.A.H. Hommels³⁰, B.P. Honan⁹⁷, J. Hong^{58c}, T.M. Hong¹³³, Y. Hong⁵¹, J.C. Honig⁵⁰, A. Höne¹¹¹, B.H. Hooberman¹⁶⁷, W.H. Hopkins⁵, Y. Horii¹¹², L.A. Horyn³⁵, S. Hou¹⁵³, J. Howarth⁵⁵, J. Hoya⁸⁶, M. Hrabovsky¹²⁵, A. Hrynevich¹⁰⁵, T. Hryn'ova⁴, P.J. Hsu⁶¹, S.-C. Hsu¹⁴³, Q. Hu³⁷, S. Hu^{58c}, Y.F. Hu^{13a,13d,al}, D.P. Huang⁹², X. Huang^{13c}, Y. Huang^{58a}, Y. Huang^{13a}, Z. Hubacek¹³⁶, F. Hubaut⁹⁸, M. Huebner²², F. Huegging²², T.B. Huffman¹²⁹, M. Huhtinen³⁴, S.K. Huiberts¹⁵, R. Hulskens⁵⁶, N. Huseynov^{77,z}, J. Huston¹⁰³, J. Huth⁵⁷, R. Hyneman¹⁴⁸, S. Hyrych^{26a}, G. Iacobucci⁵², G. Iakovidis²⁷, I. Ibragimov¹⁴⁶, L. Iconomidou-Fayard⁶², P. Iengo³⁴, R. Iguchi¹⁵⁸, T. Iizawa⁵², Y. Ikegami⁷⁹, A. Ilg¹⁸, N. Ilic¹⁶¹, H. Imam^{33a}, T. Ingebretsen Carlson^{43a,43b}, G. Introzzi^{68a,68b}, M. Iodice^{72a}, V. Ippolito^{70a,70b}, M. Ishino¹⁵⁸, W. Islam¹⁷⁵, C. Issever^{17,44}, S. Istiin^{11c,am},

J.M. Iturbe Ponce^{60a}, R. Iuppa^{73a,73b}, A. Ivina¹⁷⁴, J.M. Izen⁴¹, V. Izzo^{67a}, P. Jacka¹³⁵, P. Jackson¹,
 R.M. Jacobs⁴⁴, B.P. Jaeger¹⁴⁷, C.S. Jagfeld¹¹⁰, G. Jäkel¹⁷⁶, K. Jakobs⁵⁰, T. Jakoubek¹⁷⁴, J. Jamieson⁵⁵,
 K.W. Janas^{81a}, G. Jarlskog⁹⁴, A.E. Jaspan⁸⁸, N. Javadov^{77,z}, T. Javůrek³⁴, M. Javurkova⁹⁹, F. Jeanneau¹³⁹,
 L. Jeanty¹²⁶, J. Jejelava^{154a,aa}, P. Jenni^{50,e}, S. Jézéquel⁴, J. Jia¹⁵⁰, Z. Jia^{13c}, Y. Jiang^{58a}, S. Jiggins⁴⁸,
 J. Jimenez Pena¹¹¹, S. Jin^{13c}, A. Jinaru^{25b}, O. Jinnouchi¹⁵⁹, H. Jivan^{31f}, P. Johansson¹⁴⁴, K.A. Johns⁶,
 C.A. Johnson⁶³, D.M. Jones³⁰, E. Jones¹⁷², R.W.L. Jones⁸⁷, T.J. Jones⁸⁸, J. Jovicevic⁵¹, X. Ju¹⁶,
 J.J. Junggeburth³⁴, A. Juste Rozas^{12,v}, S. Kabana^{141c}, A. Kaczmarska⁸², M. Kado^{70a,70b}, H. Kagan¹²²,
 M. Kagan¹⁴⁸, A. Kahn³⁷, A. Kahn¹³¹, C. Kahra⁹⁶, T. Kaji¹⁷³, E. Kajomovitz¹⁵⁵, C.W. Kalderon²⁷,
 A. Kamenshchikov¹¹⁸, M. Kaneda¹⁵⁸, N.J. Kang¹⁴⁰, S. Kang⁷⁶, Y. Kano¹¹², J. Kanzaki⁷⁹, D. Kar^{31f},
 K. Karava¹²⁹, M.J. Kareem^{162b}, I. Karkanias¹⁵⁷, S.N. Karpov⁷⁷, Z.M. Karpova⁷⁷, V. Kartvelishvili⁸⁷,
 A.N. Karyukhin¹¹⁸, E. Kasimi¹⁵⁷, C. Kato^{58d}, J. Katzy⁴⁴, K. Kawade¹⁴⁵, K. Kawagoe⁸⁵, T. Kawaguchi¹¹²,
 T. Kawamoto¹³⁹, G. Kawamura⁵¹, E.F. Kay¹⁷⁰, F.I. Kaya¹⁶⁴, S. Kazakos¹², V.F. Kazanin^{117b,117a}, Y. Ke¹⁵⁰,
 J.M. Keaveney^{31a}, R. Keeler¹⁷⁰, J.S. Keller³², D. Kelsey¹⁵¹, J.J. Kempster¹⁹, J. Kendrick¹⁹,
 K.E. Kennedy³⁷, O. Kepka¹³⁵, S. Kersten¹⁷⁶, B.P. Kerševan⁸⁹, S. Ketabchi Haghigat¹⁶¹, M. Khandoga¹³⁰,
 A. Khanov¹²⁴, A.G. Kharlamov^{117b,117a}, T. Kharlamova^{117b,117a}, E.E. Khoda¹⁴³, T.J. Khoo¹⁷,
 G. Khoriauli¹⁷¹, E. Khramov⁷⁷, J. Khubua^{154b}, S. Kido⁸⁰, M. Kiehn³⁴, A. Kilgallon¹²⁶, E. Kim¹⁵⁹,
 Y.K. Kim³⁵, N. Kimura⁹², A. Kirchhoff⁵¹, D. Kirchmeier⁴⁶, C. Kirfel²², J. Kirk¹³⁸, A.E. Kiryunin¹¹¹,
 T. Kishimoto¹⁵⁸, D.P. Kisliuk¹⁶¹, C. Kitsaki⁹, O. Kivernyk²², T. Klapdor-Kleingrothaus⁵⁰, M. Klassen^{59a},
 C. Klein³², L. Klein¹⁷¹, M.H. Klein¹⁰², M. Klein⁸⁸, U. Klein⁸⁸, P. Klimek³⁴, A. Klimentov²⁷, F. Klimpel³⁴,
 T. Klingl²², T. Klioutchnikova³⁴, F.F. Klitzner¹¹⁰, P. Kluit¹¹⁵, S. Kluth¹¹¹, E. Knerner⁷⁴, T.M. Knight¹⁶¹,
 A. Knue⁵⁰, D. Kobayashi⁸⁵, M. Kobel⁴⁶, M. Kocian¹⁴⁸, T. Kodama¹⁵⁸, P. Kodys¹³⁷, D.M. Koeck¹⁵¹,
 P.T. Koenig²², T. Koffas³², N.M. Köhler³⁴, M. Kolb¹³⁹, I. Koletsou⁴, T. Komarek¹²⁵, K. Köneke⁵⁰,
 A.X.Y. Kong¹, T. Kono¹²¹, V. Konstantinides⁹², N. Konstantinidis⁹², B. Konya⁹⁴, R. Kopeliansky⁶³,
 S. Koperny^{81a}, K. Korcyl⁸², K. Kordas¹⁵⁷, G. Koren¹⁵⁶, A. Korn⁹², S. Korn⁵¹, I. Korolkov¹²,
 E.V. Korolkova¹⁴⁴, N. Korotkova¹⁰⁹, B. Kortman¹¹⁵, O. Kortner¹¹¹, S. Kortner¹¹¹, W.H. Kostecka¹¹⁶,
 V.V. Kostyukhin^{144,160}, A. Kotsokechagia⁶², A. Kotwal¹⁴⁷, A. Koulouris³⁴,
 A. Kourkoumeli-Charalampidi^{68a,68b}, C. Kourkoumelis⁸, E. Kourlitis⁵, O. Kovanda¹⁵¹, R. Kowalewski¹⁷⁰,
 W. Kozanecki¹³⁹, A.S. Kozhin¹¹⁸, V.A. Kramarenko¹⁰⁹, G. Kramberger⁸⁹, P. Kramer⁹⁶,
 D. Krasnopevtsev^{58a}, M.W. Krasny¹³⁰, A. Krasznahorkay³⁴, J.A. Kremer⁹⁶, J. Kretzschmar⁸⁸, K. Kreul¹⁷,
 P. Krieger¹⁶¹, F. Krieter¹¹⁰, S. Krishnamurthy⁹⁹, A. Krishnan^{59b}, M. Krivos¹³⁷, K. Krizka¹⁶,
 K. Kroeninger⁴⁵, H. Kroha¹¹¹, J. Kroll¹³⁵, J. Kroll¹³¹, K.S. Krowpman¹⁰³, U. Kruchonak⁷⁷, H. Krüger²²,
 N. Krumnack⁷⁶, M.C. Kruse⁴⁷, J.A. Krzysiak⁸², A. Kubota¹⁵⁹, O. Kuchinskaia¹⁶⁰, S. Kuday^{3a},
 D. Kuechler⁴⁴, J.T. Kuechler⁴⁴, S. Kuehn³⁴, T. Kuhl⁴⁴, V. Kukhtin⁷⁷, Y. Kulchitsky^{104,ad}, S. Kuleshov^{141b},
 M. Kumar^{31f}, N. Kumari⁹⁸, M. Kuna⁵⁶, A. Kupco¹³⁵, T. Kupfer⁴⁵, O. Kuprash⁵⁰, H. Kurashige⁸⁰,
 L.L. Kurchaninov^{162a}, Y.A. Kurochkin¹⁰⁴, A. Kurova¹⁰⁸, M.G. Kurth^{13a,13d}, E.S. Kuwertz³⁴, M. Kuze¹⁵⁹,
 A.K. Kvam¹⁴³, J. Kvita¹²⁵, T. Kwan¹⁰⁰, K.W. Kwok^{60a}, C. Lacasta¹⁶⁸, F. Lacava^{70a,70b}, H. Lacker¹⁷,
 D. Lacour¹³⁰, N.N. Lad⁹², E. Ladygin⁷⁷, R. Lafaye⁴, B. Laforge¹³⁰, T. Lagouri^{141c}, S. Lai⁵¹,
 I.K. Lakomiec^{81a}, N. Lalloue⁵⁶, J.E. Lambert¹²³, S. Lammers⁶³, W. Lampl⁶, C. Lampoudis¹⁵⁷,
 E. Lançon²⁷, U. Landgraf⁵⁰, M.P.J. Landon⁹⁰, V.S. Lang⁵⁰, J.C. Lange⁵¹, R.J. Langenberg⁹⁹,
 A.J. Lankford¹⁶⁵, F. Lanni²⁷, K. Lantzsch²², A. Lanza^{68a}, A. Lapertosa^{53b,53a}, J.F. Laporte¹³⁹, T. Lari^{66a},
 F. Lasagni Manghi^{21b}, M. Lassnig³⁴, V. Latonova¹³⁵, T.S. Lau^{60a}, A. Laudrain⁹⁶, A. Laurier³²,
 M. Lavorgna^{67a,67b}, S.D. Lawlor⁹¹, Z. Lawrence⁹⁷, M. Lazzaroni^{66a,66b}, B. Le⁹⁷, B. Leban⁸⁹,
 A. Lebedev⁷⁶, M. LeBlanc³⁴, T. LeCompte⁵, F. Ledroit-Guillon⁵⁶, A.C.A. Lee⁹², G.R. Lee¹⁵, L. Lee⁵⁷,
 S.C. Lee¹⁵³, S. Lee⁷⁶, L.L. Leeuw^{31c}, B. Lefebvre^{162a}, H.P. Lefebvre⁹¹, M. Lefebvre¹⁷⁰, C. Leggett¹⁶,
 K. Lehmann¹⁴⁷, N. Lehmann¹⁸, G. Lehmann Miotti³⁴, W.A. Leight⁴⁴, A. Leisos^{157,u}, M.A.L. Leite^{78c},
 C.E. Leitgeb⁴⁴, R. Leitner¹³⁷, K.J.C. Leney⁴⁰, T. Lenz²², S. Leone^{69a}, C. Leonidopoulos⁴⁸, A. Leopold¹³⁰,
 C. Leroy¹⁰⁶, R. Les¹⁰³, C.G. Lester³⁰, M. Levchenko¹³², J. Levêque⁴, D. Levin¹⁰², L.J. Levinson¹⁷⁴,

D.J. Lewis¹⁹, B. Li^{13b}, B. Li^{58b}, C. Li^{58a}, C.-Q. Li^{58c,58d}, H. Li^{58a}, H. Li^{58b}, H. Li^{58b}, J. Li^{58c}, K. Li¹⁴³, L. Li^{58c}, M. Li^{13a,13d}, Q.Y. Li^{58a}, S. Li^{58d,58c,c}, T. Li^{58b}, X. Li⁴⁴, Y. Li⁴⁴, Z. Li^{58b}, Z. Li¹²⁹, Z. Li¹⁰⁰, Z. Li⁸⁸, Z. Liang^{13a}, M. Liberatore⁴⁴, B. Liberti^{71a}, K. Lie^{60c}, J. Lieber Marin^{78b}, K. Lin¹⁰³, R.A. Linck⁶³, R.E. Lindley⁶, J.H. Lindon², A. Linss⁴⁴, E. Lipeles¹³¹, A. Lipniacka¹⁵, T.M. Liss^{167,ai}, A. Lister¹⁶⁹, J.D. Little⁷, B. Liu^{13a}, B.X. Liu¹⁴⁷, J.B. Liu^{58a}, J.K.K. Liu³⁵, K. Liu^{58d,58c}, M. Liu^{58a}, M.Y. Liu^{58a}, P. Liu^{13a}, X. Liu^{58a}, Y. Liu⁴⁴, Y. Liu^{13c,13d}, Y.L. Liu¹⁰², Y.W. Liu^{58a}, M. Livan^{68a,68b}, A. Lleres⁵⁶, J. Llorente Merino¹⁴⁷, S.L. Lloyd⁹⁰, E.M. Lobodzinska⁴⁴, P. Loch⁶, S. Loffredo^{71a,71b}, T. Lohse¹⁷, K. Lohwasser¹⁴⁴, M. Lokajicek¹³⁵, J.D. Long¹⁶⁷, I. Longarini^{70a,70b}, L. Longo³⁴, R. Longo¹⁶⁷, I. Lopez Paz¹², A. Lopez Solis⁴⁴, J. Lorenz¹¹⁰, N. Lorenzo Martinez⁴, A.M. Lory¹¹⁰, A. Lötle⁵⁰, X. Lou^{43a,43b}, X. Lou^{13a}, A. Lounis⁶², J. Love⁵, P.A. Love⁸⁷, J.J. Lozano Bahilo¹⁶⁸, G. Lu^{13a}, M. Lu^{58a}, S. Lu¹³¹, Y.J. Lu⁶¹, H.J. Lubatti¹⁴³, C. Luci^{70a,70b}, F.L. Lucio Alves^{13c}, A. Lucotte⁵⁶, F. Luehring⁶³, I. Luise¹⁵⁰, L. Luminari^{70a}, O. Lundberg¹⁴⁹, B. Lund-Jensen¹⁴⁹, N.A. Luongo¹²⁶, M.S. Lutz¹⁵⁶, D. Lynn²⁷, H. Lyons⁸⁸, R. Lysak¹³⁵, E. Lytken⁹⁴, F. Lyu^{13a}, V. Lyubushkin⁷⁷, T. Lyubushkina⁷⁷, H. Ma²⁷, L.L. Ma^{58b}, Y. Ma⁹², D.M. Mac Donell¹⁷⁰, G. Maccarrone⁴⁹, C.M. Macdonald¹⁴⁴, J.C. MacDonald¹⁴⁴, R. Madar³⁶, W.F. Mader⁴⁶, M. Madugoda Ralalage Don¹²⁴, N. Madysa⁴⁶, J. Maeda⁸⁰, T. Maeno²⁷, M. Maerker⁴⁶, V. Magerl⁵⁰, J. Magro^{64a,64c}, D.J. Mahon³⁷, C. Maidantchik^{78b}, A. Maio^{134a,134b,134d}, K. Maj^{81a}, O. Majersky^{26a}, S. Majewski¹²⁶, N. Makovec⁶², V. Maksimovic¹⁴, B. Malaescu¹³⁰, Pa. Malecki⁸², V.P. Maleev¹³², F. Malek⁵⁶, D. Malito^{39b,39a}, U. Mallik⁷⁵, C. Malone³⁰, S. Maltezos⁹, S. Malyukov⁷⁷, J. Mamuzic¹⁶⁸, G. Mancini⁴⁹, J.P. Mandalia⁹⁰, I. Mandić⁸⁹, L. Manhaes de Andrade Filho^{78a}, I.M. Maniatis¹⁵⁷, M. Manisha¹³⁹, J. Manjarres Ramos⁴⁶, K.H. Mankinen⁹⁴, A. Mann¹¹⁰, A. Manousos⁷⁴, B. Mansoulie¹³⁹, I. Manthos¹⁵⁷, S. Manzoni¹¹⁵, A. Marantis^{157,u}, G. Marchiori¹³⁰, M. Marcisovsky¹³⁵, L. Marcoccia^{71a,71b}, C. Marcon⁹⁴, M. Marjanovic¹²³, Z. Marshall¹⁶, S. Marti-Garcia¹⁶⁸, T.A. Martin¹⁷², V.J. Martin⁴⁸, B. Martin dit Latour¹⁵, L. Martinelli^{70a,70b}, M. Martinez^{12,v}, P. Martinez Agullo¹⁶⁸, V.I. Martinez Outschoorn⁹⁹, S. Martin-Haugh¹³⁸, V.S. Martoiu^{25b}, A.C. Martyniuk⁹², A. Marzin³⁴, S.R. Maschek¹¹¹, L. Masetti⁹⁶, T. Mashimo¹⁵⁸, J. Masik⁹⁷, A.L. Maslennikov^{117b,117a}, L. Massa^{21b}, P. Massarotti^{67a,67b}, P. Mastrandrea^{69a,69b}, A. Mastroberardino^{39b,39a}, T. Masubuchi¹⁵⁸, D. Matakias²⁷, T. Mathisen¹⁶⁶, A. Matic¹¹⁰, N. Matsuzawa¹⁵⁸, J. Maurer^{25b}, B. Maček⁸⁹, D.A. Maximov^{117b,117a}, R. Mazini¹⁵³, I. Maznas¹⁵⁷, S.M. Mazza¹⁴⁰, C. Mc Ginn²⁷, J.P. Mc Gowan¹⁰⁰, S.P. Mc Kee¹⁰², T.G. McCarthy¹¹¹, W.P. McCormack¹⁶, E.F. McDonald¹⁰¹, A.E. McDougall¹¹⁵, J.A. McFayden¹⁵¹, G. Mchedlidze^{154b}, M.A. McKay⁴⁰, K.D. McLean¹⁷⁰, S.J. McMahon¹³⁸, P.C. McNamara¹⁰¹, R.A. McPherson^{170,y}, J.E. Mdhluli^{31f}, Z.A. Meadows⁹⁹, S. Meehan³⁴, T. Megy³⁶, S. Mehlhase¹¹⁰, A. Mehta⁸⁸, B. Meirose⁴¹, D. Melini¹⁵⁵, B.R. Mellado Garcia^{31f}, A.H. Melo⁵¹, F. Meloni⁴⁴, A. Melzer²², E.D. Mendes Gouveia^{134a}, A.M. Mendes Jacques Da Costa¹⁹, H.Y. Meng¹⁶¹, L. Meng³⁴, S. Menke¹¹¹, M. Mentink³⁴, E. Meoni^{39b,39a}, C. Merlassino¹²⁹, P. Mermod^{52,*}, L. Merola^{67a,67b}, C. Meroni^{66a}, G. Merz¹⁰², O. Meshkov^{109,107}, J.K.R. Meshreki¹⁴⁶, J. Metcalfe⁵, A.S. Mete⁵, C. Meyer⁶³, J.-P. Meyer¹³⁹, M. Michetti¹⁷, R.P. Middleton¹³⁸, L. Mijović⁴⁸, G. Mikenberg¹⁷⁴, M. Mikestikova¹³⁵, M. Mikuž⁸⁹, H. Mildner¹⁴⁴, A. Milic¹⁶¹, C.D. Milke⁴⁰, D.W. Miller³⁵, L.S. Miller³², A. Milov¹⁷⁴, D.A. Milstead^{43a,43b}, T. Min^{13c}, A.A. Minaenko¹¹⁸, I.A. Minashvili^{154b}, L. Mince⁵⁵, A.I. Mincer¹²⁰, B. Mindur^{81a}, M. Mineev⁷⁷, Y. Minegishi¹⁵⁸, Y. Mino⁸³, L.M. Mir¹², M. Miralles Lopez¹⁶⁸, M. Mironova¹²⁹, T. Mitani¹⁷³, V.A. Mitsou¹⁶⁸, M. Mittal^{58c}, O. Miу¹⁶¹, P.S. Miyagawa⁹⁰, Y. Miyazaki⁸⁵, A. Mizukami⁷⁹, J.U. Mjörnmark⁹⁴, T. Mkrtchyan^{59a}, M. Mlynarikova¹¹⁶, T. Moa^{43a,43b}, S. Mobius⁵¹, K. Mochizuki¹⁰⁶, P. Moder⁴⁴, P. Mogg¹¹⁰, A.F. Mohammed^{13a}, S. Mohapatra³⁷, G. Mokgatitswane^{31f}, B. Mondal¹⁴⁶, S. Mondal¹³⁶, K. Mönig⁴⁴, E. Monnier⁹⁸, L. Monsonis Romero¹⁶⁸, A. Montalbano¹⁴⁷, J. Montejo Berlingen³⁴, M. Montella¹²², F. Monticelli⁸⁶, N. Morange⁶², A.L. Moreira De Carvalho^{134a}, M. Moreno Llácer¹⁶⁸, C. Moreno Martinez¹², P. Morettini^{53b}, S. Morgenstern¹⁷², D. Mori¹⁴⁷, M. Morii⁵⁷, M. Morinaga¹⁵⁸, V. Morisbak¹²⁸, A.K. Morley³⁴, A.P. Morris⁹², L. Morvaj³⁴, P. Moschovakos³⁴, B. Moser¹¹⁵, M. Mosidze^{154b}, T. Moskalets⁵⁰, P. Moskvitina¹¹⁴, J. Moss^{29,n}, E.J.W. Moyse⁹⁹, S. Muanza⁹⁸,

J. Mueller¹³³, R. Mueller¹⁸, D. Muenstermann⁸⁷, G.A. Mullier⁹⁴, J.J. Mullin¹³¹, D.P. Mungo^{66a,66b},
 J.L. Munoz Martinez¹², F.J. Munoz Sanchez⁹⁷, M. Murin⁹⁷, P. Murin^{26b}, W.J. Murray^{172,138},
 A. Murrone^{66a,66b}, J.M. Muse¹²³, M. Muškinja¹⁶, C. Mwewa²⁷, A.G. Myagkov^{118,ae}, A.J. Myers⁷,
 A.A. Myers¹³³, G. Myers⁶³, M. Myska¹³⁶, B.P. Nachman¹⁶, O. Nackenhorst⁴⁵, A.Nag Nag⁴⁶, K. Nagai¹²⁹,
 K. Nagano⁷⁹, J.L. Nagle²⁷, E. Nagy⁹⁸, A.M. Nairz³⁴, Y. Nakahama¹¹², K. Nakamura⁷⁹, H. Nanjo¹²⁷,
 F. Napolitano^{59a}, R. Narayan⁴⁰, E.A. Narayanan¹¹³, I. Naryshkin¹³², M. Naseri³², C. Nass²², T. Naumann⁴⁴,
 G. Navarro^{20a}, J. Navarro-Gonzalez¹⁶⁸, R. Nayak¹⁵⁶, P.Y. Nechaeva¹⁰⁷, F. Nechansky⁴⁴, T.J. Neep¹⁹,
 A. Negri^{68a,68b}, M. Negrini^{21b}, C. Nellist¹¹⁴, C. Nelson¹⁰⁰, K. Nelson¹⁰², S. Nemecek¹³⁵, M. Nessi^{34,f},
 M.S. Neubauer¹⁶⁷, F. Neuhaus⁹⁶, J. Neundorf⁴⁴, R. Newhouse¹⁶⁹, P.R. Newman¹⁹, C.W. Ng¹³³, Y.S. Ng¹⁷,
 Y.W.Y. Ng¹⁶⁵, B. Ngair^{33e}, H.D.N. Nguyen¹⁰⁶, R.B. Nickerson¹²⁹, R. Nicolaïdou¹³⁹, D.S. Nielsen³⁸,
 J. Nielsen¹⁴⁰, M. Niemeyer⁵¹, N. Nikiforou¹⁰, V. Nikolaenko^{118,ae}, I. Nikolic-Audit¹³⁰, K. Nikolopoulos¹⁹,
 P. Nilsson²⁷, H.R. Nindhito⁵², A. Nisati^{70a}, N. Nishu², R. Nisius¹¹¹, T. Nitta¹⁷³, T. Nobe¹⁵⁸, D.L. Noel³⁰,
 Y. Noguchi⁸³, I. Nomidis¹³⁰, M.A. Nomura²⁷, M.B. Norfolk¹⁴⁴, R.R.B. Norisam⁹², J. Novak⁸⁹, T. Novak⁴⁴,
 O. Novgorodova⁴⁶, L. Novotny¹³⁶, R. Novotny¹¹³, L. Nozka¹²⁵, K. Ntekas¹⁶⁵, E. Nurse⁹²,
 F.G. Oakham^{32,aj}, J. Ocariz¹³⁰, A. Ochi⁸⁰, I. Ochoa^{134a}, J.P. Ochoa-Ricoux^{141a}, S. Oda⁸⁵, S. Odaka⁷⁹,
 S. Oerdekk¹⁶⁶, A. Ogrodnik^{81a}, A. Oh⁹⁷, C.C. Ohm¹⁴⁹, H. Oide¹⁵⁹, R. Oishi¹⁵⁸, M.L. Ojeda⁴⁴,
 Y. Okazaki⁸³, M.W. O'Keefe⁸⁸, Y. Okumura¹⁵⁸, A. Olariu^{25b}, L.F. Oleiro Seabra^{134a},
 S.A. Olivares Pino^{141c}, D. Oliveira Damazio²⁷, D. Oliveira Goncalves^{78a}, J.L. Oliver¹⁶⁵, M.J.R. Olsson¹⁶⁵,
 A. Olszewski⁸², J. Olszowska⁸², Ö.O. Öncel²², D.C. O'Neil¹⁴⁷, A.P. O'Neill¹²⁹, A. Onofre^{134a,134e},
 P.U.E. Onyisi¹⁰, R.G. Oreamuno Madriz¹¹⁶, M.J. Oreglia³⁵, G.E. Orellana⁸⁶, D. Orestano^{72a,72b},
 N. Orlando¹², R.S. Orr¹⁶¹, V. O'Shea⁵⁵, R. Ospanov^{58a}, G. Otero y Garzon²⁸, H. Otono⁸⁵, P.S. Ott^{59a},
 G.J. Ottino¹⁶, M. Ouchrif^{33d}, J. Ouellette²⁷, F. Ould-Saada¹²⁸, A. Ouraou^{139,*}, Q. Ouyang^{13a}, M. Owen⁵⁵,
 R.E. Owen¹³⁸, K.Y. Oyulmaz^{11c}, V.E. Ozcan^{11c}, N. Ozturk⁷, S. Ozturk^{11c}, J. Pacalt¹²⁵, H.A. Pacey³⁰,
 K. Pachal⁴⁷, A. Pacheco Pages¹², C. Padilla Aranda¹², S. Pagan Griso¹⁶, G. Palacino⁶³, S. Palazzo⁴⁸,
 S. Palestini³⁴, M. Palka^{81b}, P. Palni^{81a}, D.K. Panchal¹⁰, C.E. Pandini⁵², J.G. Panduro Vazquez⁹¹, P. Pani⁴⁴,
 G. Panizzo^{64a,64c}, L. Paolozzi⁵², C. Papadatos¹⁰⁶, S. Parajuli⁴⁰, A. Paramonov⁵, C. Paraskevopoulos⁹,
 D. Paredes Hernandez^{60b}, S.R. Paredes Saenz¹²⁹, B. Parida¹⁷⁴, T.H. Park¹⁶¹, A.J. Parker²⁹, M.A. Parker³⁰,
 F. Parodi^{53b,53a}, E.W. Parrish¹¹⁶, J.A. Parsons³⁷, U. Parzefall⁵⁰, L. Pascual Dominguez¹⁵⁶, V.R. Pascuzzi¹⁶,
 F. Pasquali¹¹⁵, E. Pasqualucci^{70a}, S. Passaggio^{53b}, F. Pastore⁹¹, P. Pasuwan^{43a,43b}, J.R. Pater⁹⁷,
 A. Pathak¹⁷⁵, J. Patton⁸⁸, T. Pauly³⁴, J. Pearkes¹⁴⁸, M. Pedersen¹²⁸, L. Pedraza Diaz¹¹⁴, R. Pedro^{134a},
 T. Peiffer⁵¹, S.V. Peleganchuk^{117b,117a}, O. Penc¹³⁵, C. Peng^{60b}, H. Peng^{58a}, M. Penzin¹⁶⁰, B.S. Peralva^{78a},
 A.P. Pereira Peixoto^{134a}, L. Pereira Sanchez^{43a,43b}, D.V. Perepelitsa²⁷, E. Perez Codina^{162a}, M. Perganti⁹,
 L. Perini^{66a,66b}, H. Pernegger³⁴, S. Perrella³⁴, A. Perrevoort¹¹⁵, K. Peters⁴⁴, R.F.Y. Peters⁹⁷,
 B.A. Petersen³⁴, T.C. Petersen³⁸, E. Petit⁹⁸, V. Petousis¹³⁶, C. Petridou¹⁵⁷, P. Petroff⁶², F. Petrucci^{72a,72b},
 A. Petrukhin¹⁴⁶, M. Pettee¹⁷⁷, N.E. Pettersson³⁴, K. Petukhova¹³⁷, A. Peyaud¹³⁹, R. Pezoa^{141d},
 L. Pezzotti³⁴, G. Pezzullo¹⁷⁷, T. Pham¹⁰¹, P.W. Phillips¹³⁸, M.W. Phipps¹⁶⁷, G. Piacquadio¹⁵⁰, E. Pianori¹⁶,
 F. Piazza^{66a,66b}, A. Picazio⁹⁹, R. Piegaia²⁸, D. Pietreanu^{25b}, J.E. Pilcher³⁵, A.D. Pilkington⁹⁷,
 M. Pinamonti^{64a,64c}, J.L. Pinfold², C. Pitman Donaldson⁹², D.A. Pizzi³², L. Pizzimento^{71a,71b},
 A. Pizzini¹¹⁵, M.-A. Pleier²⁷, V. Plesanovs⁵⁰, V. Pleskot¹³⁷, E. Plotnikova⁷⁷, P. Podberezko^{117b,117a},
 R. Poettgen⁹⁴, R. Poggi⁵², L. Poggioli¹³⁰, I. Pogrebnyak¹⁰³, D. Pohl²², I. Pokharel⁵¹, G. Polesello^{68a},
 A. Poley^{147,162a}, A. Pollicchio^{70a,70b}, R. Polifka¹³⁷, A. Polini^{21b}, C.S. Pollard¹²⁹, Z.B. Pollock¹²²,
 V. Polychronakos²⁷, D. Ponomarenko¹⁰⁸, L. Pontecorvo³⁴, S. Popa^{25a}, G.A. Popeneciu^{25d}, L. Portales⁴,
 D.M. Portillo Quintero^{162a}, S. Pospisil¹³⁶, P. Postolache^{25c}, K. Potamianos¹²⁹, I.N. Potrap⁷⁷, C.J. Potter³⁰,
 H. Potti¹, T. Poulsen⁴⁴, J. Poveda¹⁶⁸, T.D. Powell¹⁴⁴, G. Pownall⁴⁴, M.E. Pozo Astigarraga³⁴,
 A. Prades Ibanez¹⁶⁸, P. Pralavorio⁹⁸, M.M. Prapa⁴², S. Prell⁷⁶, D. Price⁹⁷, M. Primavera^{65a},
 M.A. Principe Martin⁹⁵, M.L. Proffitt¹⁴³, N. Proklova¹⁰⁸, K. Prokofiev^{60c}, F. Prokoshin⁷⁷,
 S. Protopopescu²⁷, J. Proudfoot⁵, M. Przybycien^{81a}, D. Pudzha¹³², P. Puzo⁶², D. Pyatiizbyantseva¹⁰⁸,

J. Qian¹⁰², Y. Qin⁹⁷, T. Qiu⁹⁰, A. Quadt⁵¹, M. Queitsch-Maitland³⁴, G. Rabanal Bolanos⁵⁷,
 F. Ragusa^{66a,66b}, J.A. Raine⁵², S. Rajagopalan²⁷, K. Ran^{13a,13d}, D.F. Rassloff^{59a}, D.M. Rauch⁴⁴, S. Rave⁹⁶,
 B. Ravina⁵⁵, I. Ravinovich¹⁷⁴, M. Raymond³⁴, A.L. Read¹²⁸, N.P. Readioff¹⁴⁴, D.M. Rebuzzi^{68a,68b},
 G. Redlinger²⁷, K. Reeves⁴¹, D. Reikher¹⁵⁶, A. Reiss⁹⁶, A. Rej¹⁴⁶, C. Rembsler³⁴, A. Renardi⁴⁴,
 M. Renda^{25b}, M.B. Rendel¹¹¹, A.G. Rennie⁵⁵, S. Resconi^{66a}, M. Ressegotti^{53b,53a}, E.D. Ressegue¹⁶,
 S. Rettie⁹², B. Reynolds¹²², E. Reynolds¹⁹, M. Rezaei Estabragh¹⁷⁶, O.L. Rezanova^{117b,117a},
 P. Reznicek¹³⁷, E. Ricci^{73a,73b}, R. Richter¹¹¹, S. Richter⁴⁴, E. Richter-Was^{81b}, M. Ridel¹³⁰, P. Rieck¹¹¹,
 P. Riedler³⁴, O. Rifki⁴⁴, M. Rijssenbeek¹⁵⁰, A. Rimoldi^{68a,68b}, M. Rimoldi⁴⁴, L. Rinaldi^{21b,21a},
 T.T. Rinn¹⁶⁷, M.P. Rinnagel¹¹⁰, G. Ripellino¹⁴⁹, I. Riu¹², P. Rivadeneira⁴⁴, J.C. Rivera Vergara¹⁷⁰,
 F. Rizatdinova¹²⁴, E. Rizvi⁹⁰, C. Rizzi⁵², B.A. Roberts¹⁷², S.H. Robertson^{100,y}, M. Robin⁴⁴,
 D. Robinson³⁰, C.M. Robles Gajardo^{141d}, M. Robles Manzano⁹⁶, A. Robson⁵⁵, A. Rocchi^{71a,71b},
 C. Roda^{69a,69b}, S. Rodriguez Bosca^{59a}, A. Rodriguez Rodriguez⁵⁰, A.M. Rodríguez Vera^{162b}, S. Roe³⁴,
 A.R. Roepe¹²³, J. Roggel¹⁷⁶, O. Røhne¹²⁸, R.A. Rojas^{141d}, B. Roland⁵⁰, C.P.A. Roland⁶³, J. Roloff²⁷,
 A. Romaniouk¹⁰⁸, M. Romano^{21b}, A.C. Romero Hernandez¹⁶⁷, N. Rompotis⁸⁸, M. Ronzani¹²⁰, L. Roos¹³⁰,
 S. Rosati^{70a}, B.J. Rosser¹³¹, E. Rossi¹⁶¹, E. Rossi⁴, E. Rossi^{67a,67b}, L.P. Rossi^{53b}, L. Rossini⁴⁴,
 R. Rosten¹²², M. Rotaru^{25b}, B. Rottler⁵⁰, D. Rousseau⁶², D. Roussel³⁰, G. Rovelli^{68a,68b}, A. Roy¹⁰,
 A. Rozanov⁹⁸, Y. Rozen¹⁵⁵, X. Ruan^{31f}, A.J. Ruby⁸⁸, T.A. Ruggeri¹, F. Rühr⁵⁰, A. Ruiz-Martinez¹⁶⁸,
 A. Rummler³⁴, Z. Rurikova⁵⁰, N.A. Rusakovich⁷⁷, H.L. Russell³⁴, L. Rustige³⁶, J.P. Rutherford⁶,
 E.M. Rüttinger¹⁴⁴, M. Rybar¹³⁷, E.B. Rye¹²⁸, A. Ryzhov¹¹⁸, J.A. Sabater Iglesias⁴⁴, P. Sabatini¹⁶⁸,
 L. Sabetta^{70a,70b}, H.F-W. Sadrozinski¹⁴⁰, R. Sadykov⁷⁷, F. Safai Tehrani^{70a}, B. Safarzadeh Samani¹⁵¹,
 M. Safdari¹⁴⁸, P. Saha¹¹⁶, S. Saha¹⁰⁰, M. Sahinsoy¹¹¹, A. Sahu¹⁷⁶, M. Saimpert¹³⁹, M. Saito¹⁵⁸,
 T. Saito¹⁵⁸, D. Salamani³⁴, G. Salamanna^{72a,72b}, A. Salnikov¹⁴⁸, J. Salt¹⁶⁸, A. Salvador Salas¹²,
 D. Salvatore^{39b,39a}, F. Salvatore¹⁵¹, A. Salzburger³⁴, D. Sammel⁵⁰, D. Sampsonidis¹⁵⁷,
 D. Sampsonidou^{58d,58c}, J. Sánchez¹⁶⁸, A. Sanchez Pineda⁴, V. Sanchez Sebastian¹⁶⁸, H. Sandaker¹²⁸,
 C.O. Sander⁴⁴, I.G. Sanderswood⁸⁷, J.A. Sandesara⁹⁹, M. Sandhoff¹⁷⁶, C. Sandoval^{20b}, D.P.C. Sankey¹³⁸,
 M. Sannino^{53b,53a}, A. Sansoni⁴⁹, C. Santoni³⁶, H. Santos^{134a,134b}, S.N. Santpur¹⁶, A. Santra¹⁷⁴,
 K.A. Saoucha¹⁴⁴, A. Sapronov⁷⁷, J.G. Saraiva^{134a,134d}, J. Sardain⁹⁸, O. Sasaki⁷⁹, K. Sato¹⁶³, C. Sauer^{59b},
 F. Sauerburger⁵⁰, E. Sauvan⁴, P. Savard^{161,aj}, R. Sawada¹⁵⁸, C. Sawyer¹³⁸, L. Sawyer⁹³,
 I. Sayago Galvan¹⁶⁸, C. Sbarra^{21b}, A. Sbrizzi^{64a,64c}, T. Scanlon⁹², J. Schaarschmidt¹⁴³, P. Schacht¹¹¹,
 D. Schaefer³⁵, U. Schäfer⁹⁶, A.C. Schaffter⁶², D. Schaile¹¹⁰, R.D. Schamberger¹⁵⁰, E. Schanet¹¹⁰,
 C. Scharf¹⁷, N. Scharmberg⁹⁷, V.A. Schegelsky¹³², D. Scheirich¹³⁷, F. Schenck¹⁷, M. Schernau¹⁶⁵,
 C. Schiavi^{53b,53a}, L.K. Schildgen²², Z.M. Schillaci²⁴, E.J. Schioppa^{65a,65b}, M. Schioppa^{39b,39a}, B. Schlag⁹⁶,
 K.E. Schleicher⁵⁰, S. Schlenker³⁴, K. Schmieden⁹⁶, C. Schmitt⁹⁶, S. Schmitt⁴⁴, L. Schoeffel¹³⁹,
 A. Schoening^{59b}, P.G. Scholer⁵⁰, E. Schopf¹²⁹, M. Schott⁹⁶, J. Schovancova³⁴, S. Schramm⁵²,
 F. Schroeder¹⁷⁶, H-C. Schultz-Coulon^{59a}, M. Schumacher⁵⁰, B.A. Schumm¹⁴⁰, Ph. Schune¹³⁹,
 A. Schwartzman¹⁴⁸, T.A. Schwarz¹⁰², Ph. Schwemling¹³⁹, R. Schwienhorst¹⁰³, A. Sciandra¹⁴⁰,
 G. Sciolla²⁴, F. Scuri^{69a}, F. Scutti¹⁰¹, C.D. Sebastiani⁸⁸, K. Sedlaczek⁴⁵, P. Seema¹⁷, S.C. Seidel¹¹³,
 A. Seiden¹⁴⁰, B.D. Seidlitz²⁷, T. Seiss³⁵, C. Seitz⁴⁴, J.M. Seixas^{78b}, G. Sekhniaidze^{67a}, S.J. Sekula⁴⁰,
 L. Selem⁴, N. Semprini-Cesari^{21b,21a}, S. Sen⁴⁷, C. Serfon²⁷, L. Serin⁶², L. Serkin^{64a,64b}, M. Sessa^{72a,72b},
 H. Severini¹²³, S. Sevova¹⁴⁸, F. Sforza^{53b,53a}, A. Sfyrla⁵², E. Shabalina⁵¹, R. Shaheen¹⁴⁹,
 J.D. Shahinian¹³¹, N.W. Shaikh^{43a,43b}, D. Shaked Renous¹⁷⁴, L.Y. Shan^{13a}, M. Shapiro¹⁶, A. Sharma³⁴,
 A.S. Sharma¹, S. Sharma⁴⁴, P.B. Shatalov¹¹⁹, K. Shaw¹⁵¹, S.M. Shaw⁹⁷, P. Sherwood⁹², L. Shi⁹²,
 C.O. Shimmin¹⁷⁷, Y. Shimogama¹⁷³, J.D. Shinner⁹¹, I.P.J. Shipsey¹²⁹, S. Shirabe⁵², M. Shiyakova⁷⁷,
 J. Shlomi¹⁷⁴, M.J. Shochet³⁵, J. Shojaei¹⁰¹, D.R. Shope¹⁴⁹, S. Shrestha¹²², E.M. Shrif^{31f}, M.J. Shroff¹⁷⁰,
 E. Shulga¹⁷⁴, P. Sicho¹³⁵, A.M. Sickles¹⁶⁷, E. Sideras Haddad^{31f}, O. Sidiropoulou³⁴, A. Sidoti^{21b},
 F. Siegert⁴⁶, Dj. Sijacki¹⁴, J.M. Silva¹⁹, M.V. Silva Oliveira³⁴, S.B. Silverstein^{43a}, S. Simion⁶²,
 R. Simonello³⁴, N.D. Simpson⁹⁴, S. Simsek^{11b}, P. Sinervo¹⁶¹, V. Sinetckii¹⁰⁹, S. Singh¹⁴⁷, S. Singh¹⁶¹,

S. Sinha⁴⁴, S. Sinha^{31f}, M. Sioli^{21b,21a}, I. Siral¹²⁶, S.Yu. Sivoklokov¹⁰⁹, J. Sjölin^{43a,43b}, A. Skaf⁵¹, E. Skorda⁹⁴, P. Skubic¹²³, M. Slawinska⁸², K. Sliwa¹⁶⁴, V. Smakhtin¹⁷⁴, B.H. Smart¹³⁸, J. Smiesko¹³⁷, S.Yu. Smirnov¹⁰⁸, Y. Smirnov¹⁰⁸, L.N. Smirnova^{109,r}, O. Smirnova⁹⁴, E.A. Smith³⁵, H.A. Smith¹²⁹, M. Smizanska⁸⁷, K. Smolek¹³⁶, A. Smykiewicz⁸², A.A. Snesarev¹⁰⁷, H.L. Snoek¹¹⁵, S. Snyder²⁷, R. Sobie^{170,y}, A. Soffer¹⁵⁶, F. Sohns⁵¹, C.A. Solans Sanchez³⁴, E.Yu. Soldatov¹⁰⁸, U. Soldevila¹⁶⁸, A.A. Solodkov¹¹⁸, S. Solomon⁵⁰, A. Soloshenko⁷⁷, O.V. Solovyanov¹¹⁸, V. Solovyev¹³², P. Sommer¹⁴⁴, H. Son¹⁶⁴, A. Sonay¹², W.Y. Song^{162b}, A. Sopczak¹³⁶, A.L. Sopio⁹², F. Sopkova^{26b}, S. Sottocornola^{68a,68b}, R. Soualah^{64a,64c}, A.M. Soukharev^{117b,117a}, Z. Soumaimi^{33e}, D. South⁴⁴, S. Spagnolo^{65a,65b}, M. Spalla¹¹¹, M. Spangenberg¹⁷², F. Spanò⁹¹, D. Sperlich⁵⁰, T.M. Spieker^{59a}, G. Spigo³⁴, M. Spina¹⁵¹, D.P. Spiteri⁵⁵, M. Spousta¹³⁷, A. Stabile^{66a,66b}, B.L. Stamas¹¹⁶, R. Stamen^{59a}, M. Stamenkovic¹¹⁵, A. Stampekitis¹⁹, M. Standke²², E. Stancka⁸², B. Stanislaus³⁴, M.M. Stanitzki⁴⁴, M. Stankaityte¹²⁹, B. Stapf⁴⁴, E.A. Starchenko¹¹⁸, G.H. Stark¹⁴⁰, J. Stark⁹⁸, D.M. Starko^{162b}, P. Staroba¹³⁵, P. Starovoitov^{59a}, S. Stärz¹⁰⁰, R. Staszewski⁸², G. Stavropoulos⁴², P. Steinberg²⁷, A.L. Steinhebel¹²⁶, B. Stelzer^{147,162a}, H.J. Stelzer¹³³, O. Stelzer-Chilton^{162a}, H. Stenzel⁵⁴, T.J. Stevenson¹⁵¹, G.A. Stewart³⁴, M.C. Stockton³⁴, G. Stoicea^{25b}, M. Stolarski^{134a}, S. Stonjek¹¹¹, A. Straessner⁴⁶, J. Strandberg¹⁴⁹, S. Strandberg^{43a,43b}, M. Strauss¹²³, T. Strebler⁹⁸, P. Strizenec^{26b}, R. Ströhmer¹⁷¹, D.M. Strom¹²⁶, L.R. Strom⁴⁴, R. Stroynowski⁴⁰, A. Strubig^{43a,43b}, S.A. Stucci²⁷, B. Stugu¹⁵, J. Stupak¹²³, N.A. Styles⁴⁴, D. Su¹⁴⁸, S. Su^{58a}, W. Su^{58d,143,58c}, X. Su^{58a}, K. Sugizaki¹⁵⁸, V.V. Sulin¹⁰⁷, M.J. Sullivan⁸⁸, D.M.S. Sultan⁵², L. Sultanaliyeva¹⁰⁷, S. Sultansoy^{3c}, T. Sumida⁸³, S. Sun¹⁰², S. Sun¹⁷⁵, X. Sun⁹⁷, O. Sunneborn Gudnadottir¹⁶⁶, C.J.E. Suster¹⁵², M.R. Sutton¹⁵¹, M. Svatos¹³⁵, M. Swiatlowski^{162a}, T. Swirski¹⁷¹, I. Sykora^{26a}, M. Sykora¹³⁷, T. Sykora¹³⁷, D. Ta⁹⁶, K. Tackmann^{44,w}, A. Taffard¹⁶⁵, R. Tafirout^{162a}, R.H.M. Taibah¹³⁰, R. Takashima⁸⁴, K. Takeda⁸⁰, T. Takeshita¹⁴⁵, E.P. Takeva⁴⁸, Y. Takubo⁷⁹, M. Talby⁹⁸, A.A. Talyshев^{117b,117a}, K.C. Tam^{60b}, N.M. Tamir¹⁵⁶, A. Tanaka¹⁵⁸, J. Tanaka¹⁵⁸, R. Tanaka⁶², J. Tang^{58c}, Z. Tao¹⁶⁹, S. Tapia Araya⁷⁶, S. Tapprogge⁹⁶, A. Tarek Abouelfadl Mohamed¹⁰³, S. Tarem¹⁵⁵, K. Tariq^{58b}, G. Tarna^{25b}, G.F. Tartarelli^{66a}, P. Tas¹³⁷, M. Tasevsky¹³⁵, E. Tassi^{39b,39a}, G. Tateno¹⁵⁸, Y. Tayalati^{33e}, G.N. Taylor¹⁰¹, W. Taylor^{162b}, H. Teagle⁸⁸, A.S. Tee¹⁷⁵, R. Teixeira De Lima¹⁴⁸, P. Teixeira-Dias⁹¹, H. Ten Kate³⁴, J.J. Teoh¹¹⁵, K. Terashi¹⁵⁸, J. Terron⁹⁵, S. Terzo¹², M. Testa⁴⁹, R.J. Teuscher^{161,y}, N. Themistokleous⁴⁸, T. Theveneaux-Pelzer¹⁷, O. Thielmann¹⁷⁶, D.W. Thomas⁹¹, J.P. Thomas¹⁹, E.A. Thompson⁴⁴, P.D. Thompson¹⁹, E. Thomson¹³¹, E.J. Thorpe⁹⁰, Y. Tian⁵¹, V.O. Tikhomirov^{107,af}, Yu.A. Tikhonov^{117b,117a}, S. Timoshenko¹⁰⁸, P. Tipton¹⁷⁷, S. Tisserant⁹⁸, S.H. Tlou^{31f}, A. Tnourji³⁶, K. Todome^{21b,21a}, S. Todorova-Nova¹³⁷, S. Todt⁴⁶, M. Togawa⁷⁹, J. Tojo⁸⁵, S. Tokár^{26a}, K. Tokushuku⁷⁹, E. Tolley¹²², R. Tombs³⁰, M. Tomoto^{79,112}, L. Tompkins¹⁴⁸, P. Tornambe⁹⁹, E. Torrence¹²⁶, H. Torres⁴⁶, E. Torró Pastor¹⁶⁸, M. Toscani²⁸, C. Tosciri³⁵, J. Toth^{98,x}, D.R. Tovey¹⁴⁴, A. Traet¹⁵, C.J. Treado¹²⁰, T. Trefzger¹⁷¹, A. Tricoli²⁷, I.M. Trigger^{162a}, S. Trincaz-Duvold¹³⁰, D.A. Trischuk¹⁶⁹, W. Trischuk¹⁶¹, B. Trocmé⁵⁶, A. Trofymov⁶², C. Troncon^{66a}, F. Trovato¹⁵¹, L. Truong^{31c}, M. Trzebinski⁸², A. Trzupek⁸², F. Tsai¹⁵⁰, A. Tsiamis¹⁵⁷, P.V. Tsiareshka^{104,ad}, A. Tsirigotis^{157,u}, V. Tsiskaridze¹⁵⁰, E.G. Tskhadadze^{154a}, M. Tsopoulou¹⁵⁷, I.I. Tsukerman¹¹⁹, V. Tsulaia¹⁶, S. Tsuno⁷⁹, O. Tsur¹⁵⁵, D. Tsybychev¹⁵⁰, Y. Tu^{60b}, A. Tudorache^{25b}, V. Tudorache^{25b}, A.N. Tuna³⁴, S. Turchikhin⁷⁷, I. Turk Cakir^{3a}, R.J. Turner¹⁹, R. Turra^{66a}, P.M. Tuts³⁷, S. Tzamarias¹⁵⁷, P. Tzanis⁹, E. Tzovara⁹⁶, K. Uchida¹⁵⁸, F. Ukegawa¹⁶³, G. Unal³⁴, M. Unal¹⁰, A. Undrus²⁷, G. Une¹⁶⁵, F.C. Ungaro¹⁰¹, K. Uno¹⁵⁸, J. Urban^{26b}, P. Urquijo¹⁰¹, G. Usai⁷, R. Ushioda¹⁵⁹, M. Usman¹⁰⁶, Z. Uysal^{11d}, V. Vacek¹³⁶, B. Vachon¹⁰⁰, K.O.H. Vadla¹²⁸, T. Vafeiadis³⁴, C. Valderanis¹¹⁰, E. Valdes Santurio^{43a,43b}, M. Valente^{162a}, S. Valentinietti^{21b,21a}, A. Valero¹⁶⁸, L. Valéry⁴⁴, R.A. Vallance¹⁹, A. Vallier⁹⁸, J.A. Valls Ferrer¹⁶⁸, T.R. Van Daalen¹⁴³, P. Van Gemmeren⁵, S. Van Stroud⁹², I. Van Vulpel¹¹⁵, M. Vanadia^{71a,71b}, W. Vandelli³⁴, M. Vandenbroucke¹³⁹, E.R. Vandewall¹²⁴, D. Vannicola¹⁵⁶, L. Vannoli^{53b,53a}, R. Vari^{70a}, E.W. Varnes⁶, C. Varni¹⁶, T. Varol¹⁵³, D. Varouchas⁶², K.E. Varvell¹⁵², M.E. Vasile^{25b}, L. Vaslin³⁶, G.A. Vasquez¹⁷⁰, F. Vazeille³⁶, D. Vazquez Furelos¹², T. Vazquez Schroeder³⁴, J. Veatch⁵¹, V. Vecchio⁹⁷, M.J. Veen¹¹⁵, I. Veliscek¹²⁹, L.M. Veloce¹⁶¹,

F. Veloso^{134a,134c}, S. Veneziano^{70a}, A. Ventura^{65a,65b}, A. Verbytskyi¹¹¹, M. Verducci^{69a,69b}, C. Vergis²²,
 M. Verissimo De Araujo^{78b}, W. Verkerke¹¹⁵, A.T. Vermeulen¹¹⁵, J.C. Vermeulen¹¹⁵, C. Vernieri¹⁴⁸,
 P.J. Verschuur⁹¹, M. Vessella⁹⁹, M.L. Vesterbacka¹²⁰, M.C. Vetterli^{147,aj}, A. Vgenopoulos¹⁵⁷,
 N. Viaux Maira^{141d}, T. Vickey¹⁴⁴, O.E. Vickey Boeriu¹⁴⁴, G.H.A. Viehhauser¹²⁹, L. Vigani^{59b},
 M. Villa^{21b,21a}, M. Villaplana Perez¹⁶⁸, E.M. Villhauer⁴⁸, E. Vilucchi⁴⁹, M.G. Vincter³², G.S. Virdee¹⁹,
 A. Vishwakarma⁴⁸, C. Vittori^{21b,21a}, I. Vivarelli¹⁵¹, V. Vladimirov¹⁷², E. Voevodina¹¹¹, M. Vogel¹⁷⁶,
 P. Vokac¹³⁶, J. Von Ahnen⁴⁴, E. Von Toerne²², V. Vorobel¹³⁷, K. Vorobev¹⁰⁸, M. Vos¹⁶⁸, J.H. Vossebeld⁸⁸,
 M. Vozak⁹⁷, L. Vozdecky⁹⁰, N. Vranjes¹⁴, M. Vranjes Milosavljevic¹⁴, V. Vrba^{136,*}, M. Vreeswijk¹¹⁵,
 N.K. Vu⁹⁸, R. Vuillermet³⁴, O.V. Vujinovic⁹⁶, I. Vukotic³⁵, S. Wada¹⁶³, C. Wagner⁹⁹, W. Wagner¹⁷⁶,
 S. Wahdan¹⁷⁶, H. Wahlberg⁸⁶, R. Wakasa¹⁶³, M. Wakida¹¹², V.M. Walbrecht¹¹¹, J. Walder¹³⁸,
 R. Walker¹¹⁰, S.D. Walker⁹¹, W. Walkowiak¹⁴⁶, A.M. Wang⁵⁷, A.Z. Wang¹⁷⁵, C. Wang^{58a}, C. Wang^{58c},
 H. Wang¹⁶, J. Wang^{60a}, P. Wang⁴⁰, R.-J. Wang⁹⁶, R. Wang⁵⁷, R. Wang¹¹⁶, S.M. Wang¹⁵³, S. Wang^{58b},
 T. Wang^{58a}, W.T. Wang⁷⁵, W.X. Wang^{58a}, X. Wang^{13c}, X. Wang¹⁶⁷, X. Wang^{58c}, Y. Wang^{58a}, Z. Wang¹⁰²,
 C. Wanotayaroj³⁴, A. Warburton¹⁰⁰, C.P. Ward³⁰, R.J. Ward¹⁹, N. Warrack⁵⁵, A.T. Watson¹⁹,
 M.F. Watson¹⁹, G. Watts¹⁴³, B.M. Waugh⁹², A.F. Webb¹⁰, C. Weber²⁷, M.S. Weber¹⁸, S.A. Weber³²,
 S.M. Weber^{59a}, C. Wei^{58a}, Y. Wei¹²⁹, A.R. Weidberg¹²⁹, J. Weingarten⁴⁵, M. Weirich⁹⁶, C. Weiser⁵⁰,
 T. Wenaus²⁷, B. Wendland⁴⁵, T. Wengler³⁴, S. Wenig³⁴, N. Wermes²², M. Wessels^{59a}, K. Whalen¹²⁶,
 A.M. Wharton⁸⁷, A.S. White⁵⁷, A. White⁷, M.J. White¹, D. Whiteson¹⁶⁵, L. Wickremasinghe¹²⁷,
 W. Wiedenmann¹⁷⁵, C. Wiel⁴⁶, M. Wielaers¹³⁸, N. Wieseotte⁹⁶, C. Wiglesworth³⁸, L.A.M. Wiik-Fuchs⁵⁰,
 D.J. Wilbern¹²³, H.G. Wilkens³⁴, L.J. Wilkins⁹¹, D.M. Williams³⁷, H.H. Williams¹³¹, S. Williams³⁰,
 S. Willocq⁹⁹, P.J. Windischhofer¹²⁹, I. Wingerter-Seez⁴, F. Winklmeier¹²⁶, B.T. Winter⁵⁰, M. Wittgen¹⁴⁸,
 M. Wobisch⁹³, A. Wolf⁹⁶, R. Wölker¹²⁹, J. Wollrath¹⁶⁵, M.W. Wolter⁸², H. Wolters^{134a,134c},
 V.W.S. Wong¹⁶⁹, A.F. Wongel⁴⁴, S.D. Worm⁴⁴, B.K. Wosiek⁸², K.W. Woźniak⁸², K. Wraight⁵⁵,
 J. Wu^{13a,13d}, S.L. Wu¹⁷⁵, X. Wu⁵², Y. Wu^{58a}, Z. Wu^{139,58a}, J. Wuerzinger¹²⁹, T.R. Wyatt⁹⁷, B.M. Wynne⁴⁸,
 S. Xella³⁸, L. Xia^{13c}, M. Xia^{13b}, J. Xiang^{60c}, X. Xiao¹⁰², M. Xie^{58a}, X. Xie^{58a}, I. Xiotidis¹⁵¹, D. Xu^{13a},
 H. Xu^{58a}, H. Xu^{58a}, L. Xu^{58a}, R. Xu¹³¹, T. Xu^{58a}, W. Xu¹⁰², Y. Xu^{13b}, Z. Xu^{58b}, Z. Xu¹⁴⁸, B. Yabsley¹⁵²,
 S. Yacoob^{31a}, N. Yamaguchi⁸⁵, Y. Yamaguchi¹⁵⁹, M. Yamatani¹⁵⁸, H. Yamauchi¹⁶³, T. Yamazaki¹⁶,
 Y. Yamazaki⁸⁰, J. Yan^{58c}, S. Yan¹²⁹, Z. Yan²³, H.J. Yang^{58c,58d}, H.T. Yang¹⁶, S. Yang^{58a}, T. Yang^{60c},
 X. Yang^{58a}, X. Yang^{13a}, Y. Yang¹⁵⁸, Z. Yang^{102,58a}, W.-M. Yao¹⁶, Y.C. Yap⁴⁴, H. Ye^{13c}, J. Ye⁴⁰, S. Ye²⁷,
 I. Yeletskikh⁷⁷, M.R. Yexley⁸⁷, P. Yin³⁷, K. Yorita¹⁷³, K. Yoshihara⁷⁶, C.J.S. Young⁵⁰, C. Young¹⁴⁸,
 R. Yuan^{58b,i}, X. Yue^{59a}, M. Zaazoua^{33e}, B. Zabinski⁸², G. Zacharis⁹, E. Zaid⁴⁸, A.M. Zaitsev^{118,ae},
 T. Zakareishvili^{154b}, N. Zakharchuk³², S. Zambito³⁴, D. Zanzi⁵⁰, S.V. Zeißner⁴⁵, C. Zeitnitz¹⁷⁶,
 J.C. Zeng¹⁶⁷, D.T. Zenger Jr²⁴, O. Zenin¹¹⁸, T. Ženiš^{26a}, S. Zenz⁹⁰, S. Zerradi^{33a}, D. Zerwas⁶²,
 B. Zhang^{13c}, D.F. Zhang¹⁴⁴, G. Zhang^{13b}, J. Zhang⁵, K. Zhang^{13a}, L. Zhang^{13c}, M. Zhang¹⁶⁷, R. Zhang¹⁷⁵,
 S. Zhang¹⁰², X. Zhang^{58c}, X. Zhang^{58b}, Z. Zhang⁶², P. Zhao⁴⁷, Y. Zhao¹⁴⁰, Z. Zhao^{58a}, A. Zhemchugov⁷⁷,
 Z. Zheng¹⁴⁸, D. Zhong¹⁶⁷, B. Zhou¹⁰², C. Zhou¹⁷⁵, H. Zhou⁶, N. Zhou^{58c}, Y. Zhou⁶, C.G. Zhu^{58b},
 C. Zhu^{13a,13d}, H.L. Zhu^{58a}, H. Zhu^{13a}, J. Zhu¹⁰², Y. Zhu^{58a}, X. Zhuang^{13a}, K. Zhukov¹⁰⁷,
 V. Zhulanov^{117b,117a}, D. Ziemińska⁶³, N.I. Zimine⁷⁷, S. Zimmermann^{50,*}, J. Zinsser^{59b}, M. Ziolkowski¹⁴⁶,
 L. Živković¹⁴, A. Zoccoli^{21b,21a}, K. Zoch⁵², T.G. Zorbas¹⁴⁴, O. Zormpa⁴², W. Zou³⁷, L. Zwalinski³⁴.

¹Department of Physics, University of Adelaide, Adelaide; Australia.

²Department of Physics, University of Alberta, Edmonton AB; Canada.

^{3(a)}Department of Physics, Ankara University, Ankara; ^(b)Istanbul Aydin University, Application and Research Center for Advanced Studies, Istanbul; ^(c)Division of Physics, TOBB University of Economics and Technology, Ankara; Turkey.

⁴LAPP, Univ. Savoie Mont Blanc, CNRS/IN2P3, Annecy ; France.

⁵High Energy Physics Division, Argonne National Laboratory, Argonne IL; United States of America.

- ⁶Department of Physics, University of Arizona, Tucson AZ; United States of America.
- ⁷Department of Physics, University of Texas at Arlington, Arlington TX; United States of America.
- ⁸Physics Department, National and Kapodistrian University of Athens, Athens; Greece.
- ⁹Physics Department, National Technical University of Athens, Zografou; Greece.
- ¹⁰Department of Physics, University of Texas at Austin, Austin TX; United States of America.
- ¹¹^(a)Bahcesehir University, Faculty of Engineering and Natural Sciences, Istanbul;^(b)Istanbul Bilgi University, Faculty of Engineering and Natural Sciences, Istanbul;^(c)Department of Physics, Bogazici University, Istanbul;^(d)Department of Physics Engineering, Gaziantep University, Gaziantep; Turkey.
- ¹²Institut de Física d'Altes Energies (IFAE), Barcelona Institute of Science and Technology, Barcelona; Spain.
- ¹³^(a)Institute of High Energy Physics, Chinese Academy of Sciences, Beijing;^(b)Physics Department, Tsinghua University, Beijing;^(c)Department of Physics, Nanjing University, Nanjing,^(d)University of Chinese Academy of Science (UCAS), Beijing; China.
- ¹⁴Institute of Physics, University of Belgrade, Belgrade; Serbia.
- ¹⁵Department for Physics and Technology, University of Bergen, Bergen; Norway.
- ¹⁶Physics Division, Lawrence Berkeley National Laboratory and University of California, Berkeley CA; United States of America.
- ¹⁷Institut für Physik, Humboldt Universität zu Berlin, Berlin; Germany.
- ¹⁸Albert Einstein Center for Fundamental Physics and Laboratory for High Energy Physics, University of Bern, Bern; Switzerland.
- ¹⁹School of Physics and Astronomy, University of Birmingham, Birmingham; United Kingdom.
- ²⁰^(a)Facultad de Ciencias y Centro de Investigaciones, Universidad Antonio Nariño, Bogotá;^(b)Departamento de Física, Universidad Nacional de Colombia, Bogotá; Colombia.
- ²¹^(a)Dipartimento di Fisica e Astronomia A. Righi, Università di Bologna, Bologna;^(b)INFN Sezione di Bologna; Italy.
- ²²Physikalisches Institut, Universität Bonn, Bonn; Germany.
- ²³Department of Physics, Boston University, Boston MA; United States of America.
- ²⁴Department of Physics, Brandeis University, Waltham MA; United States of America.
- ²⁵^(a)Transilvania University of Brasov, Brasov;^(b)Horia Hulubei National Institute of Physics and Nuclear Engineering, Bucharest;^(c)Department of Physics, Alexandru Ioan Cuza University of Iasi, Iasi;^(d)National Institute for Research and Development of Isotopic and Molecular Technologies, Physics Department, Cluj-Napoca;^(e)University Politehnica Bucharest, Bucharest;^(f)West University in Timisoara, Timisoara; Romania.
- ²⁶^(a)Faculty of Mathematics, Physics and Informatics, Comenius University, Bratislava;^(b)Department of Subnuclear Physics, Institute of Experimental Physics of the Slovak Academy of Sciences, Kosice; Slovak Republic.
- ²⁷Physics Department, Brookhaven National Laboratory, Upton NY; United States of America.
- ²⁸Departamento de Física (FCEN) and IFIBA, Universidad de Buenos Aires and CONICET, Buenos Aires; Argentina.
- ²⁹California State University, CA; United States of America.
- ³⁰Cavendish Laboratory, University of Cambridge, Cambridge; United Kingdom.
- ³¹^(a)Department of Physics, University of Cape Town, Cape Town;^(b)iThemba Labs, Western Cape;^(c)Department of Mechanical Engineering Science, University of Johannesburg, Johannesburg;^(d)National Institute of Physics, University of the Philippines Diliman (Philippines);^(e)University of South Africa, Department of Physics, Pretoria;^(f)School of Physics, University of the Witwatersrand, Johannesburg; South Africa.
- ³²Department of Physics, Carleton University, Ottawa ON; Canada.

- ³³(^a) Faculté des Sciences Ain Chock, Réseau Universitaire de Physique des Hautes Energies - Université Hassan II, Casablanca; ^(b)Faculté des Sciences, Université Ibn-Tofail, Kénitra; ^(c)Faculté des Sciences Semlalia, Université Cadi Ayyad, LPHEA-Marrakech; ^(d)LPMR, Faculté des Sciences, Université Mohamed Premier, Oujda; ^(e)Faculté des sciences, Université Mohammed V, Rabat; Morocco.
- ³⁴CERN, Geneva; Switzerland.
- ³⁵Enrico Fermi Institute, University of Chicago, Chicago IL; United States of America.
- ³⁶LPC, Université Clermont Auvergne, CNRS/IN2P3, Clermont-Ferrand; France.
- ³⁷Nevis Laboratory, Columbia University, Irvington NY; United States of America.
- ³⁸Niels Bohr Institute, University of Copenhagen, Copenhagen; Denmark.
- ³⁹(^a) Dipartimento di Fisica, Università della Calabria, Rende; ^(b)INFN Gruppo Collegato di Cosenza, Laboratori Nazionali di Frascati; Italy.
- ⁴⁰Physics Department, Southern Methodist University, Dallas TX; United States of America.
- ⁴¹Physics Department, University of Texas at Dallas, Richardson TX; United States of America.
- ⁴²National Centre for Scientific Research "Demokritos", Agia Paraskevi; Greece.
- ⁴³(^a) Department of Physics, Stockholm University; ^(b)Oskar Klein Centre, Stockholm; Sweden.
- ⁴⁴Deutsches Elektronen-Synchrotron DESY, Hamburg and Zeuthen; Germany.
- ⁴⁵Fakultät Physik , Technische Universität Dortmund, Dortmund; Germany.
- ⁴⁶Institut für Kern- und Teilchenphysik, Technische Universität Dresden, Dresden; Germany.
- ⁴⁷Department of Physics, Duke University, Durham NC; United States of America.
- ⁴⁸SUPA - School of Physics and Astronomy, University of Edinburgh, Edinburgh; United Kingdom.
- ⁴⁹INFN e Laboratori Nazionali di Frascati, Frascati; Italy.
- ⁵⁰Physikalisch Institut, Albert-Ludwigs-Universität Freiburg, Freiburg; Germany.
- ⁵¹II. Physikalisch Institut, Georg-August-Universität Göttingen, Göttingen; Germany.
- ⁵²Département de Physique Nucléaire et Corpusculaire, Université de Genève, Genève; Switzerland.
- ⁵³(^a) Dipartimento di Fisica, Università di Genova, Genova; ^(b)INFN Sezione di Genova; Italy.
- ⁵⁴II. Physikalisch Institut, Justus-Liebig-Universität Giessen, Giessen; Germany.
- ⁵⁵SUPA - School of Physics and Astronomy, University of Glasgow, Glasgow; United Kingdom.
- ⁵⁶LPSC, Université Grenoble Alpes, CNRS/IN2P3, Grenoble INP, Grenoble; France.
- ⁵⁷Laboratory for Particle Physics and Cosmology, Harvard University, Cambridge MA; United States of America.
- ⁵⁸(^a) Department of Modern Physics and State Key Laboratory of Particle Detection and Electronics, University of Science and Technology of China, Hefei; ^(b)Institute of Frontier and Interdisciplinary Science and Key Laboratory of Particle Physics and Particle Irradiation (MOE), Shandong University, Qingdao; ^(c)School of Physics and Astronomy, Shanghai Jiao Tong University, Key Laboratory for Particle Astrophysics and Cosmology (MOE), SKLPPC, Shanghai; ^(d)Tsung-Dao Lee Institute, Shanghai; China.
- ⁵⁹(^a) Kirchhoff-Institut für Physik, Ruprecht-Karls-Universität Heidelberg, Heidelberg; ^(b)Physikalisches Institut, Ruprecht-Karls-Universität Heidelberg, Heidelberg; Germany.
- ⁶⁰(^a) Department of Physics, Chinese University of Hong Kong, Shatin, N.T., Hong Kong; ^(b)Department of Physics, University of Hong Kong, Hong Kong; ^(c)Department of Physics and Institute for Advanced Study, Hong Kong University of Science and Technology, Clear Water Bay, Kowloon, Hong Kong; China.
- ⁶¹Department of Physics, National Tsing Hua University, Hsinchu; Taiwan.
- ⁶²IJCLab, Université Paris-Saclay, CNRS/IN2P3, 91405, Orsay; France.
- ⁶³Department of Physics, Indiana University, Bloomington IN; United States of America.
- ⁶⁴(^a) INFN Gruppo Collegato di Udine, Sezione di Trieste, Udine; ^(b)ICTP, Trieste; ^(c)Dipartimento Politecnico di Ingegneria e Architettura, Università di Udine, Udine; Italy.
- ⁶⁵(^a) INFN Sezione di Lecce; ^(b)Dipartimento di Matematica e Fisica, Università del Salento, Lecce; Italy.
- ⁶⁶(^a) INFN Sezione di Milano; ^(b)Dipartimento di Fisica, Università di Milano, Milano; Italy.

- ^{67(a)}INFN Sezione di Napoli; ^(b)Dipartimento di Fisica, Università di Napoli, Napoli; Italy.
^{68(a)}INFN Sezione di Pavia; ^(b)Dipartimento di Fisica, Università di Pavia, Pavia; Italy.
^{69(a)}INFN Sezione di Pisa; ^(b)Dipartimento di Fisica E. Fermi, Università di Pisa, Pisa; Italy.
^{70(a)}INFN Sezione di Roma; ^(b)Dipartimento di Fisica, Sapienza Università di Roma, Roma; Italy.
^{71(a)}INFN Sezione di Roma Tor Vergata; ^(b)Dipartimento di Fisica, Università di Roma Tor Vergata, Roma; Italy.
^{72(a)}INFN Sezione di Roma Tre; ^(b)Dipartimento di Matematica e Fisica, Università Roma Tre, Roma; Italy.
^{73(a)}INFN-TIFPA; ^(b)Università degli Studi di Trento, Trento; Italy.
⁷⁴Institut für Astro- und Teilchenphysik, Leopold-Franzens-Universität, Innsbruck; Austria.
⁷⁵University of Iowa, Iowa City IA; United States of America.
⁷⁶Department of Physics and Astronomy, Iowa State University, Ames IA; United States of America.
⁷⁷Joint Institute for Nuclear Research, Dubna; Russia.
^{78(a)}Departamento de Engenharia Elétrica, Universidade Federal de Juiz de Fora (UFJF), Juiz de Fora; ^(b)Universidade Federal do Rio De Janeiro COPPE/EE/IF, Rio de Janeiro; ^(c)Instituto de Física, Universidade de São Paulo, São Paulo; Brazil.
⁷⁹KEK, High Energy Accelerator Research Organization, Tsukuba; Japan.
⁸⁰Graduate School of Science, Kobe University, Kobe; Japan.
^{81(a)}AGH University of Science and Technology, Faculty of Physics and Applied Computer Science, Krakow; ^(b)Marian Smoluchowski Institute of Physics, Jagiellonian University, Krakow; Poland.
⁸²Institute of Nuclear Physics Polish Academy of Sciences, Krakow; Poland.
⁸³Faculty of Science, Kyoto University, Kyoto; Japan.
⁸⁴Kyoto University of Education, Kyoto; Japan.
⁸⁵Research Center for Advanced Particle Physics and Department of Physics, Kyushu University, Fukuoka ; Japan.
⁸⁶Instituto de Física La Plata, Universidad Nacional de La Plata and CONICET, La Plata; Argentina.
⁸⁷Physics Department, Lancaster University, Lancaster; United Kingdom.
⁸⁸Oliver Lodge Laboratory, University of Liverpool, Liverpool; United Kingdom.
⁸⁹Department of Experimental Particle Physics, Jožef Stefan Institute and Department of Physics, University of Ljubljana, Ljubljana; Slovenia.
⁹⁰School of Physics and Astronomy, Queen Mary University of London, London; United Kingdom.
⁹¹Department of Physics, Royal Holloway University of London, Egham; United Kingdom.
⁹²Department of Physics and Astronomy, University College London, London; United Kingdom.
⁹³Louisiana Tech University, Ruston LA; United States of America.
⁹⁴Fysiska institutionen, Lunds universitet, Lund; Sweden.
⁹⁵Departamento de Física Teórica C-15 and CIAFF, Universidad Autónoma de Madrid, Madrid; Spain.
⁹⁶Institut für Physik, Universität Mainz, Mainz; Germany.
⁹⁷School of Physics and Astronomy, University of Manchester, Manchester; United Kingdom.
⁹⁸CPPM, Aix-Marseille Université, CNRS/IN2P3, Marseille; France.
⁹⁹Department of Physics, University of Massachusetts, Amherst MA; United States of America.
¹⁰⁰Department of Physics, McGill University, Montreal QC; Canada.
¹⁰¹School of Physics, University of Melbourne, Victoria; Australia.
¹⁰²Department of Physics, University of Michigan, Ann Arbor MI; United States of America.
¹⁰³Department of Physics and Astronomy, Michigan State University, East Lansing MI; United States of America.
¹⁰⁴B.I. Stepanov Institute of Physics, National Academy of Sciences of Belarus, Minsk; Belarus.
¹⁰⁵Research Institute for Nuclear Problems of Byelorussian State University, Minsk; Belarus.

- ¹⁰⁶Group of Particle Physics, University of Montreal, Montreal QC; Canada.
- ¹⁰⁷P.N. Lebedev Physical Institute of the Russian Academy of Sciences, Moscow; Russia.
- ¹⁰⁸National Research Nuclear University MEPhI, Moscow; Russia.
- ¹⁰⁹D.V. Skobeltsyn Institute of Nuclear Physics, M.V. Lomonosov Moscow State University, Moscow; Russia.
- ¹¹⁰Fakultät für Physik, Ludwig-Maximilians-Universität München, München; Germany.
- ¹¹¹Max-Planck-Institut für Physik (Werner-Heisenberg-Institut), München; Germany.
- ¹¹²Graduate School of Science and Kobayashi-Maskawa Institute, Nagoya University, Nagoya; Japan.
- ¹¹³Department of Physics and Astronomy, University of New Mexico, Albuquerque NM; United States of America.
- ¹¹⁴Institute for Mathematics, Astrophysics and Particle Physics, Radboud University/Nikhef, Nijmegen; Netherlands.
- ¹¹⁵Nikhef National Institute for Subatomic Physics and University of Amsterdam, Amsterdam; Netherlands.
- ¹¹⁶Department of Physics, Northern Illinois University, DeKalb IL; United States of America.
- ¹¹⁷^(a)Budker Institute of Nuclear Physics and NSU, SB RAS, Novosibirsk; ^(b)Novosibirsk State University Novosibirsk; Russia.
- ¹¹⁸Institute for High Energy Physics of the National Research Centre Kurchatov Institute, Protvino; Russia.
- ¹¹⁹Institute for Theoretical and Experimental Physics named by A.I. Alikhanov of National Research Centre "Kurchatov Institute", Moscow; Russia.
- ¹²⁰Department of Physics, New York University, New York NY; United States of America.
- ¹²¹Ochanomizu University, Otsuka, Bunkyo-ku, Tokyo; Japan.
- ¹²²Ohio State University, Columbus OH; United States of America.
- ¹²³Homer L. Dodge Department of Physics and Astronomy, University of Oklahoma, Norman OK; United States of America.
- ¹²⁴Department of Physics, Oklahoma State University, Stillwater OK; United States of America.
- ¹²⁵Palacký University, Joint Laboratory of Optics, Olomouc; Czech Republic.
- ¹²⁶Institute for Fundamental Science, University of Oregon, Eugene, OR; United States of America.
- ¹²⁷Graduate School of Science, Osaka University, Osaka; Japan.
- ¹²⁸Department of Physics, University of Oslo, Oslo; Norway.
- ¹²⁹Department of Physics, Oxford University, Oxford; United Kingdom.
- ¹³⁰LPNHE, Sorbonne Université, Université de Paris, CNRS/IN2P3, Paris; France.
- ¹³¹Department of Physics, University of Pennsylvania, Philadelphia PA; United States of America.
- ¹³²Konstantinov Nuclear Physics Institute of National Research Centre "Kurchatov Institute", PNPI, St. Petersburg; Russia.
- ¹³³Department of Physics and Astronomy, University of Pittsburgh, Pittsburgh PA; United States of America.
- ¹³⁴^(a)Laboratório de Instrumentação e Física Experimental de Partículas - LIP, Lisboa; ^(b)Departamento de Física, Faculdade de Ciências, Universidade de Lisboa, Lisboa; ^(c)Departamento de Física, Universidade de Coimbra, Coimbra; ^(d)Centro de Física Nuclear da Universidade de Lisboa, Lisboa; ^(e)Departamento de Física, Universidade do Minho, Braga; ^(f)Departamento de Física Teórica y del Cosmos, Universidad de Granada, Granada (Spain); ^(g)Dep Física and CEFITEC of Faculdade de Ciências e Tecnologia, Universidade Nova de Lisboa, Caparica; ^(h)Instituto Superior Técnico, Universidade de Lisboa, Lisboa; Portugal.
- ¹³⁵Institute of Physics of the Czech Academy of Sciences, Prague; Czech Republic.
- ¹³⁶Czech Technical University in Prague, Prague; Czech Republic.
- ¹³⁷Charles University, Faculty of Mathematics and Physics, Prague; Czech Republic.

- ¹³⁸Particle Physics Department, Rutherford Appleton Laboratory, Didcot; United Kingdom.
- ¹³⁹IRFU, CEA, Université Paris-Saclay, Gif-sur-Yvette; France.
- ¹⁴⁰Santa Cruz Institute for Particle Physics, University of California Santa Cruz, Santa Cruz CA; United States of America.
- ¹⁴¹^(a)Departamento de Física, Pontificia Universidad Católica de Chile, Santiago; ^(b)Universidad Andres Bello, Department of Physics, Santiago; ^(c)Instituto de Alta Investigación, Universidad de Tarapacá, Arica; ^(d)Departamento de Física, Universidad Técnica Federico Santa María, Valparaíso; Chile.
- ¹⁴²Universidade Federal de São João del Rei (UFSJ), São João del Rei; Brazil.
- ¹⁴³Department of Physics, University of Washington, Seattle WA; United States of America.
- ¹⁴⁴Department of Physics and Astronomy, University of Sheffield, Sheffield; United Kingdom.
- ¹⁴⁵Department of Physics, Shinshu University, Nagano; Japan.
- ¹⁴⁶Department Physik, Universität Siegen, Siegen; Germany.
- ¹⁴⁷Department of Physics, Simon Fraser University, Burnaby BC; Canada.
- ¹⁴⁸SLAC National Accelerator Laboratory, Stanford CA; United States of America.
- ¹⁴⁹Department of Physics, Royal Institute of Technology, Stockholm; Sweden.
- ¹⁵⁰Departments of Physics and Astronomy, Stony Brook University, Stony Brook NY; United States of America.
- ¹⁵¹Department of Physics and Astronomy, University of Sussex, Brighton; United Kingdom.
- ¹⁵²School of Physics, University of Sydney, Sydney; Australia.
- ¹⁵³Institute of Physics, Academia Sinica, Taipei; Taiwan.
- ¹⁵⁴^(a)E. Andronikashvili Institute of Physics, Iv. Javakhishvili Tbilisi State University, Tbilisi; ^(b)High Energy Physics Institute, Tbilisi State University, Tbilisi; Georgia.
- ¹⁵⁵Department of Physics, Technion, Israel Institute of Technology, Haifa; Israel.
- ¹⁵⁶Raymond and Beverly Sackler School of Physics and Astronomy, Tel Aviv University, Tel Aviv; Israel.
- ¹⁵⁷Department of Physics, Aristotle University of Thessaloniki, Thessaloniki; Greece.
- ¹⁵⁸International Center for Elementary Particle Physics and Department of Physics, University of Tokyo, Tokyo; Japan.
- ¹⁵⁹Department of Physics, Tokyo Institute of Technology, Tokyo; Japan.
- ¹⁶⁰Tomsk State University, Tomsk; Russia.
- ¹⁶¹Department of Physics, University of Toronto, Toronto ON; Canada.
- ¹⁶²^(a)TRIUMF, Vancouver BC; ^(b)Department of Physics and Astronomy, York University, Toronto ON; Canada.
- ¹⁶³Division of Physics and Tomonaga Center for the History of the Universe, Faculty of Pure and Applied Sciences, University of Tsukuba, Tsukuba; Japan.
- ¹⁶⁴Department of Physics and Astronomy, Tufts University, Medford MA; United States of America.
- ¹⁶⁵Department of Physics and Astronomy, University of California Irvine, Irvine CA; United States of America.
- ¹⁶⁶Department of Physics and Astronomy, University of Uppsala, Uppsala; Sweden.
- ¹⁶⁷Department of Physics, University of Illinois, Urbana IL; United States of America.
- ¹⁶⁸Instituto de Física Corpuscular (IFIC), Centro Mixto Universidad de Valencia - CSIC, Valencia; Spain.
- ¹⁶⁹Department of Physics, University of British Columbia, Vancouver BC; Canada.
- ¹⁷⁰Department of Physics and Astronomy, University of Victoria, Victoria BC; Canada.
- ¹⁷¹Fakultät für Physik und Astronomie, Julius-Maximilians-Universität Würzburg, Würzburg; Germany.
- ¹⁷²Department of Physics, University of Warwick, Coventry; United Kingdom.
- ¹⁷³Waseda University, Tokyo; Japan.
- ¹⁷⁴Department of Particle Physics and Astrophysics, Weizmann Institute of Science, Rehovot; Israel.
- ¹⁷⁵Department of Physics, University of Wisconsin, Madison WI; United States of America.

¹⁷⁶Fakultät für Mathematik und Naturwissenschaften, Fachgruppe Physik, Bergische Universität Wuppertal, Wuppertal; Germany.

¹⁷⁷Department of Physics, Yale University, New Haven CT; United States of America.

^a Also at Borough of Manhattan Community College, City University of New York, New York NY; United States of America.

^b Also at Bruno Kessler Foundation, Trento; Italy.

^c Also at Center for High Energy Physics, Peking University; China.

^d Also at Centro Studi e Ricerche Enrico Fermi; Italy.

^e Also at CERN, Geneva; Switzerland.

^f Also at Département de Physique Nucléaire et Corpusculaire, Université de Genève, Genève; Switzerland.

^g Also at Departament de Fisica de la Universitat Autonoma de Barcelona, Barcelona; Spain.

^h Also at Department of Financial and Management Engineering, University of the Aegean, Chios; Greece.

ⁱ Also at Department of Physics and Astronomy, Michigan State University, East Lansing MI; United States of America.

^j Also at Department of Physics and Astronomy, University of Louisville, Louisville, KY; United States of America.

^k Also at Department of Physics, Ben Gurion University of the Negev, Beer Sheva; Israel.

^l Also at Department of Physics, California State University, East Bay; United States of America.

^m Also at Department of Physics, California State University, Fresno; United States of America.

ⁿ Also at Department of Physics, California State University, Sacramento; United States of America.

^o Also at Department of Physics, King's College London, London; United Kingdom.

^p Also at Department of Physics, St. Petersburg State Polytechnical University, St. Petersburg; Russia.

^q Also at Department of Physics, University of Fribourg, Fribourg; Switzerland.

^r Also at Faculty of Physics, M.V. Lomonosov Moscow State University, Moscow; Russia.

^s Also at Faculty of Physics, Sofia University, 'St. Kliment Ohridski', Sofia; Bulgaria.

^t Also at Graduate School of Science, Osaka University, Osaka; Japan.

^u Also at Hellenic Open University, Patras; Greece.

^v Also at Institutio Catalana de Recerca i Estudis Avancats, ICREA, Barcelona; Spain.

^w Also at Institut für Experimentalphysik, Universität Hamburg, Hamburg; Germany.

^x Also at Institute for Particle and Nuclear Physics, Wigner Research Centre for Physics, Budapest; Hungary.

^y Also at Institute of Particle Physics (IPP); Canada.

^z Also at Institute of Physics, Azerbaijan Academy of Sciences, Baku; Azerbaijan.

^{aa} Also at Institute of Theoretical Physics, Ilia State University, Tbilisi; Georgia.

^{ab} Also at Instituto de Fisica Teorica, IFT-UAM/CSIC, Madrid; Spain.

^{ac} Also at Istanbul University, Dept. of Physics, Istanbul; Turkey.

^{ad} Also at Joint Institute for Nuclear Research, Dubna; Russia.

^{ae} Also at Moscow Institute of Physics and Technology State University, Dolgoprudny; Russia.

^{af} Also at National Research Nuclear University MEPhI, Moscow; Russia.

^{ag} Also at Physics Department, An-Najah National University, Nablus; Palestine.

^{ah} Also at Physikalischs Institut, Albert-Ludwigs-Universität Freiburg, Freiburg; Germany.

^{ai} Also at The City College of New York, New York NY; United States of America.

^{aj} Also at TRIUMF, Vancouver BC; Canada.

^{ak} Also at Universita di Napoli Parthenope, Napoli; Italy.

^{al} Also at University of Chinese Academy of Sciences (UCAS), Beijing; China.

^{am} Also at Yeditepe University, Physics Department, Istanbul; Turkey.

* Deceased